



Chapter 4

The Texas Geothermal Resource: Regions and Geologies Ripe for Development

K. Wisian, S. Bhattacharya, M. Richards

The total amount of heat in the upper ten kilometers of the Texas subsurface is approximately one million exajoules. That is roughly half a million times Texas' annual electricity generation of 500 million megawatt hours. Put simply, even accounting for low efficiency of extraction, there is enough energy to meet electric and thermal demand in Texas for thousands of years just a short distance under our feet.

I. Introduction

Texas is known as the energy State. It has led the growth and development of the world's petroleum industry, and is responsible for the United States becoming a world leader for gas production as a result of the shale boom. And in the last two decades, a different form of energy production boomed in Texas – wind. Texas leapt into the lead in wind power production nationally after initially lagging behind other states at the beginning of this century (DOE, 2022). Texas has the opportunity to become a global leader of yet another source of energy – geothermal. In this Chapter, we explore the abundant subsurface heat that may provide the next opportunity for Texas to lead the world in energy – the concept of 'Geothermal Anywhere.'

Texas is not on the list of conventional geothermal production zones in the United States. To date, geothermal energy production has been (with negligible exceptions) concentrated west of the Rockies in a region referred to by geologists as the Great Basin. Traditional hydrothermal resources, referred to in this Report as Conventional Hydrothermal Systems ("CHS"), are geographically limited. CHS requires the presence of natural, dynamic or static water/steam in the subsurface. The location of these systems is connected with tectonics, either volcanism or deep fault lines. These geological settings, in turn, occur mainly in the Great Basin, a geographic range that includes most of Nevada, reaches north to the Columbia Plateau in

<https://doi.org/10.26153/tsw/44071>



central Oregon and southern Idaho, encompasses half of Utah to the Wasatch Mountain Range to the east and the Sierra Nevada mountains of California to the west, and stretches south through the Mojave Desert and Imperial Valley in California and Sonoran Desert in Mexico.

Additionally, the Pacific coastal area of the western United States and Hawaii have visible tectonic activity. Worldwide, the close coupling of geothermal development and tectonics occurs around the “Ring of Fire” of the Pacific Ocean, the East African Rift, and one-off hotspots (Iceland and Hawaii, for example), as well as near other tectonic plate boundaries.

Texas is hot. The total amount of heat in the upper 6.2 miles (ten kilometers) of the Texas subsurface is approximately one million exajoules (Tester, et al., 2006). That is; 10^{24} joules, 9.4×10^{20} British thermal units, 163,000 billion barrels of oil equivalent, or 2.8×10^{11} gigawatt hours. Pick your units any way you want - Texas has roughly half a million times its annual electricity generation of 500 million megawatt hours in geothermal energy potential just below the surface of its ranches, farms, cities, and towns (EIA, 2022). This however is energy content, not extractable energy. The purpose of this Report is to provide policy-makers, investors, and the general public a greater appreciation as to how much of this energy is recoverable, both in the near term, and with the application of new technologies in the future.

The history of geothermal energy in Texas is comparatively brief. There have been small periods of interest and research in the past, mainly in the 1970s and 1980s. The unique Gulf Geopressure Zone, located in the subsurface along the Texas Gulf Coast, generated interest in the past, and has sustained intermittent attention since. A geothermal demonstration plant in Pleasant Bayou in Brazoria County was built and operated briefly in the 1990s (John, et al., 1998). Excellent fundamental work was done in the period between 1979 and 1990, and the publications resulting from this work form a solid foundation of understanding about the State’s geothermal resources, as referenced in this Chapter¹. Since this foundational work was performed in Texas, technologies, science, and the world’s priorities with regard to clean energy technologies have significantly changed, and altered

the lens through which we should view the geothermal opportunity in Texas.

Recent and continuing advancements in drilling technologies, as well as technologies related to the conversion of heat into electricity, are changing the picture and opening the door to Texas adding a significant new power source to its grid, as well as creating and leading a major new world-wide industry - geothermal energy. These technological advances are breaking the geographic constraint of days past of where geothermal can be developed, creating an opportunity for the emergence of the next generation of “geothermal anywhere.” In light of this new paradigm, as well as the increased availability of subsurface data, we re-examine the geothermal potential of Texas.

First, some caveats: in this Chapter, we focus on the subsurface, as opposed to on specific geothermal technologies. Technologies such as Direct Use heat and power production concepts are considered in detail in other Chapters. Additionally, Conventional Hydrothermal Systems (“CHS”), though limited in Texas, do exist, and will be addressed in this Chapter. The semi-conventional gulf coast geopressure resource is perhaps the most currently exploitable opportunity in the realm of CHS. Geopressure allows for both the thermal and mechanical energy of over-pressured, deep formations to be harnessed, resulting in more economically attractive geothermal projects, which may also be co-produced with gas.

II. What’s New

A significant difference between this study and previous work performed in Texas is the inclusion of all types of geothermal resources in our analysis - not just CHS, geopressure, and Direct Use. The “geothermal anywhere” paradigm opens opportunities for application of new technologies, and exploitation of resources in new regions that may have previously been infeasible. The next generation of geothermal anywhere takes advantage of multiple proven and emergent technologies to enable the creation of artificial systems to extract heat from the crust, without relying on nature to concentrate the heat in visible surface anomalies. These proven and

¹For a concise listing please search the Bureau of Economic Geology Bookstore with “geothermal”
https://store.beg.utexas.edu/search?controller=search&orderby=position&orderway=desc&search_query=Geothermal&submit_search=



emergent technologies are covered elsewhere in this Report. We refer to these collectively as Next Generation technologies.

Geothermal anywhere opens up all of Texas, not just the select areas of the past, to geothermal energy production. As such, geothermal anywhere will demand new ways of city planning. For example, when power generation is embedded in a decentralized, organic way at the scale of a few or tens of megawatts per plant, cities will need to fold geothermal infrastructure into growth plans as now they do with power substations. This approach means the generation is close to the customer or what grid operators call the demand, or load center.

The State's geothermal resources are, in many instances particularly along the Gulf Coast industrial regions in Texas, co-located with industrial off-takers, which means industry in the future may have their own on-site geothermal energy source, and use it in whatever way is most efficient for them. Thus, an area of continued research for geothermal in Texas will be the integration of geothermal energy use and urban/growth planning.

With the flourish of recent technological advancements, deep oil and gas producing basins are becoming viable as geothermal producers. Even hard-rock zones, such as the Llano uplift, could become geothermal energy producers. The energy industry is increasingly interested in the potential of energy generation that can take advantage of vast existing infrastructure already in place in areas such as the Permian Basin oil and gas fields, and underneath decommissioned coal power plants. In part, stakeholders see the expansion of low or zero-carbon technologies as a crucial enabling technology in their plans to mitigate greenhouse gasses created by their continuing oil & gas production.

III. Risk Reduction vs. Conventional Geothermal and Oil & Gas

Perceived risk is a crucial difference between developing an oil and gas field and a geothermal resource. Oil and gas risk remains high until the well is completed in the production zone, due to the local and small-scale heterogeneities in key production factors such as porosity and permeability. While the ability to predict these variables in advance has improved considerably in recent

decades, a fundamental level of risk for successfully completing a producing zone remains. A similar risk exists in Conventional Hydrothermal System development, but perhaps not in some new technologies, as will be explored further below. The usual geothermal targets, which are hot fluid upflow channels and a sufficient rate of fluid flow, can be challenging to pin down in advance, and therefore success cannot be known until the expensive process of drilling the well is mostly complete.

Next Generation geothermal methods permit the exploration of geothermal resources beyond Conventional Hydrothermal Systems dominated by advection and convection (moving fluids) to permit exploration in conduction dominated systems, such as sedimentary basins or stable hard-rock cratons.

Conduction is a diffusive process, which is the exchange of energy between adjacent molecules and electrons. It is the dominant heat transfer mechanism for most of the lithosphere, as the rigid lithosphere is unable to support large convection cells. In a conductive (diffusive) setting, temperature does not vary laterally nearly as rapidly as other rock properties such as porosity or mineral content. In other words, you will not find a change of ten degrees across one centimeter (0.4 inches), whereas you might find a complete mineralogy change across the same distance due to depositional or diagenetic controls.

The Earth's core is as hot as the surface of the sun, and in general, the Earth's temperature increases with depth, although it does not do so at a uniform rate. In theory, a desired target temperature can always be reached, it is just a matter of at what depth, and in what rock formation it will occur. Estimates of heat transfer in conduction dominated systems are governed by Fourier's Law. The rate at which heat is conducted through a material (heat flow) is directly proportional to the temperature gradient across the material and the thermal conductivity of the material, and is inversely proportional to the thickness of the material. Therefore, geothermal gradients and conductivity of the rock as well as fractures are key to understanding heat transfer. Variations of thermal conductivity related to the change of lithology have a significant impact on temperatures.

The geothermal gradient element of Fourier's Law are calculated from drilling data. Temperatures measured-while-drilling ("MWD") or measured at the bottom of



the hole via a Bottom Hole Temperature (“BHT”) tool after drilling is complete are highly disturbed (generally registering as cooler than equilibrium) by the drilling activity itself and require correction. Errors in estimation of both conductivity and expected geothermal gradient prior to drilling can mean deeper drilling is needed, or worse, that you reach the desired temperature in a different formation and with different properties than planned. The fact that if drilling continues, it will eventually hit the desired temperature, does not minimize the need for fundamental geologic and geophysics analysis of a project site. Detailed pre-drill geological studies are still critical to the success of a project.

Thus, while the risk in Next Generation geothermal is reduced compared to Conventional Geothermal Systems and oil and gas, it is not eliminated. Understanding local technical details is a high-skill pursuit, and represents employment opportunities for talent looking to transfer their efforts from oil and gas operations.

As in all other forms of energy and mineral resources, the pursuit of random drilling programs is not a recipe for success. Wells, including geothermal wells of all types, are expensive prospects, typically millions to tens of millions of dollars per well. Before committing to expenditures of that sort, the best possible understanding of the subsurface is needed. While, in general terms, the Earth does get hotter the deeper one drills, the variations are immense. As we will see later in this Chapter, some areas of Texas can probably produce viable geothermal energy from wells a few kilometers deep, while other areas would need a well nearly ten kilometers deep to reach the same temperatures. This variability does not include the local variations driven by the presence of salt domes, faults and fractures, rock and fluid types, and many other complications in drilling to extract heat from the Earth.

This Chapter will provide an up-to-date assessment of Texas’ geothermal potential at the whole-State level down to the regional/basin level and, in some cases, to the county level. We will look at the resource (temperature), as well as the other geologic and geophysical aspects of the various regions of Texas.

IV. Texas Regions

Texas is diverse geologically and geographically (Figures 4.1 and 4.2). It ranges from deep sedimentary basins to basement uplift, and from mountains to coastal plains. The State’s mineral and energy resources are similarly heterogeneous. Texas’ oil and gas development is distinctly zoned in time and space, with areas such as East Texas, the coast, offshore, and the Permian Basin (among others) experiencing one or more periods of intense exploration and production.

In this Chapter, we will divide Texas up into specific regions based on multiple factors. We will then assess the geothermal potential of these regions as the data permits, bearing in mind that some regions have very limited data. Broadly speaking, we break Texas into two types of regions. The first set of regions have abundant oil and gas exploration data, while the second set generally has a much lower density of data available (Figure 4.3). The regions we explore in this Chapter include:

1. Sedimentary basins

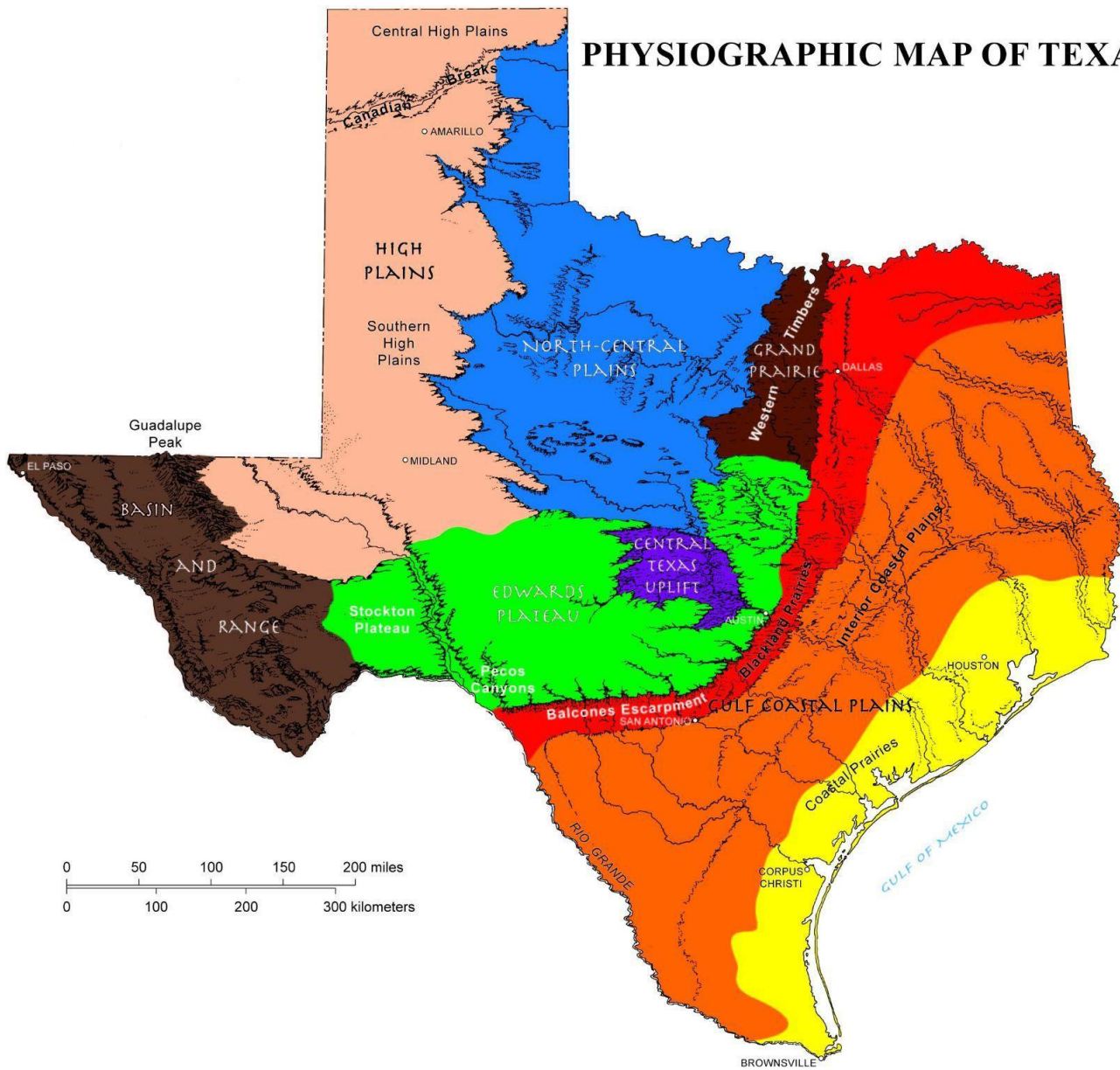
- a. North-Central/Fort Worth Basin
- b. The Gulf Coast/Geopressure Zone
- c. East Texas
- d. West Texas/Permian Basin
- e. Panhandle/Anadarko Basin

2. Other regions

- a. The Llano Uplift
- b. Central Texas/Hill Country
- c. El Paso/The Basin and Range



PHYSIOGRAPHIC MAP OF TEXAS



PROVINCE	MAX. ELEV. (ft)	MIN. ELEV. (ft)	TOPOGRAPHY	GEOLOGIC STRUCTURE	BEDROCK TYPES
Gulf Coastal Plains					
Coastal Prairies	300	0	Nearly flat prairie, <1 ft/mi to Gulf	Nearly flat strata	Deltaic sands and muds
Interior Coastal Plains	800	300	Parallel ridges (questas) and valleys	Beds tilted toward Gulf	Unconsolidated sands and muds
	1000	450	Low rolling terrain	Beds tilted south and east	Chalks and marls
	1250	450	Low stairstep hills west; plains east	Strata dip east	Calcareous east; sandy west
	3000	450	Flat upper surface with box canyons	Beds dip south; normal faulted	Limestones and dolomites
	2000	1200	Steep-walled canyons		Limestones and dolomites
	4200	1700	Mesa-formed terrain; highs to west	Unfaulted, near-horizontal beds	Carbonates and alluvial sediments
	2000	800	Knobby plain; surrounded by questas	Centripetal dips, strongly faulted	Granites; metamorphics; sediments
	3000	900	Low north-south ridges (questas)	West dip; minor faults	Limestones; sandstones; shales
High Plains					
Central	4750	2900	Flat prairies slope east and south	Slight dips east and south	Eolian silts and fine sands
Canadian Breaks	3800	2350	Highly dissected; local solution valleys		
Southern	3800	2200	Flat; many playas; local dune fields		
	8750	1700	North-south mountains and basins	Some complex folding and faulting	Igneous; metamorphics; sediments

Figure 4.1. Texas Physiographic Regions. The Physiographic Regions of Texas encompass a large, sweeping coastal plain in the southern and eastern third of the State, the “Hill Country” and Llano uplift in the center of the State, various plains in the north and north-central area and mountainous basin and range terrain in the far west. These zones correlate closely with geology (Figure 4.2).

Source: Wermund, 1996.



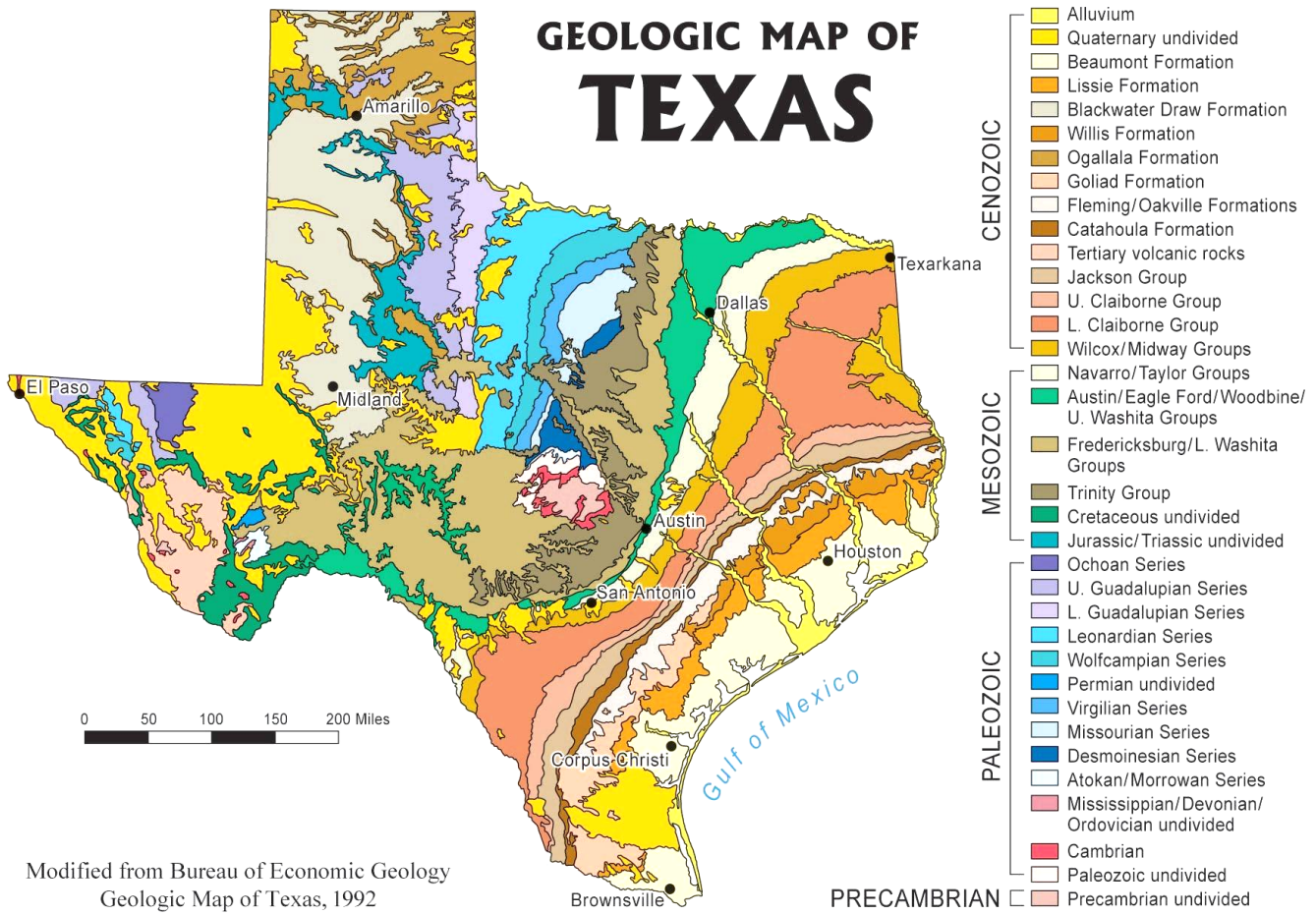


Figure 4.2. Geologic Map of Texas. Similarly varied as the physiographic zones, the geology of Texas ranges from relatively young coastal sediments to “dinosaur age” Cretaceous limestones in central Texas to volcanic and Precambrian igneous formations in west Texas and the Llano area. Source: Hartman & Scranton, 1992.

A. The Foundational Data

This heterogeneity in hydrocarbon resource exploration creates a parallel heterogeneity in the geothermal data available for Texas (Figure 4.3). The data points in Figure 4.3 represent the foundational data on the thermal state of the lithosphere of Texas. Each point is a well that has been logged at some time, usually during or shortly after drilling. In areas with oil and gas production, the density of data points is very high, however as noted above, BHT measurements are generally not at equilibrium conditions. Correspondingly, where there is no petroleum potential, the map is mostly blank. This is not to say that there are no wells in the empty map areas, as there are ubiquitous and relatively shallow water wells. However, wells of this type rarely have useful recorded information and their temperatures, if known, are disturbed by the aquifer flow.

Although this dataset where present is very dense, it is usually not particularly robust and accurate regarding temperatures. This is a concern since the temperature measurement is the sought after information. Other well log data such as porosity and mineralogy are generally much more reliable. The “gold standard” data is an equilibrium temperature of the rocks, measured long after the well is drilled and the disturbance of drilling has passed. However, when a well is drilled, the return to thermal equilibrium takes on the order of months to years. It is not economically viable to let a completed well sit idle for that long to get good temperature data. Therefore, the temperature is typically measured before the drilling-induced temperature disturbance returns to the in-situ equilibrium value. This disturbed value may be up to tens of degrees different from equilibrium. Typically, the temperature is collected in the form of a BHT shown on the strip log of a well and/or recorded as



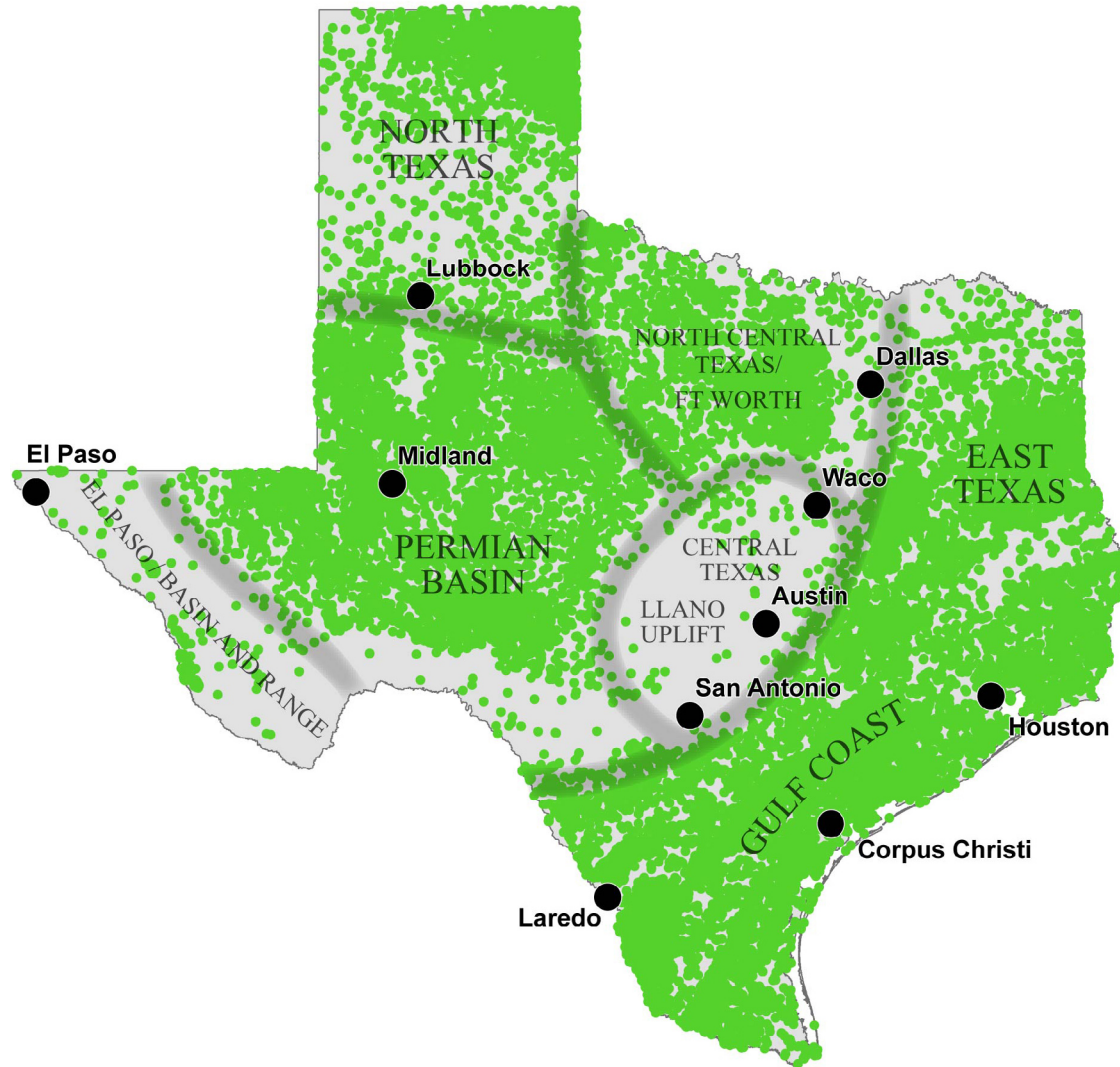


Figure 4.3. The SMU-NGDS (National Geothermal Data System) geothermal dataset for Texas, geothermal.smu.edu. Also shown are the approximate boundaries of the regions discussed in this Chapter. Source: Adapted from Blackwell, et al., 2011a.

a maximum temperature on the well log header. Thus we resort to applying crude corrections to the measured (disturbed) temperature to get an estimate of the equilibrium (undisturbed) temperatures (Schumacher & Moeck, 2020). Undisturbed temperatures are critical to understanding the resource in place. And where it is possible to obtain precision, equilibrium temperature data is valuable in and of itself and as a calibration for the “noisy” BHT data.

A similar problem to the potential for temperature errors exists in the data on rock thermal conductivities. Thermal conductivity, (“k”), is the measurement of how well a rock

conducts heat and, inversely, how well it can act as an insulating “blanket” and thus is also a critical parameter in understanding geothermal potential. These values are rarely experimentally measured. There are rock physics models for estimating k based on the rock composition, such as mineral type and percentage, porosity, and fluid content. As with temperatures, however, k estimates are crude and subject to considerable error (Vasseur, et al., 1995; Vacquier, et al., 1988; Jennings, et al., 2019).

Thermal conductivity is critical for extrapolating temperatures below known points. Assuming that BHT can be corrected to yield the in-situ temperature at the



bottom of a well, can temperatures below that point be accurately estimated? Figure 4.7, the temperature map of Texas at 6.2 mile (10 kilometer) depth, is not a map of measured data - there are no temperatures from that depth. Instead, it is calculated using heat flow, an estimate using the temperature difference (gradient) times the thermal conductivity, detailed stratigraphic columns for assigning k values, depth to the basement (e.g., the thickness of sediments), and radiogenic heat production. All these parameters are part of the temperature-at-depth model (Batir & Richards, 2021; Negraru, et al., 2008).

With greater numbers of data points, the aerial coverage of temperature is improved, but unless the raw BHT's are appropriately corrected, then the end temperatures are only estimates based on wrong inputs - thus, more inaccurate data are not always better. With a greater number of and more accurate thermal conductivity measurements, the details of the temperatures throughout the stratigraphy improve, thereby refining the details at all depths. This is why improving k estimates and BHT corrections are worth a significant investment. The sum total of the errors in temperature and k can add up to be on the order of 25 percent (Batir & Richards, 2020) - a variance that can induce investors and project managers to invest in improving geothermal technology.

Despite the awareness of data concerns discussed above, numbers can be a significant compensating factor. The extraordinary density of data points allows, as we will show later in this Chapter, the aggregation of "noisy" data into a more coherent picture. Thus, we can make relatively well informed assessments of most regions in this Report, though in some regions only at larger scales/lower resolution. Understanding the data limitations is of utmost importance, as it highlights areas for future research, with an eye toward risk reduction, realizing that the thermal picture could change with better data. This provides a focus for specific items of data collection for project success.

B. Future Research

Both BHT and k determination are high priority issues for further research, as they would provide a substantial return on investment in reducing uncertainty in our understanding of the resource. In particular, BHT and k are possible subjects for machine learning approaches

because of the nature of the data available. As is well demonstrated in Batir and Richards (2020), a detailed knowledge of radiogenic heat production throughout the stratigraphic column and into the basement is also a key variable needed in refining temperatures at depth. Note also that a Report such as this one, while a source of information for planning geothermal development, is not sufficient in and of itself for siting a project. The uncertainties and heterogeneities in the data mean that detailed site-specific geologic and geophysical studies are still an essential step in building a geothermal prospect.

V. Texas as a Whole

A. Heat Flow

Heat flow, as used in this Report, is the conductive transfer of heat through the upper crust. When compiling heat flow data, every effort is made to eliminate heat flow data affected by convection (Blackwell, et al., 1990; Richards, et al., 2012). In the Texas case, with no active magma movement in the subsurface, this leaves water movement in the ground, which can swamp the conductive signal even with very slow fluid movement. This is most often caused by shallow groundwater flow, which can mask the deeper conductive heat flow. These disturbances can be readily recognized in good quality data.

In broad terms, the heat flow of Texas can be divided up into a few main areas (see Figure 4.4). A large swath of elevated heat flow exists along the Gulf Coast and broadens out into inland East Texas, with values generally in the 65 to 85 milliwatts per square meter range. A broad area of low to moderate heat flow (about 30 to 60 milliwatts per square meter) runs from central Texas up through the panhandle. The highest heat flows are confined to far western Texas along the Rio Grande, and in the El Paso area. This zone has the highest heat flows in Texas, exceeding 90 milliwatts per square meter, and represents the eastern end of the Basin and Range province of the western United States, a well-known rich conventional geothermal producing region outside of Texas.



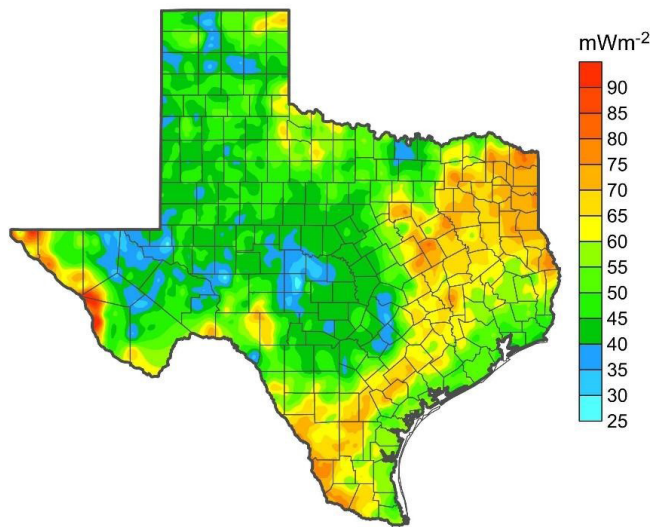


Figure 4.4. This heat flow map generally presents the best estimate of the average shallow crustal conductive heat flow (the heat continually flowing from the hot core to the surface of the Earth).
 Source: SMU Geothermal Laboratory Texas Heat Flow Map (Blackwell, et al., 2011a).

B. Temperature at Depth

Estimated temperatures at various depths below the surface in Texas are shown in Figures 4.5 through 4.8. Besides obviously becoming hotter with depth, the general temperature patterns follow that of the heat flow map. This pattern is to be expected, since heat flow is directly proportional to thermal gradient via the thermal conductivity. As the individual regions will be discussed in detail below, one main point that will be highlighted; in terms of temperature, the Gulf Coast and East Texas are largely comparable to the Permian Basin section of Texas. The Permian Basin is part of the Basin and Range physiographic province that stretches from Oregon to central Mexico. The Basin and Range physiographic province has high heat flow and temperatures due to extensional thinning of the crust. The high temperatures along the coast and in East Texas are due to multiple factors, including the low thermal conductivity of the sediments, which act as a “blanket” to contain the heat. For the same reason, parts of the Fort Worth basin of North Texas also show up as distinct areas of elevated temperatures.

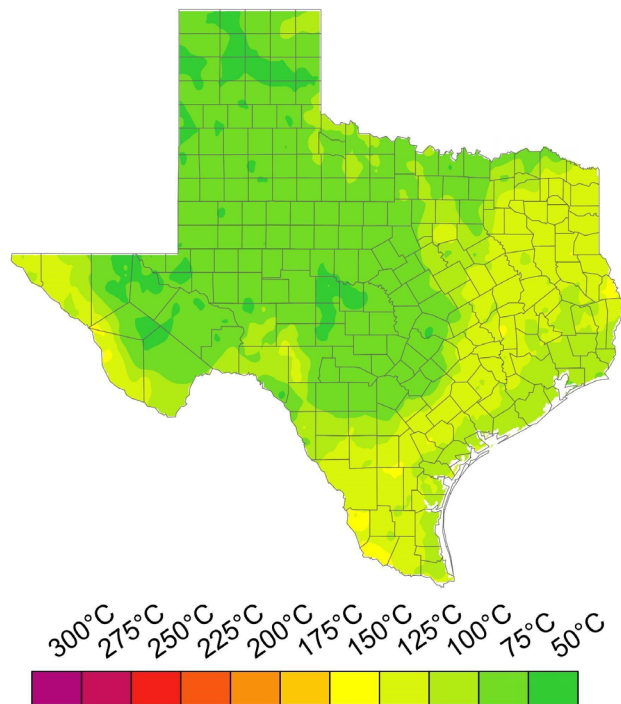


Figure 4.5. This represents a cut through Texas at a depth that is reasonably accessible and useful for direct-use applications. At this depth, temperatures in some regions are getting into the range at which a modern binary geothermal plant can effectively operate (around 125-150 °C or 257-302 °F). Also, a general trend of higher temperatures along the coast from South Texas into East Texas and the far west is emerging at this depth. Source: SMU Geothermal Laboratory Texas Heat Flow Map (Blackwell, et al., 2011b).

Also, when looking at the deeper temperatures, Texas’ relatively low heat flow areas still get reasonably hot (greater than 125 °C, or 257 °F) by four miles in depth (6.5 kilometers). As power conversion technology continues to advance and drilling costs decrease, these regions will rapidly become more economically viable for geothermal development. These areas are beginning to attract interest and funding, but more is still to be done to prove the viability of these lower-grade resources for development. Thus, in an over simplified, first order reconnaissance, East Texas and the Gulf Coast plus the Permian Basin are Texas’ most attractive geothermal resource areas.



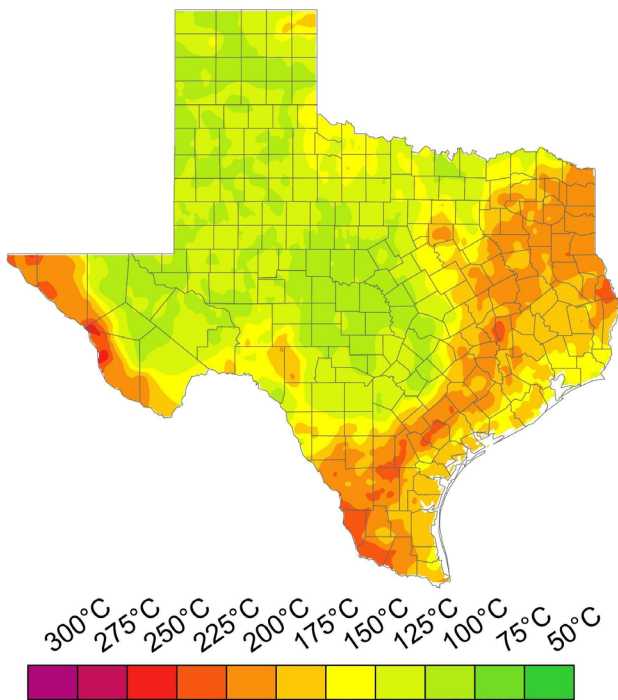


Figure 4.6. Most of the oil and gas drilling is shallower than this depth, and therefore, the temperatures represent primarily calculated values, tuned to fit the rare well penetrations drilled to this depth. As mapped, much of the State is at or near conventional minimum viable temperatures for geothermal power generation. Source: SMU Geothermal Laboratory Temperature Map at 6.5 kilometers (21,320 feet) Depth. (Blackwell, et al., 2011b).

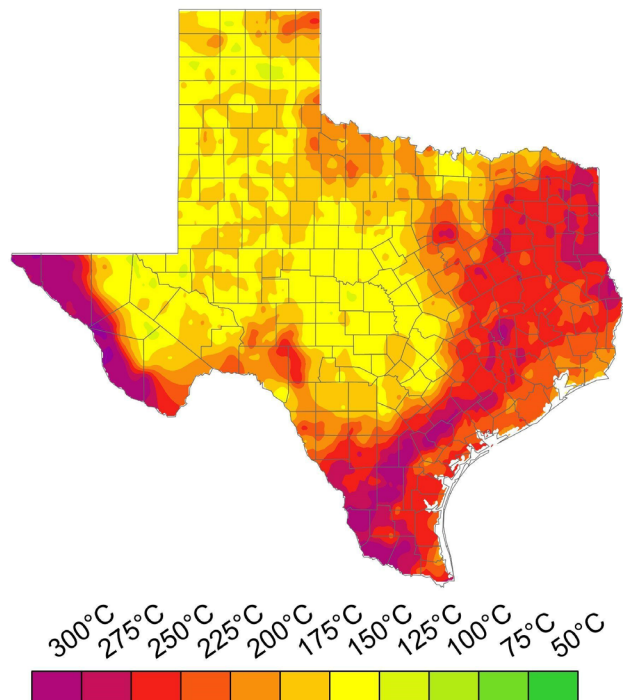


Figure 4.7. Rarely do the oil and gas industry drill to these depths outside the Permian Basin, but drillers do have the capability. Temperatures at this depth are all calculated, not measured. This depth is at the deep end of reasonably envisioned geothermal drilling. At this depth, the entire State is at temperatures that could economically generate power if brought to the surface. Source: SMU Geothermal Laboratory Temperature Map at 10.0 kilometers (32,808 ft) Depth (Blackwell, et al., 2011b).

C. Heat Flow Versus Heat Content:

A brief explanation of heat flow, heat content, and temperature-at-depth are helpful at this point. The Earth's core is approximately 6,000 °C (10,800 °F). The surface of the Earth has an average temperature of approximately 15 °C (59 °F). The core-to-surface temperature gradient creates a heat flow outward through the surface of the Earth of approximately 90 milliwatts per square meter. Integrating this heat flow over the entire Earth surface yields an estimate of total heat flow of about 47 terawatts thermal that is continually flowing past us into space (Davies & Davies, 2010). Such heat flow yields a lot of energy, if it can be tapped. This is because rock is a thermal "sink" or "battery." Also, note that converting thermal energy into electricity is less than 100 percent efficient.

For example, at the temperatures in the Gulf Coast geopressure region available subsurface at about 2.2 miles (3.5 kilometers), the thermal-to-electrical conversion efficiency is only about 5 percent with current technology.

VI. North - Central Texas

The historical record reports flowing geysers in many north-central Texas communities. Waco was known as the "City of Geysers," and the town of Mineral Springs built multiple hotels around their springs. Geothermal hot water was used to preheat the boiler for the community hospital in Marlin (Woodruff & McBride, 1979). The water table in the past was closer to the surface, allowing the heated water to flow along breaks and faults in the rocks to reach the surface.



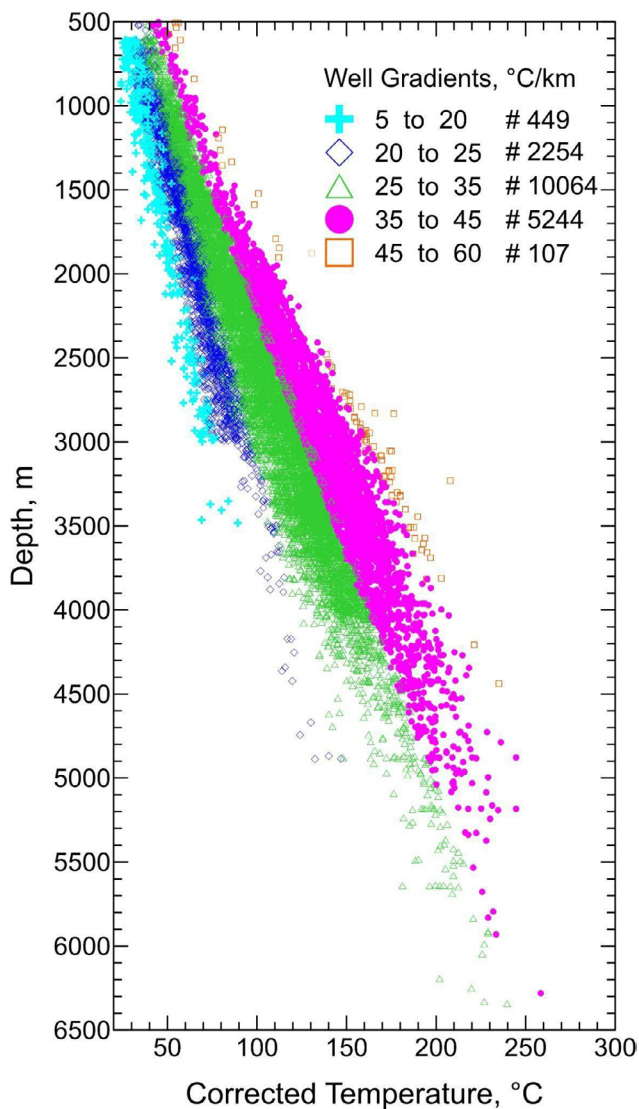


Figure 4.8. The well temperatures plotted are corrected using the SMU-Harrison Correction method. Well-site gradients (depth - surface) are subdivided to depict geothermal gradients of 'high' (35 to 60 °C per kilometer), 'normal' (25 to 35 °C per kilometer), and 'low' (5 to 25 °C per kilometer). In the legend, the number of site values for each gradient interval are shown after the interval, with the gradients from 25 - 35 °C per kilometer being the most common with a count of over 10,000 wells. High gradients deeper than three kilometers are of most interest as a geothermal resource. Source: *The SMU-NGDS Data of Texas Wells Corrected Bottom-Hole Temperatures and Blackwell, et al., 2011a:b.*

Evaluation and research of the regional thermal regime focused initially on the Balcones, Luling, Mexia, and Talco fault zones, and on Cretaceous aquifers located in North and Central Texas (Woodruff & McBride, 1979). These faults roughly follow the edge of the Llano granitic exposure in Central Texas, then arch up towards Dallas before running east into northeast Texas (Figure 4.1).

On the other side of the buried Ouachita Overthrust Belt from East Texas is the North Texas region (Negraru et al., 2008). This stratigraphic and structural change in the geology is the cause for a decrease in heat flow in North Texas compared to East Texas. The current thermal data suggest the basement rock beneath the Fort Worth Basin is Precambrian granite, similar to the Llano Uplift observed at the surface in central Texas (Figure 4.9). The gas-producing zones in the Barnett formation are associated with local thermal anomalies from multiple paleotectonic events that brought heat into the zone, one of them possibly from the Ouachita Thrust Fault (Negraru, et al., 2008).

The geothermal resources for North - Central Texas are considered low to moderate, as the thermal gradients are rarely over 35 °C per kilometer, with most well gradients between 20 °C and 30 °C per kilometer (Figure 4.10). The wells drilled deeper than 2.2 miles (three kilometers) are scattered, with only three more than 13,120 feet (4,000 meters). These deeper wells are of most interest to review for their temperature at the bottom of the hole, especially if they have been shut-in for months to years and have achieved an equilibrium temperature. The deepest wells are the Ellenburger injection wells, reported to inject at rates from 1,500 barrels of water per month (240 cubic meters per month) up to 100 times that rate (Frohlich, 2012). The injected fluids are at surface air temperatures, thus considered a cold water for the formation. The thermal impact of this much fluid injected over a decade into the Ellenburger Formation has not been mapped, and is thus a target for further research.

A. Detailed Review of Barnett Shale Play: Hood, Johnson, Parker, and Tarrant Counties

The Barnett Shale play provides a significant quantity of new oil and gas well data from the past 20 years. In this Section, we examine the thermal data for Hood, Johnson, Parker, and Tarrant Counties. The entire play includes Jack, Wise, and Denton counties, all on the northern edge of the play (Figure 4.10). Although many oil



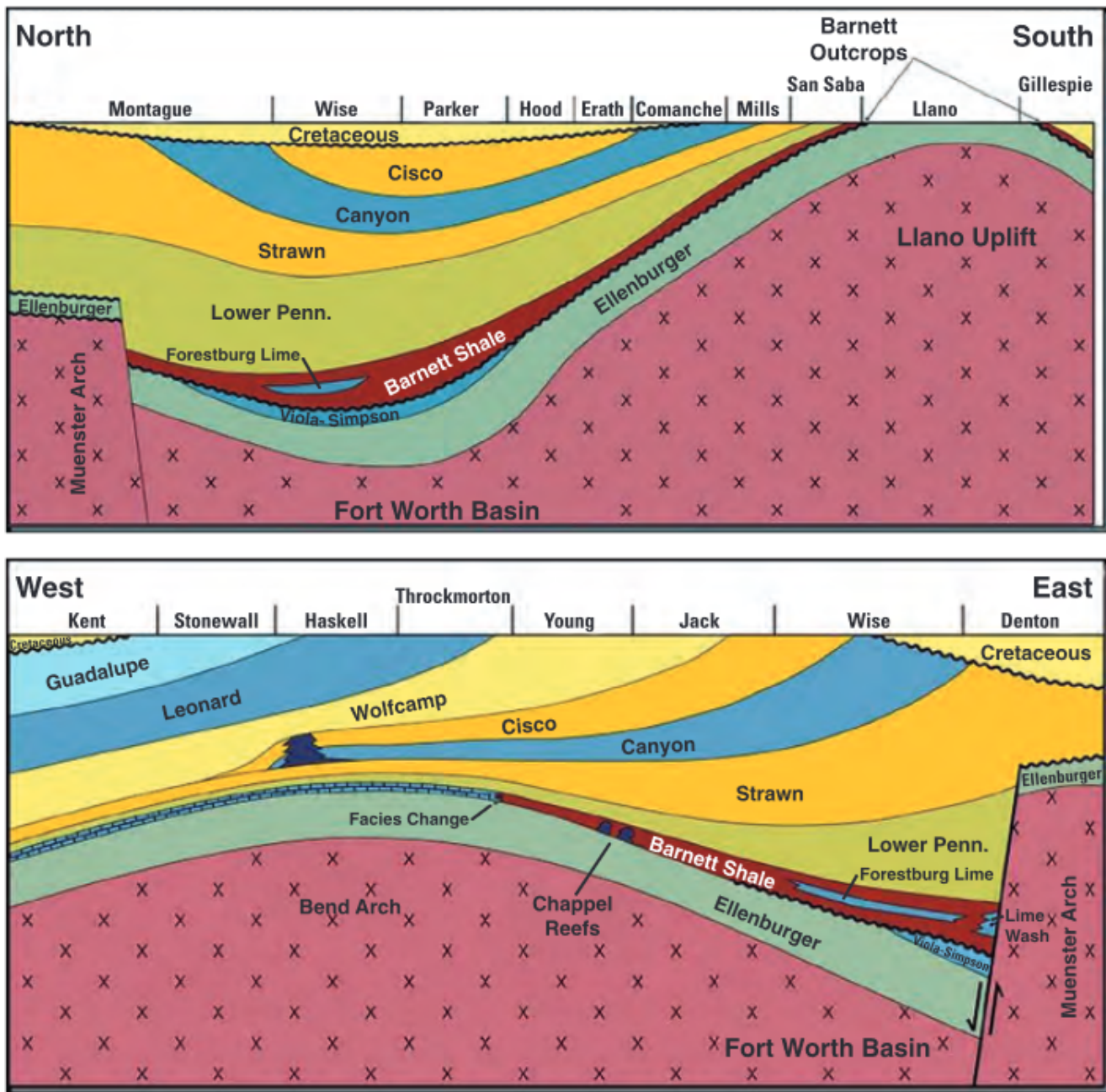


Figure 4.9. Fort Worth Basin stratigraphy across North Central Texas. County names are listed at the top of the sections for reference. *Source: Burner & Smosna, 2011.*

and gas wells are drilled in Jack and Wise counties, the related well log headers have not had the temperature extracted from them yet to use in a geothermal resource calculation. The available BHT data within the National Geothermal Data System are corrected for drilling impact using the Southern Methodist University (“SMU”) Harrison Correction (Blackwell, et al., 2011b; Richards & Blackwell, 2012; Blackwell, et al., 2010). These temperatures and related thermal gradients are plotted in Figures 4.11 and 4.12.

These well locations are a small subset of the drilled wells. Most of the wells are drilled into the Barnett Shale for production, and the Ellenburger Formation below it for injection. The Ellenburger Formation is part of a carbonate system with a high porosity and permeability karst structure. As shown in the temperature-depth plot (Figure 4.11), the general trend of maximum temperatures is within the 100 to 150 °C (212 to 300 °F) range at the depths currently drilled. There are higher thermal gradients (35 to 60 °C per kilometer), especially in Johnson County.



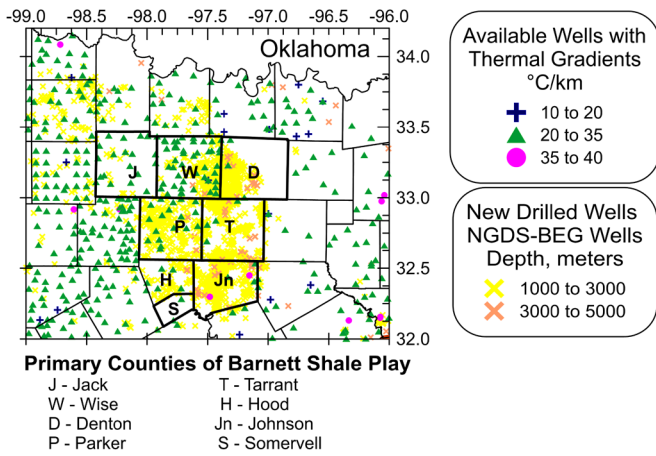


Figure 4.10. Map of North - Central Well Locations. Existing wells used in previous maps are shown as “thermal gradients,” and new additional data shown as “NGDS-BEG well depths.” The thermal gradient wells were used to map the 2011 Heat Flow map and Temperature-at-Depth maps (Figures 4.5 through 4.7). Additional wells with temperature data have been provided by BEG, plotted by their depths, will be included in future resource assessments. These newer wells are primarily from the Barnett Shale Play and show a significant increase in data density in the area. Source: *Future of Geothermal Energy in Texas, 2023*.

As this is only an initial review of the data, these higher values need to be examined for geological reasoning behind the higher gradients. They may represent zones of fluid movement, or correlate to higher oil and gas thermal maturation.

One area of concern for using the Barnett Shale play as a geothermal resource is the potential of induced seismicity. In Barnett Shale play, induced seismicity related to oil and gas operations is linked to injected water causing reactivation of deep faults (Hornbach, et al., 2015) below the Ellenburger formation. The injection of the produced fluids in a large well for an extended time changes the stress dynamics and can lead to induced seismicity. There is now a network of seismometers across Texas, run by TexNet of the University of Texas at Austin’s Bureau of Economic Geology, to improve the monitoring and understanding of this phenomenon (TexNet, 2022). This concern is offset, however, by the technological developments of the geothermal anywhere movement. These approaches use much less or no fracking fluids, nor do they inject spent fluids back into the subsurface, thereby reducing the risk of induced seismicity.

B. Detailed Review of Dallas County

Dallas is not considered a place for deep well drilling because the Ouachita overthrust brought basement rocks closer to the surface than in counties to the east and west of Dallas (Woodruff, et al., 1984). Dallas County does have high flow groundwater aquifers, flowing through three cretaceous sandstone aquifers: the Hosston/Trinity, the Paluxy, and the Woodbine Sandstone. In the 1980s, there was an assessment of geothermal resources across Texas, and in eastern Dallas County groundwater from wells drilled into the Trinity formation were measured to be more than 54 °C (130 °F) (Woodruff et al., 1984). Today temperatures of approximately 54 °C represent an opportunity to use the geothermal resources for Direct Use applications.

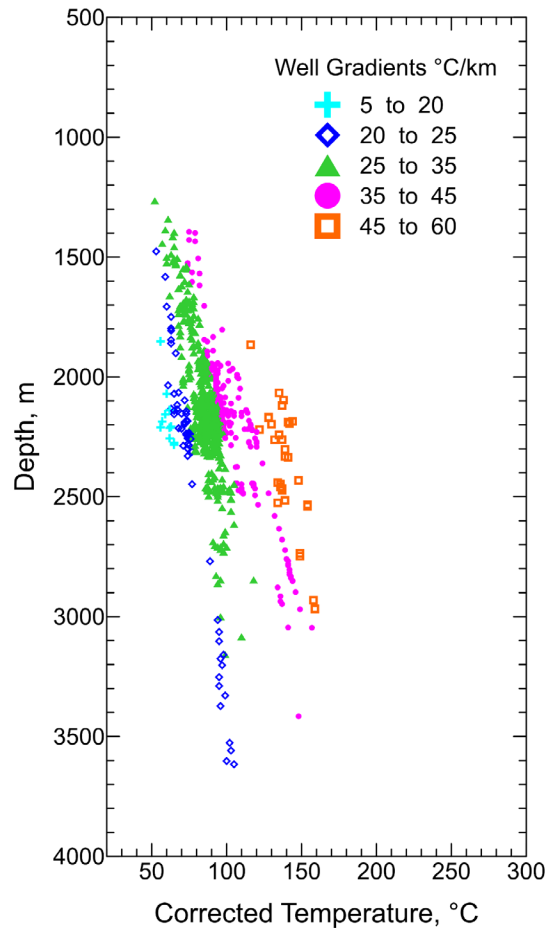


Figure 4.11. Corrected well temperatures and gradients for the Barnett Shale play. The well sites are plotted for comparison to values plotted in Figure 4.10. Source: *Future of Geothermal Energy in Texas, 2023*.



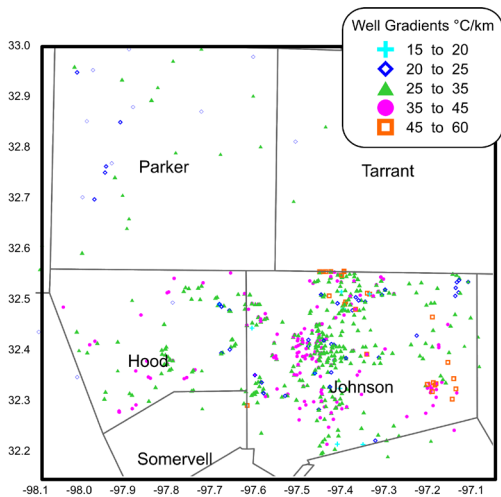


Figure 4.12. Well temperatures and gradients for the southwestern Barnett Shale counties. The locations correspond to the data in Figure 4.11. Source: *Future of Geothermal Energy in Texas, 2023.*

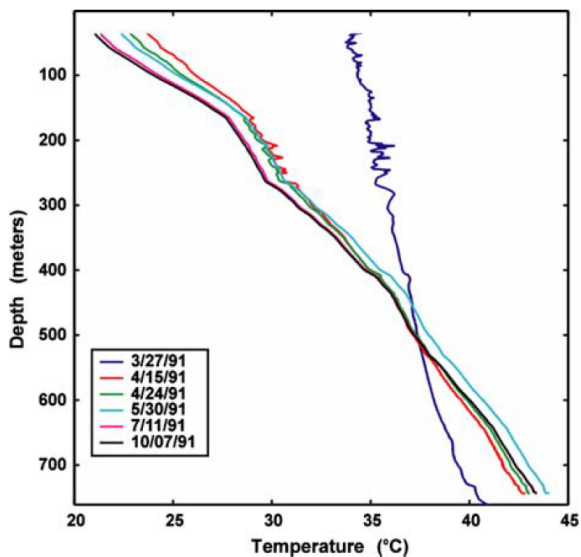


Figure 4.13. Temperature Measurement Series for Mobil New Exploration Ventures (“MNEV”) Well. The well is located in Farmer’s Branch and represents the typical drilling influence of drilling muds on well temperatures measured after drilling. The temperature changed from too cold at depth to warmer temperatures as the impact of the drilling fluids subsided over seven months to reach equilibrium with the surrounding formations. Source: *Negraru et al., 2008.*

Only one oil and gas well has been drilled in Dallas County: the Mobil New Exploration Ventures (“MNEV”) well. It is located on the property of the Mobil Research campus in Farmer’s Branch, on the north side of Dallas County. Mobil worked with the SMU Geothermal Laboratory to collect temperature logs over seven months at intervals along the borehole length (Negraru, et al., 2008) (Figure 4.13). The results highlight that wells recently drilled contain temperatures hotter than equilibrium at the surface, yet colder at the bottom than a BHT would record. Seven months later, the final temperature log shows the well reached a thermal equilibrium within the surrounding formations with a cooled surface value and a hotter temperature at depth. Well temperatures return to equilibrium temperatures at a rate based on the type of mineralogy, permeability, amount and type of mud, and the surface and/or drill head temperatures.

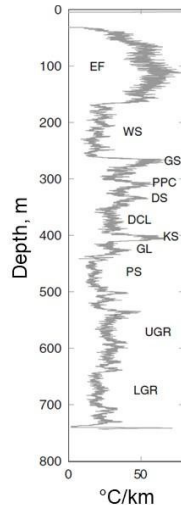
As part of the research for the MNEV well, thermal conductivity values were measured (Table 4.1) (Negraru, et al., 2008). The Eagle Ford Shale is located at the top of the stratigraphic column at this location in Dallas County. These measurements are unique in that they were analyzed shortly after being brought to the surface. Typically, a shale sample dries out before analysis, and the anisotropy of the clay particles causes thermal values to be too high (Negraru, et al., 2008; Blackwell, et al., 1990). This is not the best-case scenario, because the deeper sediments will have higher thermal conductance because of decreased porosity and increased mineral aging (Pribnow & Sass, 1995). Thus, further work and research with regard to actual k values will be helpful for refining the geothermal resource of a location.

As part of the research completed on geothermal resources, the SMU Geothermal Laboratory focused for more than 40 years on collecting temperatures in wells that are at equilibrium with the surrounding geological setting, similar to the MNEV well. This focus on temperature measurements with high precision logging probes is the foundation of a database of well measurements included in the SMU Node of the National Geothermal Data System (“NGDS”). Wells such as these are essential tools in determining the accuracy of a collection of raw BHT data, and the type of temperature correction to use on them.



Table 4.1. Measured Thermal Conductivities (k) for the MNEV Well. Geological formations listed in the Table correspond to their temperature gradients plotted to the right. Eagle Ford Shale, etc. Note the strong and relatively consistent correlation of k with lithology, such that shales are low (1.0 to 1.5 watts per meter Kelvin), limestones are approximately 2.0 watts per meter Kelvin, and the sand - sandstone formations are the highest with values of over 3 watts per meter Kelvin. Source: adapted after Negraruet et al., 2008.

Formation	Calculated average thermal conductivity ($Wm^{-1} K^{-1}$)
Eagle Ford Shale	1.13
Woodbine Sand	2.95
Grayson Shale	1.37
Main Street Limestone	2.05
Paw Paw Clay	1.25
Weno Formation	1.72
Denton Shale	1.58
Duck Creek Limestone	1.99
Kiamichi Shale	1.06
Goodland Limestone	2.10
Paluxy Sandstone	3.42
Glenrose Formation	2.05



The ability to collect equilibrium temperatures is rare. To do so means a well is shut-in for months to years. As geothermal research uses well temperatures, the full borehole equilibrium temperature logs help calibrate other raw BHT temperatures nearby, or within the same geological setting. Correcting for all the possible parameters is complex (Jordan, et al., 2016), and instead, a common practice is to apply a uniform correction across the entire well data set (Richards, et al., 2012). The temperature data within the NGDS on the SMU Node follows the SMU-Harrison Correction method (Blackwell, et al., 2011b; Richards & Blackwell 2012).

VII. I-35 Corridor and North East Texas

A review of the possible geothermal resources was the focus of a Texas State Energy Conservation Office grant to the SMU Geothermal Laboratory (Blackwell, et al., 2010). This assessment focused on well temperatures at different depths to determine where geothermal resource potential existed. The findings were limited in the North Texas area because BHT data were unavailable from the Barnett Shale Play. Still, the results represent the general

trend of North Texas having cooler geothermal resources at the same depths as those in East Texas and the Gulf Coastal region (Figure 4.14).

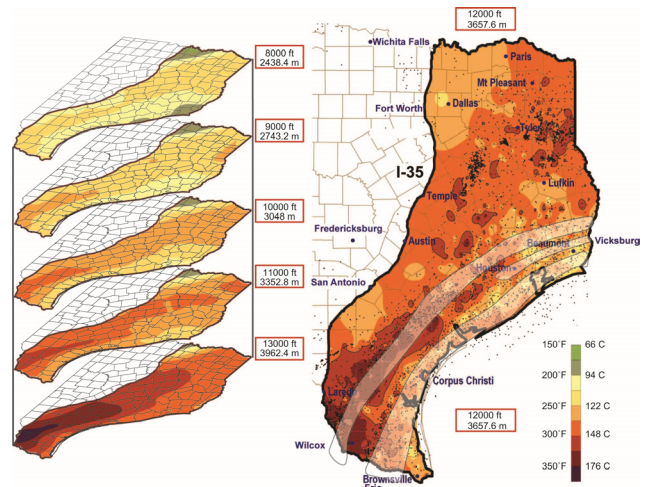


Figure 4.14. On the left are Isotherm maps for North and East Texas at six depths between 8,000 and 13,000 feet (2,440 and 3,963 meters), based on well data. Marked on the 12,000 feet isotherm map (on the right) are the Wilcox, Vicksburg, and Frio formation focused oil & gas regions. Source: SMU Geothermal Laboratory maps with overlays by Weijermars, et al., 2018.

VIII. The Texas Gulf Coast

The Gulf Coast Region, located in Texas and Louisiana, is approximately 750 miles (1,200 kilometers) long and 100 miles (160 kilometers) wide onshore (Wallace, et al., 1978; Davis, et al., 1981). Figures 4.15 and 4.16 show the location of the Gulf Coast and generalized stratigraphy. The geology of the Gulf Coast area is complex due to the cyclical deposition of prograding deltaic sedimentary facies during the Paleogene and Neogene (Tertiary). During this time, the uplift of the Rocky Mountains during the Laramide Orogeny provided an enormous sedimentary influx deposited on the continental shelf in the form of wedges that thicken and dip toward the gulf. This rapid deposition caused the growth of syndepositional normal fault systems parallel to the coastline by the movements of deep units and the collapse of shallow deposits (Ewing & Salvador, 1991). The development of growth faults resulted in the landward thickening of sand packages inside each fault compartment, like a prism. As a result, porous sandstone reservoirs were displaced downward



and came in contact with impermeable shale across the fault. This developed the clastic reservoirs in the Gulf Coast (Figure 4.15).

The Gulf Coast region has the highest overpressure and geothermal temperature gradient in sedimentary basins in Texas. The U.S. Geological Survey (Burke, et al., 2012) published the regional extent of the overpressure in the Gulf of Mexico, including the onshore coast. Sediments and fluids in an “overpressure” situation are at a higher than expected pressure than if the sediments had been deposited and buried slowly. Instead, the sediments are buried quickly and are not allowed to accommodate and dewater as normal, leading to a situation where the fluids will vigorously flow to the surface without pumping if a well is drilled into them - ‘gushers’ to use oil and gas vernacular.

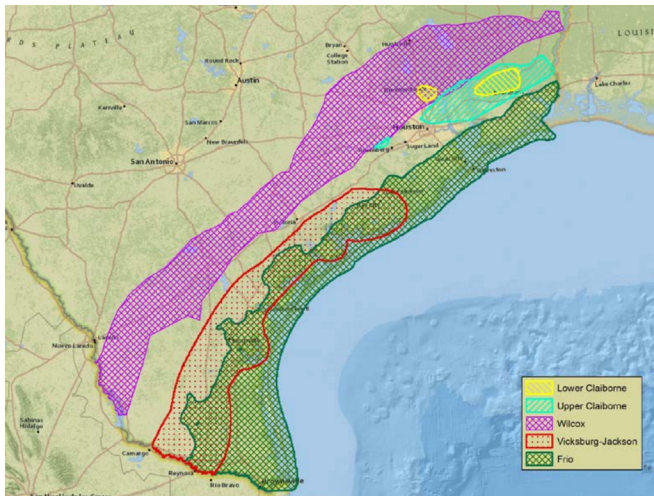


Figure 4.15. The geologic trends of potential geothermal reservoirs in the Gulf Coast, Texas. Source: Esposito and Augustine, 2012.

These high overpressure and high geothermal gradients develop in the Gulf Coast due to many geologic processes and products over time, such as high sedimentation rate, sandstone, and clay diagenesis (smectite-to-illite), salt diapirs, and migration of pore fluid through faults (Nagihara and Smith, 2008; Christie, 2014). Salt diapirs can impact the 3-D thermal picture of a target due to salt’s relatively high thermal conductivity. Disequilibrium compaction is another potential factor, but it is temperature-independent and can occur at any depth as long as the pressurized zone has not been breached through faults and fractures.

PERIOD	EPOCH	AGE	GROUP OR FORMATION	
QUAT.	HOL.			
	REL.	Calabrian	Undifferentiated	
TERTIARY	NEOGENE	PLIOCENE	Piacenzian Zanclean	Undifferentiated
		MIOCENE	Messinian Tortonian Serravallian Langhian Burdigalian Aquitanian	Fleming Fm.
	PALEOGENE	OLIGOCENE	Chattian	Anahuac Fm. Catahoula Fm. Frio Fm.
			Rupelian	Vicksburg
		EOCENE	Priabonian Bartonian Lutetian Ypresian	Jackson Claiborne Gp. Wilcox
			PALEO.	Thanetian Selandian Danian
	CRETACEOUS	UPPER	Maastrichtian	Navarro (Dimos Fm. / Escondido Fm.)
			Campanian	Taylor Gp. (Anacacho Ls. / San Miguel Fm. / Ozan Fm. / Annona Chalk)
			Santonian Coniacian	Austin Gp. / Tokio Fm. / Eutaw Fm.
			Turonian Cenomanian	Eagle Ford Woodbine/ Tuscaloosa Washita Gp. (Buda Limestone) Fredericksburg Gp. (Edwards Ls. / Paluxy) Glen Rose (Rodessa Fm.)
LOWER		Aptian	Pearsall Fm. – James Ls.	
			Sligo Fm.	
		Barremian Hauterivian	Hosston Fm. (Travis Peak Fm.)	
		Valanginian Berriasian	Cotton Valley	
JURASSIC		UPPER	Tithonian	Bossier Fm.
			Kimmeridgian	Haynesville Fm. / Gilmer Ls. Smackover Fm. Norphlet Fm.
	Oxfordian			
	MID	Callovian Bathonian	Louann Salt Werner Fm.	
		L	Hettangian	
TRIA.	UP.	Rhaetian Norian Carnian	Eagle Mills Fm.	

Figure 4.16. Generalized Stratigraphy of the Gulf Coast region. Source: Adapted from Swanson, et al., 2013.



McKenna (1997) suggests that hot fluids expelled from overpressured sediments and migrating upward through faults cause high heat flow anomalies along the Wilcox fault zone in the Texas coastal plain (Figure 4.17). In contrast, the Frio Fault zone (Figures 4.17 and 4.18) has no thermal anomalies. Further work will be needed to understand the reasons behind thermal anomalies across various fault zones in the Gulf Coast. The contribution from radiogenic heat varies, depending on the sediment thickness in the Gulf Coast (Christie, 2014; Nagihara, et al., 1996). Very few studies have been published to understand the relation between overpressure and high geothermal gradient in the Gulf Coast, and to decouple them (Cornelius & Emmet, 2020). In several areas, the geopressure gradient is more than 0.7 pounds per square inch per foot (also known as hard overpressure), corresponding to greater than 7,500 feet (2,286 meters) depth along the coast. Inland, the geopressured gradient decreases.

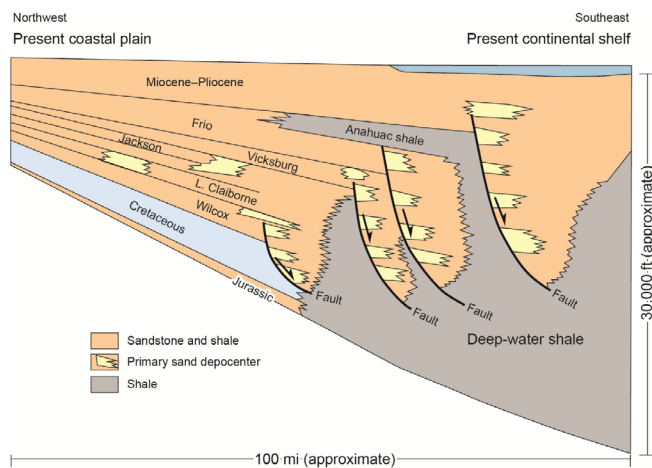


Figure 4.17. Schematic cross-section through the central area of the Texas Gulf Coast. Source: Adapted from Land and Fisher, 1987.

A. Potential Gulf Coast Geothermal Reservoirs and Reservoir Properties

Based on the publicly available pressure, temperature, porosity, permeability, and salinity data, a few formations (Frio, Wilcox, and Edward Group) could be potential conventional geothermal reservoirs. These formations are of particular interest due to several attributes, including overpressure, high geothermal gradient, relatively high water production, and extensive oil and gas industry experience.

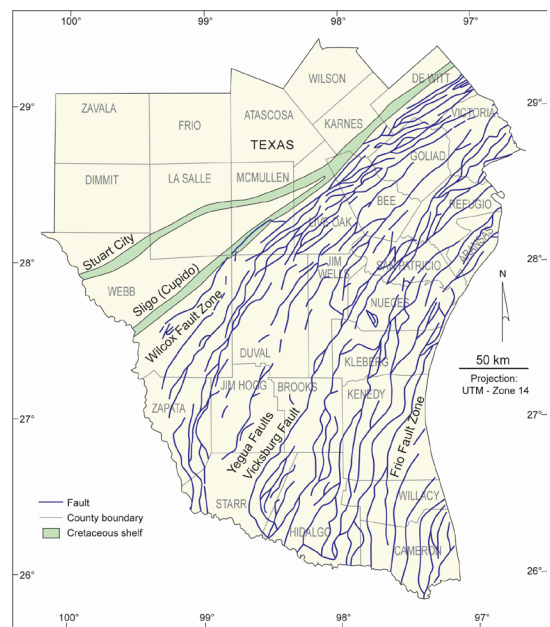


Figure 4.18. Spatial location of major fault zones (Wilcox, Vicksburg, and Frio fault zones) in the Gulf Coast, Texas. Source: McKenna, 1997.

1. Frio Formation

The Frio Formation is a major hydrocarbon producer from the Paleogene in the Gulf of Mexico. It is composed of a sequence of deltaic and marginal-marine sandstones and shales. In terms of structural elements, the Frio Formation is defined by a series of salt diapirs and associated faulting, growth faults, and associated shale ridges (Bruce, 1973; Galloway, et al., 1982; Swanson, et al., 2013). These elements can be a potential conduit of heat from the deep subsurface. In addition, the development of growth faults due to rapid sedimentation helps develop potential clastic reservoir wedges. Such reservoirs are thicker toward the fault and thinner away from the fault. However, some of the faults are very shallow and may contribute instead to heat loss.

Most Frio sandstones are lithic arkoses and feldspathic litharenites (Land, 1984). Litharenites or lithic arenites are types of sandstones with a large fraction of rock fragments greater than five percent. Compositional variation controls the reservoir quality of the Frio sandstones. The reservoir quality of Frio sandstone varies regionally and with depth due to a combination of changes in rock composition, degree of diagenesis, and geothermal gradient. Loucks, et al., (1984) reported good to excellent reservoir quality in the Frio sandstones in the upper and middle Texas Gulf Coast. The permeability is



as high as 1,000 millidarcy in this area (1 millidarcy is 10–16 square meters). Based on data from NRG (2006) and Nehring (1992), the average porosity of Frio sandstone reservoirs, excluding the Hackberry trend in southwest Louisiana, is 27 percent, and the average permeability is 685 millidarcy.

In contrast, the reservoir quality is poor in the lower Texas Gulf Coast. Permeability measured in sandstone cores deeper than 2.5 miles (four kilometers) in the Lower Texas Gulf Coast averages one to two millidarcy. Secondary porosity in the Frio sandstones is volumetrically significant (Loucks, et al., 1979). Lindquist (1976; 1977) concluded that most deep Frio reservoirs are cemented with late-forming kaolinite, Fe-rich calcite, and dolomite. This cement would result in poor heat production due to internal fluid flow barriers, which cannot be fractured effectively due to the presence of kaolinite. In contrast, permeability in deep sandstones in the Upper Texas Gulf Coast ranges up to hundreds of millidarcies. This higher permeability is interpreted as the result of the less well developed late carbonate cementation stage. According to Hovorka, et al. (2001) and other studies, the formation water salinity in the Frio is around 100,000 parts per million (Macpherson, 1992; Kreitler, et al., 1990), potentially causing the formation of mineral scaling and corrosion of pipes if formation fluids are produced in a geothermal system.

2. Wilcox Formation

The Paleogene-aged Wilcox Group extends across the entire Texas Gulf Coast. The formation is composed of a wedge of sandstone and shale that thickens and dips toward the coast. The Wilcox has been interpreted to be primarily deposited in a deltaic setting (Endicott, 1995; Fisher, et al., 1969; Lofton & Adams, 1971; Womack, 1971; Edwards, 1981; Dutton & Loucks, 2010). The Wilcox is divided into three parts. The first two are the sandstone-rich upper and lower sections, which represent two major progradational cycles, and the third is the shale-rich middle section, which in part represents a major transgression.

The quality of the Wilcox sandstones varies spatially and with depth. Porosity and permeability of the Wilcox sandstone vary between 5 and 25 percent and 0.01 to 100 millidarcy; however, there are sections where higher porosity and permeability are present. Dutton and Loucks (2010) studied the impact of temperature dependent

burial diagenesis on porosity and permeability of the Wilcox sandstones in onshore wells. Primary porosity and permeability are reduced as temperature increases, while the secondary porosity remains unchanged. These sandstones show progressive porosity and permeability reduction from an average of 33 percent at 38 °C (100 °F) to 12 percent at 132 °C (270 °F), with minor loss beyond that due to burial and compaction (Figure 4.19). Bebout, et al. (1982) mention the variation of formation temperature within the Wilcox relative to dip, the lithology, the location of growth faults, and the location along the Gulf Coast. Formation water salinity increases with depth in the hydro pressured zone, and it varies in the overpressure zone between 20,000 to 100,000 parts per million (Bebout, et al., 1981).

The geothermal gradient in the Wilcox is 2.1 to 3.1 °F per 100 feet (38 to 57 °C per kilometer). A previous study (Blackwell et al., 2010) found the temperature range of the formation to be 88 °C and 205 °C (190 °F and 400 °F). Such temperatures, coupled with the near lithostatic geopressure and high permeability and porosity, point to moderate potential for geothermal development.

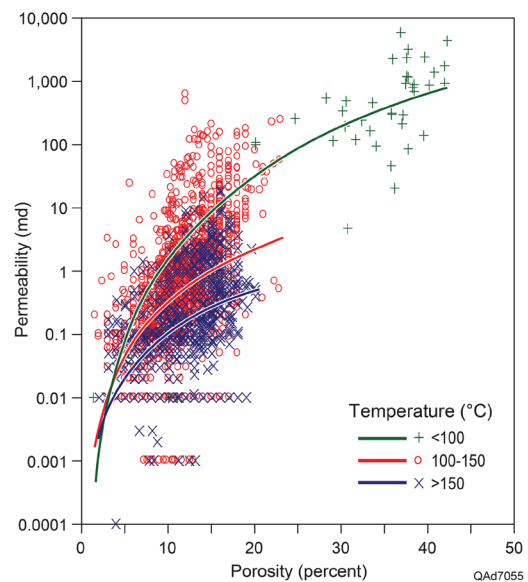


Figure 4.19: Different trends of porosity-permeability in the Wilcox sandstones at different temperatures. Source: Adapted from Dutton and Loucks, 2010. Reprinted from *Marine and Petroleum Geology*, 27, 1, Dutton and Loucks, *Diagenetic controls on evolution of porosity and permeability in lower Tertiary Wilcox sandstones from shallow to ultradeep (200–6700m) burial, Gulf of Mexico Basin, U.S.A., 69–81, Copyright (2010), with permission from Elsevier.*



3. Edwards Group

The deeper Cretaceous-aged Edwards Group, near the Stuart City Reef, is another potential geothermal reservoir often overlooked in most published studies. The Edwards Group was deposited in shallow-marine environments and underwent normal early diagenesis, forming dolomites and micrites at places (Longman & Mensch, 1978). The Stuart City Reef is divided into two portions: Lower Edwards (“B”), which is interpreted to be a barrier-type reef margin, and upper Edwards (“A”), which is primarily bioherms (Waite, 2009). The average porosity and permeability of the Edward Group are 14 percent and 41 millidarcy. The Edward Group contains fractures and vugs, which enhance its pore volume and fluid flow.

4. Smackover/Norphlet Formation

The Jurassic-aged Norphlet and Smackover formations in South Texas pinch out in the deep subsurface against subjacent Paleozoic rocks of the Ouachita Fold Belt. There has been limited mapping of these formations due to limited available geophysical log data. Although the primary depocenter of the Norphlet Formation (based on available data) is in Alabama and Mississippi, it is known to be present in Texas. It is overlain by Smackover Formation and underlain by Louann Salt. The Norphlet is dominated by alluvial-fan, wadi-, playa-, and eolian deposits (Budd, 1981). The depositional environment initially controls porosity and permeability. Aeolian deposits have the best porosity and permeability values. Diagenetic processes modify the porosity of the Norphlet Formation. Quartz cementation above 200 °F (93 °C) reduced porosity. Chlorite grain coating at places preserved the porosity of the Norphlet formation (Dixon, et al., 1989). The porosity of the Norphlet formation is 10 to 26 percent, and permeability varies between 0.1 and 650 millidarcy, depending on the facies (Godo, 2019). Due to its deposition in a sabkha environment and stratigraphic position above the salt, the salinity is very high and can reach about 240,000 parts per million of total dissolved solids (Godo, 2019). Several normal faults are present in the Norphlet formation, which may provide the high heat flow required for geothermal development.

The saturating fluids in the Smackover and Norphlet formations have variable hydrogen sulfide (“H₂S”) concentrations, which is essential to consider in reservoir evaluation and economics. H₂S is toxic and can corrode

metal pipes. Several Smackover and Norphlet oil fields produce sour gas, and H₂S concentration increases with increasing temperature (greater than 175 °C or 347 °F) in certain fields due to thermochemical sulfate reduction (McBride, et al., 1987; Claypool & Mancini, 1989; Shew, 1992). The H₂S concentrations range from 25 percent to 42 percent.

5. Estimated Thermal Resource in the Gulf Coast

The thermal resource base of the Gulf Coast is estimated to be 46,000 exajoules, and the methane volume entrained in the brine is 23,700 x 10¹² standard cubic feet, with a thermal equivalent of 25,000 exajoules (White & Williams, 1975), considering only Tertiary rocks. Wallace, et al. (1979) extended this study to the underlying Cretaceous rocks and estimated thermal energy of 110,000 exajoules, including onshore and offshore geopressured areas. This estimate does not include energy stored in methane. Esposito and Augustine (2012) at the National Renewable Energy Laboratory (“NREL”) reassessed the potential of onshore geopressured geothermal energy from the Gulf Coast. They identified five major geopressured-geothermal formations in Texas: lower Wilcox, lower Frio, Vicksburg–Jackson, lower Claiborne, and upper Claiborne. They also concluded that the Vicksburg–Jackson in south Texas has high quality geothermal resources because of thick sandstone and high temperatures. However, this study was done at a high level and does not provide enough granularity. The reservoir properties used in this study are average estimates of the entire formation in the entire study area. Based on petrophysical measurements of core, Vicksburg has very low permeability in south Texas, in the range of 0.2 to 0.7 millidarcy, in the lower Gulf Coast (Swanson, et al., 1976; Rich & Kozik, 1971; Loucks, 1978). The above discussion relates primarily to conventional hydrothermal development. The Vicksburg–Jackson, lower Claiborne, and the upper Claiborne formations all may work well as targets for development if Closed Loop Geothermal Systems are used.

6. Type of Potential Geothermal Development in the Gulf Coast

The upper and middle Gulf Coast can support Conventional Hydrothermal System development based on the available reservoir property information. These reservoirs will support conventional in-situ formation fluid-production-



based geothermal, and ‘geothermal anywhere’ concepts like Engineered and Advanced Geothermal Systems focused on high temperature rock. On the other hand, the lower Gulf Coast region of south Texas seems favorable for unconventional ‘geothermal anywhere’ type development, which can include drilling multilaterals and multi-stage fracturing (referred to as Next Generation EGS in this Report), since high porosity and permeability, required for Conventional Hydrothermal System development, are generally not present or are very restricted. These features elevate risk for conventional projects.

7. Stress Direction and Seismicity in the Gulf Coast

The present day principal maximum horizontal stress (“SHmax”) direction in the Gulf Coast is northeast to southwest, with minor stress field rotations locally (Snee & Zoback, 2018). Generally, the direction of hydraulic fractures tends to parallel SHmax, if these sections are hydraulically fractured for geothermal resources. The growth of the vertical hydraulic fracture depends on the contrast of SHmin between different beds. If the height of these fractures is high, they can inadvertently intersect other unfavorable zones rather than creating a desired fracture network to enhance fluid flow through these rocks.

There are no known occurrences of present day tectonic activity in this region, however, induced seismicity has been found to correlate with hydraulic fracturing of the Eagle Ford Shale in the Gulf Coast (Fasola, et al., 2019). This seismicity is somewhat in contrast to induced seismicity mainly related to saltwater disposal in the Permian Basin. Many Eagle Ford region earthquakes are distributed linearly along the Karnes fault zone and North Live Oak fault zone (Li, et al., 2021). Li, et al. (2021) also show several faults that have not been mapped previously. The depth range of these earthquake clusters varies between 2 to 10 kilometers in depth. Figure 4.20 shows the location of faults and recent earthquakes in the Eagle Ford play in south Texas.

If the development plan of geothermal resources in the Gulf Coast includes modern techniques, such as multi-stage fracturing along multi-laterals, induced seismicity must be monitored closely. This is because the strike of the growth faults is mostly along a northeast to southwest direction (Figure 4.18), which is parallel or subparallel to

the present day SHmax. Also, the sand wedges, which are potential geothermal reservoirs, were deposited towards the downthrown side of the growth faults. The thickness of these sand packages decreases away from the faults towards the southeast basinal side. Therefore, hydraulic fracturing sites targeting these reservoirs are likely to be close to the faults, some of which may be critically stressed, and need to be appropriately instrumented and monitored as the circulating fluids could enhance fault slip potential. This seismic potential affects most of the reservoirs of the Gulf Coast region.

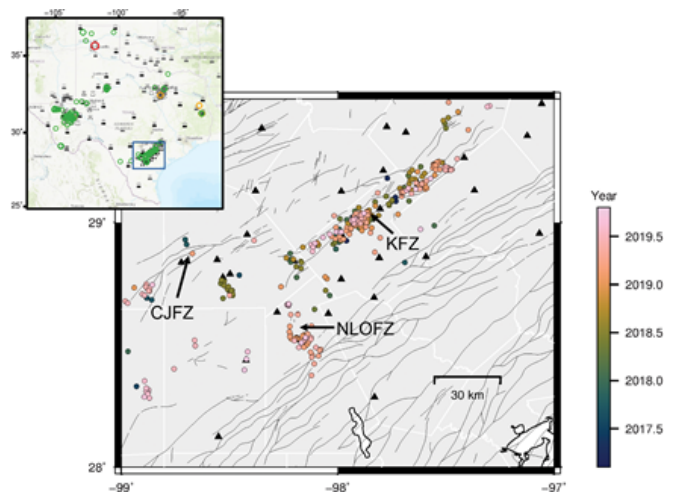


Figure 4.20. Map of the Eagle Ford Shale play, with locations of broadband seismic stations (in black triangles), earthquake locations (in colored circles), and previously mapped faults (in black lines) [after Li, et al., 2021]. Faults are interpreted by Ewing, et al. (1990). There are different fault zones in the area, including the Charlotte–Jourdanton fault zone (CJFZ), the Karnes fault zone (KFZ), and the North Live Oak fault zone (NLOFZ). *Source: Adapted from Li, et al., 2021 and Ewing, et al., 1990.*

8. Pleasant Bayou Test Wells in the Gulf Coast

The University of Texas at Austin, Bureau of Economic Geology (“Bureau or BEG”) was involved in drilling two pilot test wells (Pleasant Bayou 1 and 2) in Brazoria County, located between Houston and Galveston. Pleasant Bayou Well No. 1 was drilled in 1978 and plugged back and completed as a brine disposal well because of hole instability problems. The Pleasant Bayou Well No. 2 was offset 500 feet (152.4 meters) from the No. 1 well, drilled to 16,500 feet, and completed in 1979 (Riney, 1991). Well



No. 2 targeted the lower Frio Formation C-zone; the total thickness at the wellbore of this zone is composed of 125 feet (38.1 meters) of sandstone. Thick sandstones in this well have a porosity of about 18 percent. The well is bound on the southwest by large growth faults, which create compartments (Hamlin & Tyler, 1988). Based on the local geology interpreted from seismic and wireline data, there is also a possibility of many small scale faults and fault splays from the large growth fault in this region.

The initial pressure and temperature recorded at 14,560 feet (4,438 meters) was 11,116 pounds per square inch and 156 °C (306 °F). The well produced 20,000 barrels per day of water for a total of about 3.7 x 1E6 barrels from 1981 to 1983. With regard to energy output, the well produced approximately 0.5 megawatts electric from heat and one megawatt electric from co-produced gas (Riney, 1991). The produced brine was principally a sodium (“NaCl”) solution with substantial calcium and ions, including potassium and magnesium. The salinity was 130,000 parts per million total dissolved solids.

9. Jackson County in the Gulf Coast

Jackson County sits approximately in the middle of the Gulf Coast region inland from Matagorda Bay, approximately 100 miles (160 kilometers) southwest from Houston, and 110 miles (177 kilometers) northeast of Corpus Christi. With the central proximity of the county, Jackson County was chosen for our review as an example county for the Gulf Coastal zone, with the goal of gaining a greater understanding of the geothermal resources outside of the Eagle Ford Shale play. This study was accomplished as part of the University of Texas Geothermal Entrepreneurship Organization project (“GEO”) funded by DOE (Batir & Richards, 2020; 2021).

The previous geothermal resources mapping of Jackson County was completed as part of Blackwell, et al. (2011a), heat flow maps and temperature-at-depth maps (Blackwell, et al., 2011b), the 2010 Interstate 35 East project (Blackwell, et al., 2010), and was originally part of the 2004 Geothermal Map of North America (Blackwell & Richards, 2004a; 2004b). Therefore, it has been a decade since the last review of geothermal resources in this area. Currently available data includes a BHT dataset accessible through the National Geothermal Data System (“NGDS”) Borehole Observation file updated from recently drilled oil and gas well logs.

The previous mapping efforts used a thermal conductivity model for the Gulf Coastal region based on low thermal conductance in young unconsolidated sediments that increased conductance as the geology became older and further away from the shore (Blackwell & Richards, 2004a). The most recent 2020 (Batir & Richards, 2020; 2021) assessment incorporated the Pitman and Rowan (2012) thermal conductivity values assigned to Gulf Coast formations, although their work is based on research in Louisiana. There are some differences between the Gulf Coast depositional settings along the Gulf Coast from the speed of deposition to proximity to the shoreline at the time. Still, it was determined that when the formation descriptions were the same, these mineral-based thermal conductivity values by Pitman and Rowan (2012) were an improvement over a generalized model previously used. McKenna and Sharp (1989) measured thermal conductivities in South Texas were also used as a second boundary condition. As discussed earlier in the Chapter, the lack of thermal conductivity sample analyses for rocks in Texas is a limitation currently for the accurate mapping of the geothermal resources in Texas.

Using the oil and gas temperature data, there was an increase in data sites from 80 wells in 2011 (Blackwell, et al., 2011b) to 215 wells in the 2020 (Batir & Richards, 2020) project. The additional BHT data are distributed similarly over the county to the original 80 well sites allowing for an infilling of data. The SMU-Harrison correction was applied to the raw BHT data (Blackwell & Richards 2004). Combined with the more detailed thermal conductivity and stratigraphic column for the county, these data allowed for an update in the Jackson County heat flow map (Figure 4.21).

There are similar trends between the 2020 and the 2011 heat flow maps, going from higher heat flow in the northwest portion of the county and decreasing slightly to the southeast. With the additional data, the spatial resolution of the mapping increased between the 2011 and the 2020 datasets that produced a different pattern, yet the general trends are consistent. The county heat flow in the 2020 map ranges from 65 to 80 milliwatts per square meter, and the 2011 map is from 50 to 65 milliwatts per square meter. The new BHT data include an increased gradient that supports the increase in heat flow, although the prominent increase is more directly tied to the more representative thermal conductivity values.



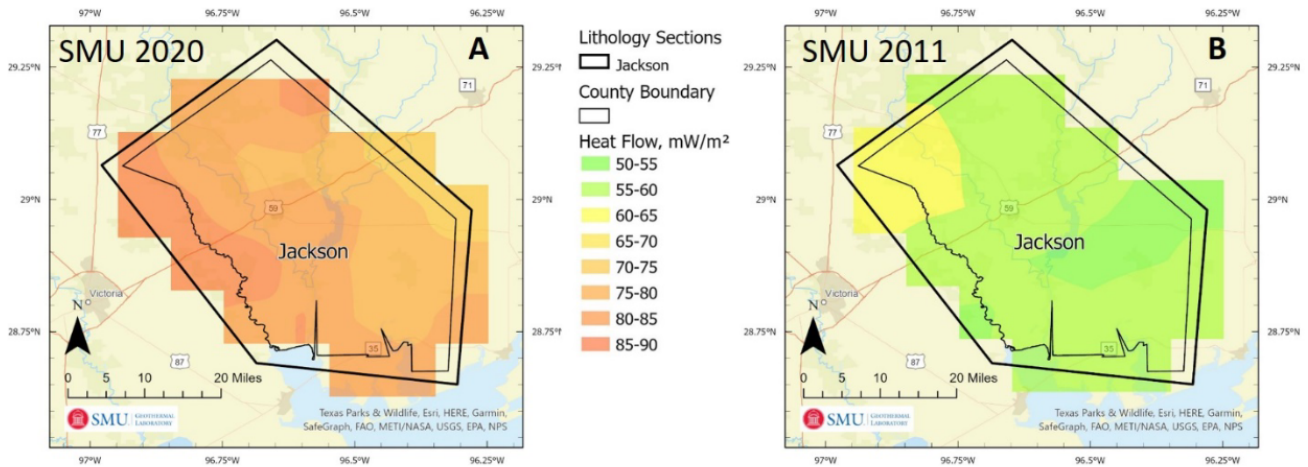


Figure 4.21. A comparison of heat flow maps for Jackson County with the most recent one in 2020 (Batir and Richards) using an updated thermal conductivity model and more BHT data points than the 2011 Blackwell, et al. map (this is a subset of the U.S heat flow map). Sources: *Batir and Richards, 2020 and Blackwell, et al., 2011.*

As part of the calculations for the temperatures-at-depth, especially those depths beyond any measured BHT, the radiogenic heat production of the sediments and basement rock is used as one of the parameters (Batir & Richards 2020). A maximum depth of 8 miles (13 kilometers) usually defines the thickness of the sedimentary formations; deeper than that is considered basement (igneous or metamorphic rock types). The sedimentary section in Jackson County is determined by geophysical studies to be as deep as 9.3 miles (15 kilometers). Therefore, Batir and Richards (2020) updated their basement thickness models for Jackson and Webb Counties. In doing so, the radiogenic heat production values improved the accuracy and resolution of the resulting deep temperatures.

Using the updated temperatures, radiogenic heat production, thermal conductivity, and detailed stratigraphic column, the temperatures were calculated at 6.2 miles (ten kilometers). Figures 4.22, 4.23, 4.24 are the maps of the temperatures at 3.5 kilometers, five kilometers, and 10 kilometers (11,480, 16,400, 32,800 feet, respectively).

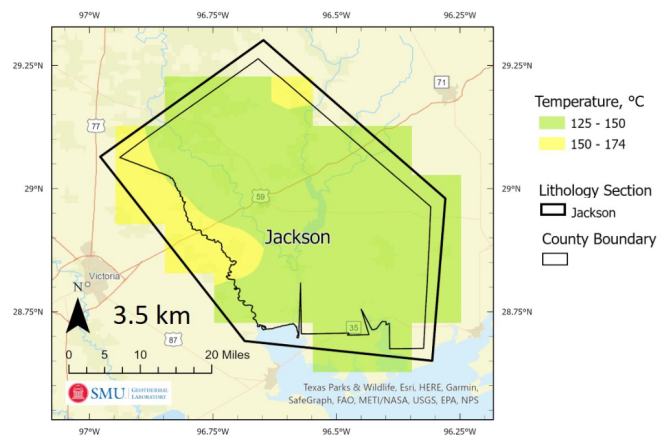


Figure 4.22. Map of temperatures below Jackson County at a depth of 3.5 km (11,480 ft). The temperatures range from 125 °C to over 150 °C (257 to 302 °F), with the warmer temperatures in the northwest portion of the county. At this depth, approximately one third of the BHT sites are drilled to or deeper than this depth and were therefore used in the calculation. Source: *Adapted after Batir and Richards 2020; 2021.*

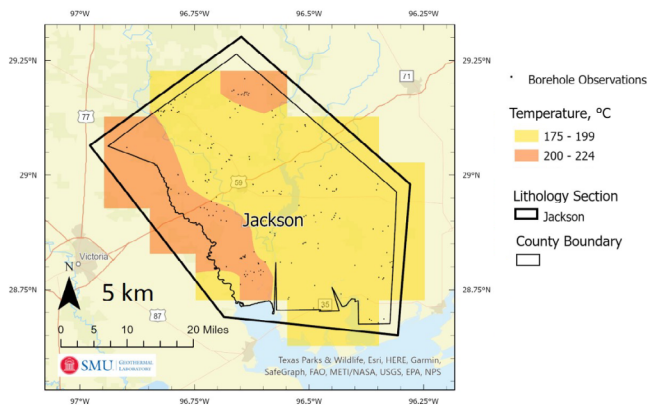


Figure 4.23. Map of temperatures below Jackson County at a depth of 5.0 km (16,400 ft). The temperatures range from 175 °C to over 200 °C (347 to 392 °F), with the warmer temperatures in the northwest portion of the county. At this depth, there are 8 wells drilled near or deeper than this depth used in the calculation, with temperatures ranging from 180 to 220 °C (356 to 428 °F). Source: Adapted after Batir and Richards 2020; 2021.

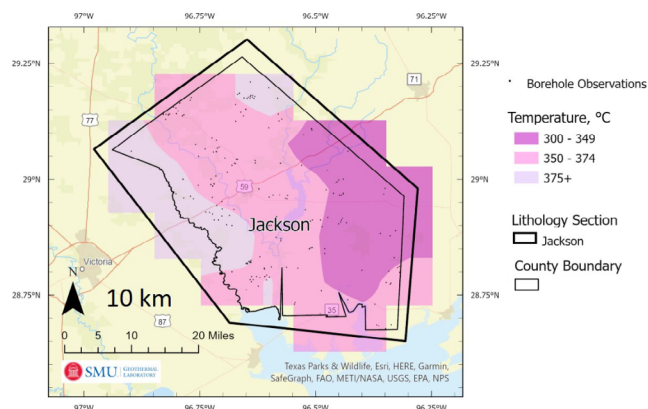


Figure 4.24. Map of temperatures below Jackson County at a depth of 10 km (32,800 ft). The temperatures range from 300 °C to over 375 °C (572 to 707 °F). The warmer temperatures continue to be towards the northwest, somewhat following the increased thickness in sediments to the southeast being younger and cooler. At this depth, the temperatures are all extrapolated with no direct measurements. Source: Adapted after Batir and Richards 2020; 2021.

Jackson County is not in the middle of a highly active oil and gas play, such as the Eagle Ford or Barnett Shale play, yet the use of the existing oil and gas well data and past research of the geology and geophysics shows how the geothermal resource can be determined and that there are high temperatures available for resource use in all types of geothermal projects.

IX. East Texas

The boundaries for East, North, South Texas, and the Gulf Coast can be overlapping depending on how they are defined. The I-35 report (Blackwell et al., 2010; Richards & Blackwell, 2012) discusses the four areas as they sit along or are east of Interstate 35 from the Mexican border to Oklahoma (Figure 4.14). For this study, the focus has been based on geological regions, and as such, the geology of East Texas is known for the “tight” formations (little fluid content) and impacted by deep salt structures, causing the formations to dip in different directions relative to the nearby salt structures as they moved upward, creating local faults and anticlines (Figure 4.25). The deep Jurassic Louann Salt is hypothesized to have been deposited on a flat surface in the Gulf Coast of the East Texas Basin (Figure 4.26). The basin filled over millions of years in sequences of deep water and shallow water environments. Deposits of shales and mudstones formed during the shallow water periods, while during transgressive, deep water events, sandstones to limestones were formed (Granata, 1960). The shoreline of East Texas Basin moved inward and outward, depositing shale-sand sequences to produce groups of thick formations such as the Cotton Valley Group, Nueva Leon Group, and Trinity Group. The Cotton Valley Group thickness is typically between 2,400 to 3,700 meters (8,000 to 12,000 feet) and at drill depths of 2,400 to 3,000 meters (about 8,000 to 10,000 feet).

Along the eastern border of Texas is the Sabine Uplift, which contains basement rocks that differ in radiogenic heat production from the rest of the Gulf Coast and East Texas basement. The uplift is considered a mid-rift high caused by an area of stability with less subsidence relative to the East Texas and South Louisiana rift basins (Granata, 1960). The results are major transform faults bounding the Sabine Uplift on its northeast and southwest sides. As additional Laramide compression caused folding and faulting, a restraining side-step formed northeast to southwest as a shear fault system in the area of East Texas (Adams, 2009).



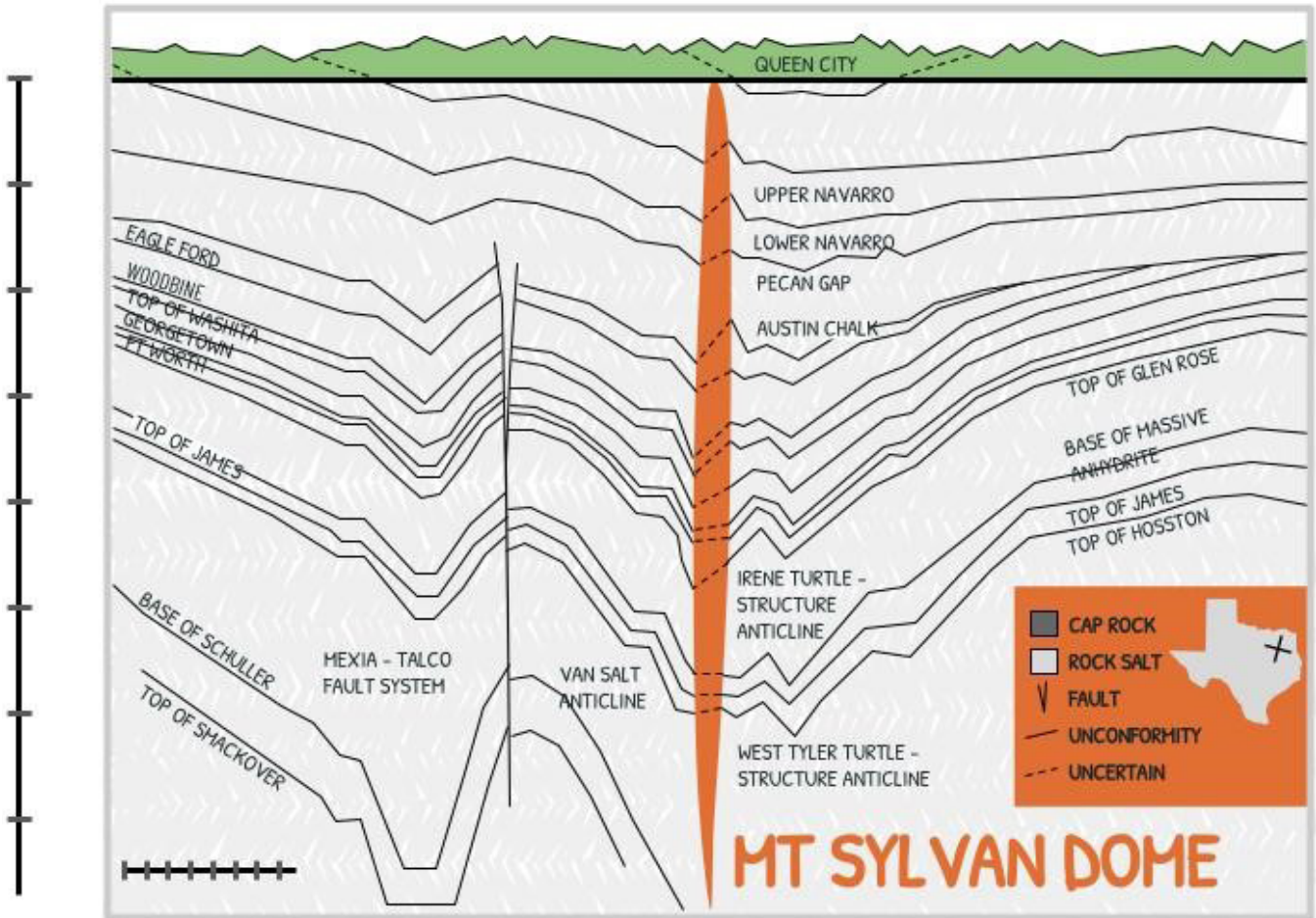


Figure 4.25. Structural cross-section across the East Texas Basin. Source: Adapted from Wood and Guevara, 1981.



ERA	SYSTEM	SERIES	GROUP	FORMATION	ISOPACH MAP INTERVALS
CENOZOIC	TERTIARY	EOCENE		WILCOX	
		PALEOCENE		MIDWAY	
MESOZOIC	UPPER CRETACEOUS	GULFIAN	NAVARRO	ARKADELPHIA NACATOCH	
			TAYLOR	SARATOGA	
				HARLBROOK	
				ANNONA	
				OZAN	
			AUSTIN	AUSTIN (UNDIFFERENTIATED)	
			EAGLE FORD		
			WOODBINE (TUSCALOOSA)		
			HANESS		
			BUDA		
			GRAYSON		
			WASHITA		
	LOWER CRETACEOUS	COHANCHEAN		MAINSTREET	
				PAW PAW WENO	
				DENTON	
				FORT WORTH	
				DUCK CREEK	
				KIAHICHI	
			FREDERICKSBURG	GOODLAND	
				WALNUT	
				RUSK	
				FERRY LAKE	
				RODESSA	
				BEXAR	
JURASSIC	COAHUILAN		JAMES		
			PINE ISLAND		
			SLIGO		
			HOSSTON		
		NUEVA LEON	SCHULER		
			BOSSIER		
		HAYNESVILLE			
		SHACKOVER			
		NORPHLET			
		LOUANN			
		WERNER			
		COTTON VALLEY			
PALEOZOIC	PENN.		MOREHOUSE		
			EAGLE MILLS		

Figure 4.26. Stratigraphic column of the East Texas Basin. Source: Adapted from Granata, 1960.

A. East Texas Geothermal Resources

The geothermal resources within East Texas were discussed as part of the Gulf Coast Geothermal-Geopressure studies (John, et al., 1988). The area's first regional heat flow mapping was part of the 1992 Geothermal Map of North America (Blackwell, et al., 1990). The heat flow was calculated to be between 50 to 60 milliwatts per square meter, considered similar to the central United States heat flow. The 2004 Geothermal Map of North America (Blackwell & Richards, 2004) shows this region, highlighting the use of oil and gas well BHT data with a thermal conductivity model based on sediment thickness and age, such that the thick young sediments were assigned a low thermal conductivity (about 1.4 watts per meter-Kelvin). More recently, with the addition of oil and gas BHT data, the heat flow in the area was re-evaluated at 60 to 80 milliwatts per square

meter and displayed a variability not previously realized. This new outcome highlights the value of updating assessments based on new data availability. Generally, specific research studies in East Texas show a trend of decreasing heat flow the further the resource is from the Sabine Uplift.

Differences in the predictions of heat flow between the original assessments and modern assessments highlight the importance of thermal conductivity measurements. The one set of k measurements for East Texas are from Fairway Field and discussed below. The regional gradient map (Figure. 4.27) shows the current BHT locations within the NGDS are the area's primary source of saved BHT data. Counties with additional BHT locations since the Blackwell, et al. (2011a) and the Richards and Blackwell (2012) maps are emphasized by their thicker borders and discussed in the next Section.



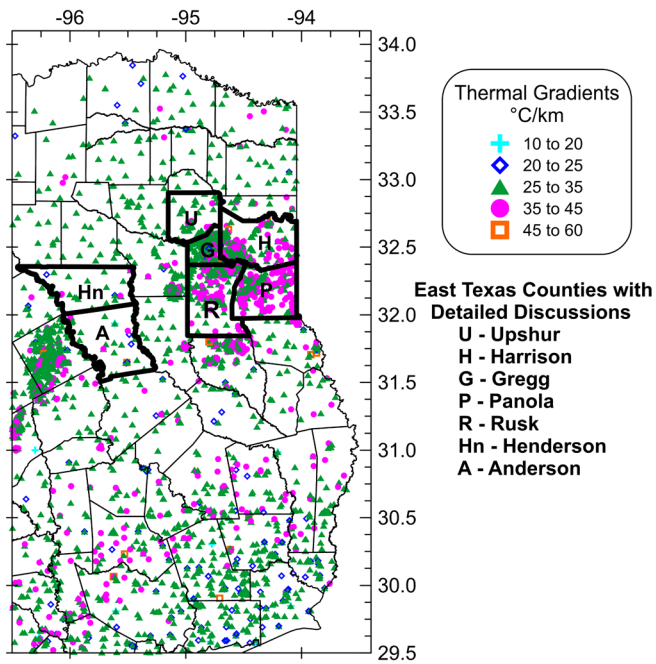


Figure 4.27. East Texas Bottom-hole Temperature Well Sites in the National Geothermal Data System. The thermal gradients are one component of the heat flow calculation. Thickly bordered counties are discussed in this section. Pink circles and orange squares are sites with higher than the regional gradients. The deepest BHT data are plotted on top if more than one for the same site or close to each other. *Source: Future of Geothermal Energy in Texas, 2023.*

East Texas is a large and somewhat heterogeneous region, so we will examine some representative areas in greater detail. Studies to be discussed in this Section include the Richards and Blackwell (2012) I-35 corridor study of the entire eastern Texas region, as well as Kweik, et al. (2014) and Kweik (2014), which focused on the oil and gas Fairway Field in Henderson and Anderson Counties. The Batir, et al. (2018) study of the Longview area included Gregg, Rusk, Panola, and Harrison Counties. Lastly, the most recent review of Upshur County geothermal resources was completed for a private company by Batir and Richards (2020, unpublished report).

1. Detailed Review of Fairway Field: Henderson and Anderson Counties

The Fairway oil field is located in East Texas near the town of Poynor, bordering Henderson and Anderson Counties. The field produced oil continuously for over 60 years (Webster, et al., 2018) (Figure 4.27). Hunt Oil Company

granted access to the SMU Geothermal Laboratory for Kweik to review the field, which has over 2,900 open-hole well logs and pressure surveys, for his Master’s research project (Kweik, et al., 2014; Kweik, 2014). These data comprise open-hole (BHT) and closed (shut-in) temperature logs, pressure logs, fluid production, and injection data. Taken together, these data provide an opportunity to analyze temperature variations associated with fluid migration and field development over time.

The density of data within the field allowed for a review of time sequence trends and the ability to determine a weighted average for parameters based on hundreds of wells. The field averaged temperature gradient of 35 °C per kilometer (1.92 °F per foot), the field average thermal conductivity of 1.98 watts per meter-Kelvin, and the conductive heat flow value is 69±6 milliwatts per square meter. The porosity ranges from 7.2 percent to 10.8 percent. The permeability varies between formations and across the field from eight millidarcy to 43.7 millidarcy.

An unexpected result in this field was the increase in reservoir temperatures of more than 10 °C (20 °F) over more than 50 years. The structure of Fairway Field is of a dome (turtle structure), allowing for the higher temperatures deeper to flow up as fluids are extracted, and pressures changed over the 50 years of production. This pattern represents an influx of heat over this time rather than a decrease, highlighting the ability to bring warmer temperatures into production over the life of a field. The availability of pressure-survey temperature data and fluid data provides a unique understanding of such dynamic geothermal resources (Kweik, et al., 2014; Kweik, 2014).

Fairway Field illustrates how sedimentary basins have considerable potential for geothermal development. In this field, the James Limestone formation is the primary source for fluid production from 1960 to 2012. As mentioned above, the temperatures increased in this field over the 50 years of operation. The increase in temperature caused the “heat loss” to become a negative number. A “heat loss” of -1.7×10^{17} joules was calculated (Kweik, et al., 2014).

As part of this project, core samples of the James Limestone were analyzed for thermal conductivity, resulting in an averaged value of 2.60 watts per meter-Kelvin for this formation (Table 4.2). The detailed core



Table 4.2. Thermal conductivity and porosity values for James Limestone cores from seven wells across the field at various depths; Source: Adapted after Kweik, et al., 2014; Kweik, 2014.

Well #	Depth, m (feet)	Porosity %	Sample Plug Orientation To Lamination	Divided Bar Thermal Conductivity (Wm ⁻¹ K ⁻¹)
647-3	3000 (9,842)	9.11	Parallel	2.42
649-3	3008 (9,868)	6.67	Parallel	2.95
746-3	3012 (9,880)	0.54	Perpendicular	2.45
452-2	3027 (9,930)	0.00	Parallel	2.50
747-2	3042 (9,978)	4.55	Perpendicular	2.78
548-3	3052 (10,009)	16.56	Parallel	2.20
149-2	3055 (10,021)	7.11	Parallel	2.83
Average Thermal Conductivity for James Limestone				2.6 ± 0.4

analysis across the 45 square miles (115 square kilometers) highlights the amount of variation in thermal conductivity and porosity that can occur even within one field (Kweik, 2014). For some rock types, the thermal conductivity changes with the direction of the bedding being analyzed. This difference is referred to as anisotropy. From the results of the James Limestone, thermal conductivity varies inconsistently with the change in bedding direction.

2. Detailed Review of Sabine Uplift: Rusk, Gregg, Harrison, and Upshur Counties

The Eastman Chemical plant, southeast of Longview, Texas, was the central point for a study to evaluate a Deep Direct Use (“DDU”) application of geothermal energy to improve the efficiency of a gas power plant (Turchi, et al., 2020). The warm geothermal resource was modeled for its ability to produce supercooled fluids for turbine inlet cooling. Normally geothermal fluids are used to generate electricity from the extracted heat. For the Eastman Chemical plant projects, the geothermal heat energy was used to drive a chiller process that instead made supercooled fluids (4 °C or 39 °F) to be stored in an on-site tank. These fluids were for inlet cooling of the gas plant, when the outside air temperature was at least 16 °C

(60 °F) or hotter, to increase the efficiency of the plant. The Eastman Chemical company provided their time and data for this DOE Geothermal Technologies Office study conducted by the National Renewable Energy Laboratory, SMU Geothermal Laboratory, and TAS Energy (Batir, et al., 2018; Turchi, et al., 2020).

Examination of the geothermal resources focused on depths of the Lower Cretaceous Trinity Group (Travis Peak / Hosston, James, Pettet / Sligo) between approximately 5,576 to 8,856 feet (1,700 to 2,700 meters) and the Upper Jurassic Cotton Valley Group (Schuler and Bossier), approximately 8,200 to 10,988 feet (2,500 to 3,350 meters) for the application. Below the Cotton Valley Group are the Haynesville and/or Smackover Formations, which are expected to be above 150 °C (300 °F) below depths of 11,480 feet (3.5 kilometers) in Rusk, Harrison, and Gregg Counties, and less than 150 °C in Upshur County (Figures 4.26 and 4.28).

The recent geothermal resource mapping differs from previous research in the area by the SMU Geothermal Laboratory as part of the Geothermal Map of North America (Blackwell & Richards, 2004) and the Geothermal Map of the United States (Blackwell, et al., 1990). The past two projects used a model for thermal conductivity



values based primarily on the age and thickness of the sedimentary basin. This model meant increased thermal conductivities moving from south to north across the Gulf Coastal Plain and East Texas.

The DDU study provided the ability to review the local detailed stratigraphic column and assign thermal conductivity values based on well location, formation thickness, and on mineralogy related to those in Louisiana (Pitman & Rowan, 2012). The Pitman and Rowan (2012) report determined thermal conductivities based on rock mineralogy for each formation, instead of from core samples on a divided bar. The minerals within the formations are similar, yet as discussed above in Fairway Field, it is expected that there are formational changes both laterally and vertically over a region that are not possible to take into consideration without more thermal conductivity sample analyses.

As site heat flow values are based on thermal conductivity and local temperature gradient, the variation in BHT data is a significant component in the heat flow value. Therefore, large error bars (± 25 °C or ± 77 °F) become the most significant error component in all future calculations. To account for the potential for BHT error, data are examined initially both as raw data for outliers and then mapped. The mapping process uses a gridding method capable of removing data that are more than two standard deviations from the surrounding values. As the amount of data points increases, more points can be averaged as a smoothing method to arrive at an improved value.

By incorporating the Pittman and Rowan (2012) thermal conductivity values for each formation, the overall heat flow values increased by approximately 5 to 10 milliwatts per meter squared over the previously calculated heat flow values in the Blackwell and Richards (2004) and Blackwell, et al. (2011) maps. Within the 12.4 mile (20 kilometer) radius near the city of Longview, heat flow varies from 65 to 95 milliwatts per meter squared (Figure 4.29), which is a higher typical variability than in regional mapping where the data are smoothed. Usual differences are approximately 10 to 20 milliwatts per meter squared. In Figure 4.29, the heat flow values show the general trend of hotter resources to the southeast in Rusk, Gregg, and Harrison counties.

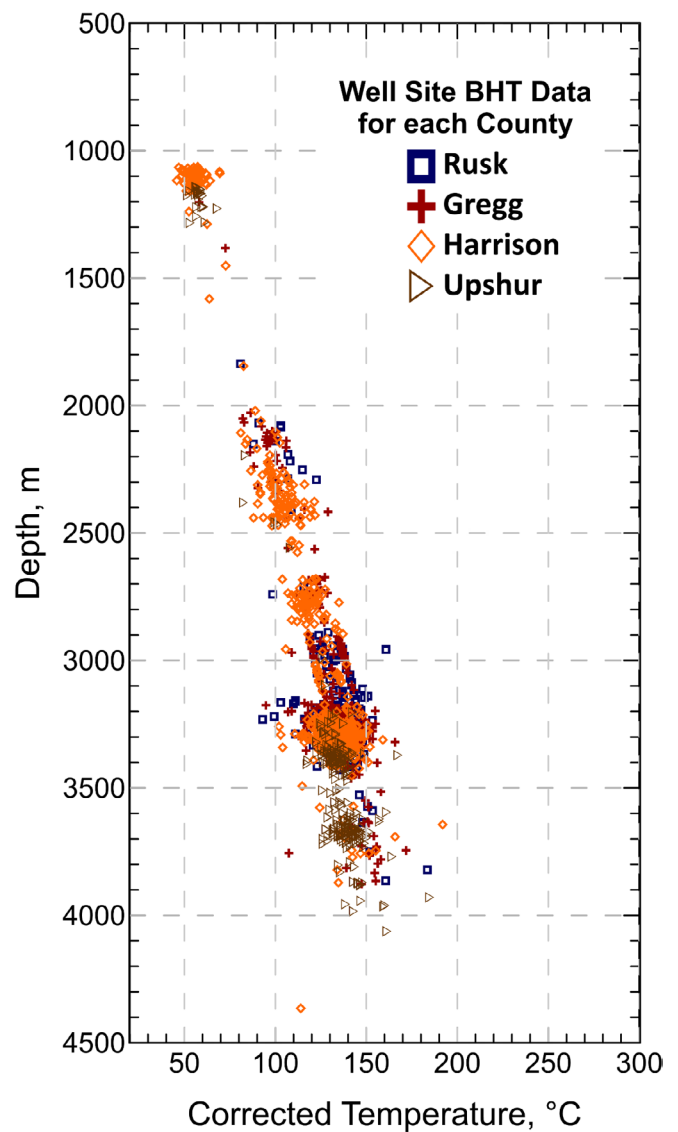


Figure 4.28. East Texas Corrected Temperatures for Upshur, Gregg, Rusk, and Harrison Counties. The well temperatures in Upshur County are primarily the deepest, yet approximately the same temperatures as the wells 500 to 1000 meters shallower in the other counties to the southeast and closer to the Sabine Uplift. Source: *Future of Geothermal Energy in Texas, 2023*.

A heat flow of 55 to 65 milliwatts per meter squared is considered normal for the Central United States, therefore, there is more stored thermal energy in the East Texas basins than in many portions of the Central United States. This increase in heat is related to the sediments acting like a protective layer or a thermal blanket above the more radiogenically active basement rock of the Sabine Uplift.



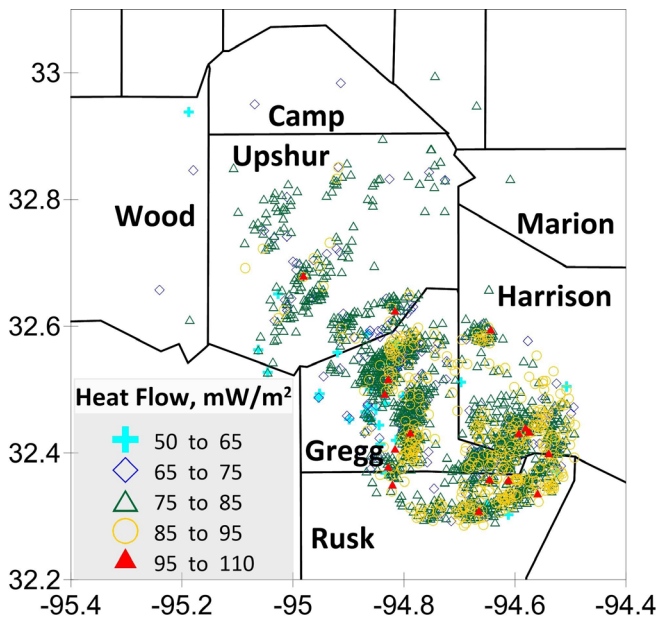


Figure 4.29. East Texas Updated Heat Flow. The heat flow trends warmer to the southeast towards the Sabine Uplift, which is located along the border of Texas and Louisiana. Sources: Batir and Richards, 2018 and Batir and Richards, unpublished 2020.

Another way to look at the available geothermal resources is using the Heat-in-Place or heat density calculations to provide the total thermal energy stored within a defined 3D volume. The denser the heat, the hotter it is within that area of rock. The DDU study (Batir, et al. 2018; Turchi, et al., 2020) follows the methodology of Zafar and Cutright (2014), who used the 3-D model to calculate the amount of heat being stored. For this study, the Travis Peak Formation was chosen because of the direct-use project constraints for production from wells. The Travis Peak thickness component and the temperatures through the formation are shown as the heat indicator (Figure 4.30). The top of the Travis Peak Formation lies between 6,560 to 7,872 feet (2,000 to 2,700 meters) below sea level, trending locally deeper to the northeast. On average, the Travis Peak is 1,804 feet (550 meters) thick, yet can vary from 984 to over 1,968 feet (300 to over 600 meters) in thickness. The calculated amount of heat stored ranges from 150 to over 275 megajoules per meter cubed as the thermal gradient and thickness of formation change, thus creating variations in the mapped heat density. There are no major faults mapped within the 12.4 miles (20 kilometers) area of this study, so the possibility of fault-driven fluids is unlikely.

The heat density map for the Travis Peak formation highlights the potential for geothermal resources to be variable within sedimentary formations. For the geothermal industry, this variability within sedimentary geothermal resources could be identified in a similar manner to the historic hydrothermal systems of the western United States. Although oil and gas fields are large geographic areas, there is usually an ideal location for drilling that can be identified to maximize production and profit.

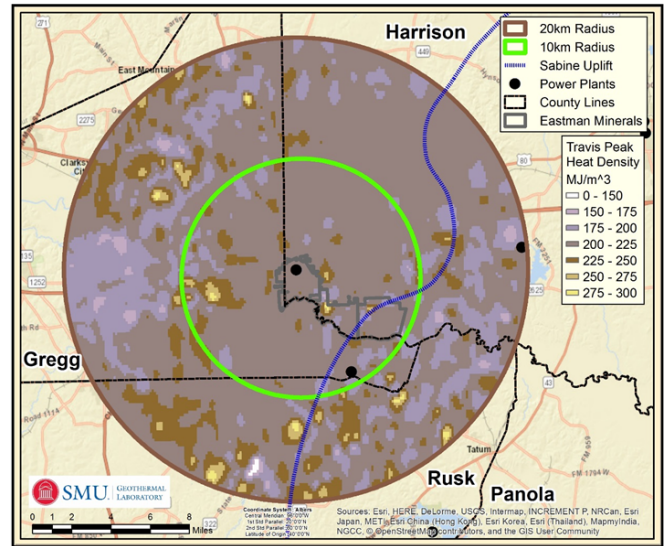


Figure 4.30. The Heat Density or Heat-in-Place Map of the Travis Peak Formation. This map represents the stored thermal resource and shows the local variations using the most advanced methods for calculation. The western edge of the Sabine Uplift is shown as a blue line on the eastern side of the map. Source: Adapted after Batir, et al. 2018 and Turchi, et al., 2020.

To better understand how much energy is stored within the Travis Peak formation, illustrated in this 6.2 mile (20 kilometer) circle in Figure 4.30, one megajoule is equal to the energy consumed in 0.278 kilowatt hour. Figure 4.30 uses megajoules per meter cubed units. Based on the volume of a cylinder, 3.1416 times ten square kilometers times 0.550 kilometer (the average thickness) = 172.8 cubed kilometers or 172.8x1E9 cubed meters. Using an average heat density for Travis Peak of 200 megajoules per meter cubed, there are 345.6 x 1E11 megajoules per meter cubed within the 6.2 miles (20 kilometer) cylinder of Travis Peak rocks and fluids. Not all of the heat will be extractable; usually about 1 to 10 percent of the resource. If 1 percent is used, then 345.6 x 1E9 megajoules per meter



cubed of energy is available. The equivalent of 345.6×10^9 megajoules per meter cubed times 0.278 kilowatt-hour = 96×10^9 kilowatt-hours. If the average home uses 10,632 kilowatt-hours per year (EIA, 2022), approximately 500,000 homes could be powered for over 18 years based on this stored heat. Thus, more than enough energy is stored within this formation to meet the residential power demand within this 6.2 mile (20 kilometer) circle.

Upshur County has three northeast to southwest oil and gas trends providing well data for initial geothermal resource analysis. As with most of Texas, the number of existing drilled wells is 4,193 in Upshur County (Batir & Richards, 2020), far greater than the current 313 BHT extracted from well log headers in the dataset (Figures 4.28 and 4.31). The available well data follow the three drilling trends. The grid size for the Upshur project maps is set to 0.05° latitude/longitude to include at least one data point within each grid cell and smooth the gradients. This grid size is similar to the size used in the Geothermal

Map of North America (Blackwell & Richards, 2004a,b) and the Geothermal Map of the United States (Blackwell, et al, 2011a).

In general, as shown by the 11,480 feet (3.5 kilometers) temperature gradients (Figure 4.31), Upshur County is consistent in thermal gradient with a small heat flux of about 1.76 to 1.82°F per 100 feet (32 to 33°C per kilometer). Of interest in this figure are the deep salt intrusions having little to no direct impact on the thermal picture at the 11,480 feet (3.5 kilometers) or even deeper at 18,040 feet (5.5 kilometers) (Batir & Richards, 2020 unpublished report). The average temperature at 14,760 feet (4.5 kilometers) is 160°C (320°F), although the deepest BHT measurement is 4.1 kilometer. Upshur County is an example of a county with lower heat flow, yet temperatures are able to sustain geothermal development, especially with the ability to mix geothermal resources with other renewable energy sources, such as solar and biomass.

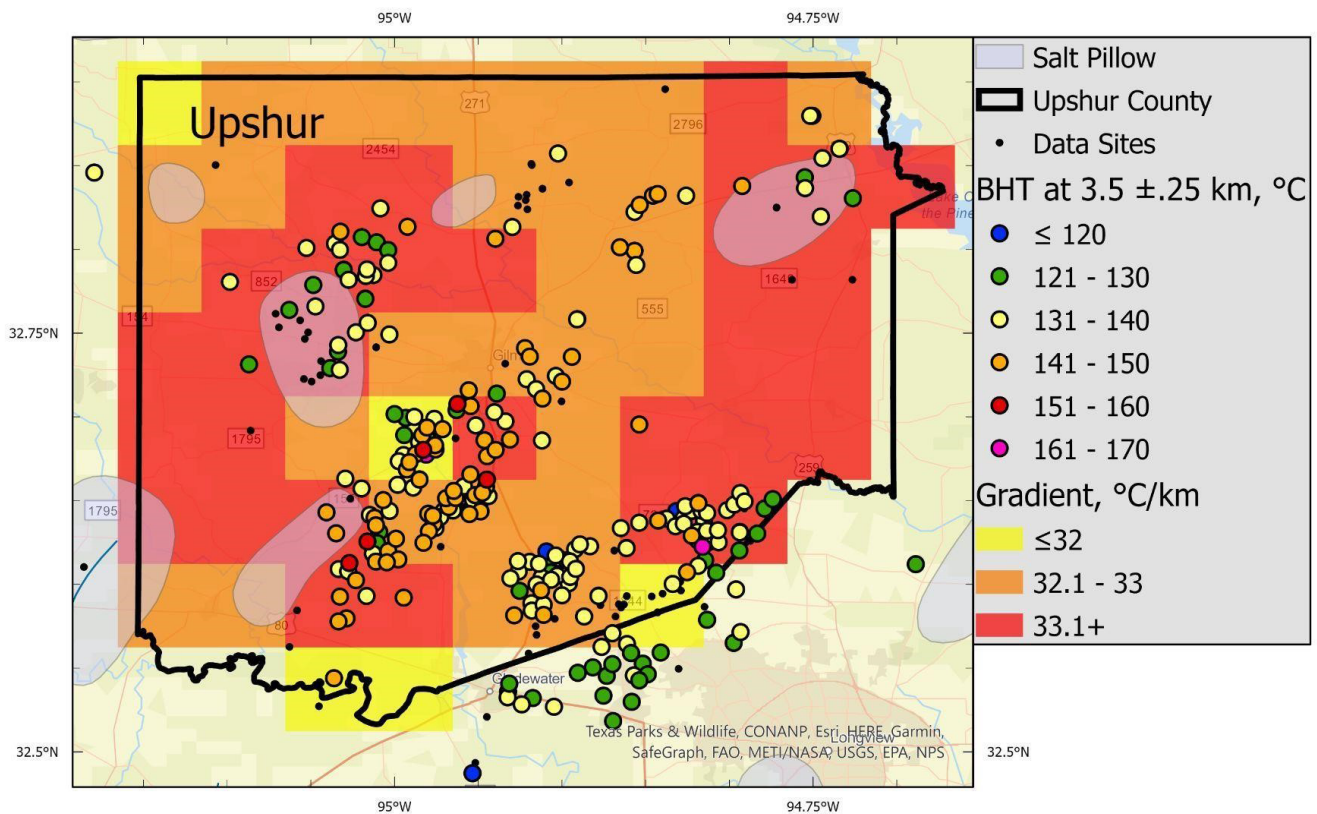


Figure 4.31. Map of 3.5 kilometers Corrected Well Temperatures and Gradients for Upshur County. The average temperature at this depth is $136 \pm 7^\circ\text{C}$. BHT measurements in this depth are between 115°C to 170°C , although the highest grid value is 144°C because of averaging within the cell. 274 wells penetrate the 3.25 to 3.75 kilometer depth range. Source: Adapted after Batir and Richards (2020).



X. Permian Basin (West Texas):

The stratigraphic column of Upshur County follows the same general formations shown in Figure 4.26. Using the correlation between the Pittman and Rowan (2012) mineralogy for these formations, the well averaged thermal conductivity varies between 2.38 and 2.42 watts per meter Kelvin. The base of the sediment thickness is determined to be between 13,740 to 13,900 feet (4.19 to 4.24 kilometers).

The northern counties of East Texas are currently mapped similarly to Upshur County resources and not expected to change compared to the temperature-at-depth maps from 2011 (Blackwell, et al., 2011b) (Figures 4.5 through 4.7).

The Permian Basin of West Texas and south to east New Mexico (Figure 4.32) is the most important onshore sedimentary basin in the United States in terms of energy resources production. The basin has been producing hydrocarbons from multiple formations for over a century, resulting in one of the most extensive datasets for subsurface characterization and energy exploration, including geothermal energy. With changes in the energy business trends over the years, the Permian Basin has always been a top choice of onshore operators for resource exploration and development due to discovery thinking, new technologies, and favorable rock properties in the subsurface. The thickness of the sedimentary strata in the basin is more than 26,000 feet (7,925 meters), containing multiple reservoirs of varying sizes for geothermal resource development.

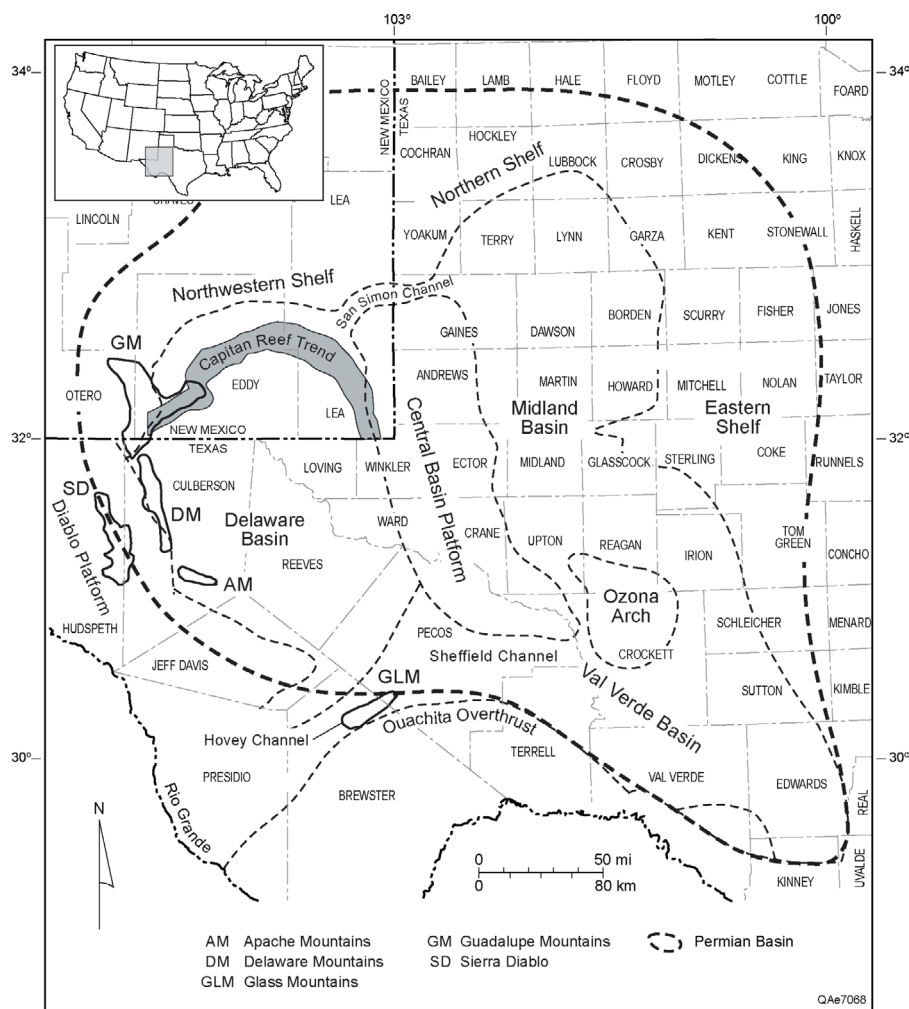


Figure 4.32. Location of the Permian Basin and sub-basins in west Texas and southeastern New Mexico, United States. Source: Dutton, et al., 2004.



The Permian Basin started from an ancient broad, shallow, gently dipping depression known as the Tobosa Basin. The Tobosa Basin records clastic and carbonate sediments from the Cambrian through Mississippian. The Tobosa Basin went through tectonic evolution due to the collision of the North American Craton with South America from Early Pennsylvanian through Early Permian, which resulted in the development of the deep Delaware Basin and Midland Basin, separated by the shallow Central Basin Platform (Figure 4.33). Vast deposits of clastics deposited in the deep basins and carbonates deposited on the shelves resulted in a mixed carbonate-siliciclastic pattern (Figure 4.33). Figure 4.34 shows the stratigraphy of the formations in the Permian Basin. Polyphase fault systems developed in the Permian Basin, which also involved reactivation of basement-rooted faults. Major faulting, folding, subsidence, tilting, and uplift of the basin reshaped the basin geometry and deposition of sediment.

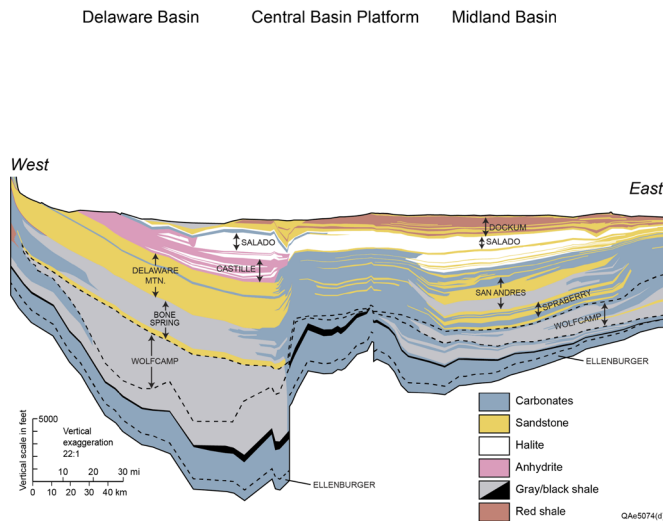


Figure 4.33. The east to west cross section of the Permian Basin and current trends of operation, including conventional, unconventional reservoirs, saltwater disposal, produced water, and enhanced oil recovery Source: Adapted after Scanlon, et al., 2017. Permission received from the American Chemical Society. Further permissions related to the material excerpted should be directed to the American Chemical Society.

The Greater Permian Basin's Delaware and Val Verde basins are deep and have a relatively high geothermal gradient. Keay, et al. (2021) generated a basin-wide temperature model and opined that depths deeper than 10,000 feet (3,048 meters) in both Delaware and Midland basins mostly correspond to temperatures over 100 °C, which is suitable for low-enthalpy geothermal systems (Figure 4.35). Figure 4.36 shows a generalized geothermal gradient from a well across multiple formations in the Delaware Basin. Heat flow data in the Permian Basin are sparse. Blackwell, et al. (2011) reported average heat flow in Crockett County 57 milliwatts per meter squared with a standard deviation of ±13 milliwatts per meter squared.

System	Epoch/Series/Stage	Age (Ma)	U.S. Epoch/Series/Stage	W-NW Shelf New Mexico	Delaware Basin	NW Shelf Texas	Central Basin Platform	Midland Basin	
CARBONIFEROUS	Pennsylvanian	299	Virgilian	Cisco	Cisco	Cisco	Cisco	Cisco/Cline	
		303	Kasimovian	Canyon	Canyon	Canyon	Canyon	Canyon	
		307	Missourian	Strawn	Strawn	Strawn	Strawn	Strawn	
		315	Desmoinesian	Atoka	Atoka	Atoka	Atoka	Atoka/Bend	
			Bashkirian	Morrow	Morrow	Morrow			
	Mississippian	323	Serpukhovian	Chesterian	Barnett	Barnett	Barnett	Barnett	Barnett
		331	Visean	Meramecian					
		347	Osagean						
		359	Tournasian	Kinderhookian	Mississippian Limestone	Mississippian Limestone	Mississippian Limestone	Mississippian Limestone	Mississippian Limestone
DEVONIAN	Late	372	Famennian		Woodford	Woodford	Woodford	Woodford	
		382	Frasnian						
		388	Givetian						
	Middle	393	Eifelian						
		408	Emsian						
	Early	411	Pragian			Thirtyone	Thirtyone	Thirtyone	
		419	Lochkovian						
		423	Pridoli	Winston	Fasken	Winston	Fasken	Winston	Fasken
		427	Ludlow	Wink	Wink	Wink	Wink	Wink	
	SILURIAN	433	Wenlock						
444		Llandovery							
458		Fusselfman		Fusselfman	Fusselfman	Fusselfman	Fusselfman		
			Montoya	Montoya	Montoya	Montoya	Montoya		
ORDOVICIAN	Middle	470	Simpson Group	Simpson Group	Simpson Group	Simpson Group	Simpson Group		
		485	Ellenburger	Ellenburger	Ellenburger	Ellenburger	Ellenburger		
CAMBRIAN	Late	485	Bliss	Bliss	Bliss	Bliss	Bliss		
							Wilberns		
								Riley	

Figure 4.34. Cambrian-Carboniferous stratigraphy of the Permian Basin, deemed feasible for deep geothermal resources. Sources: Adapted after Ruppel, 2019; Ogg, et al., 2016; Kerans and Kempter, 2002; Kerans, et al., 2014; Hurd, et al., 2016; Nestell, et al., 2019.



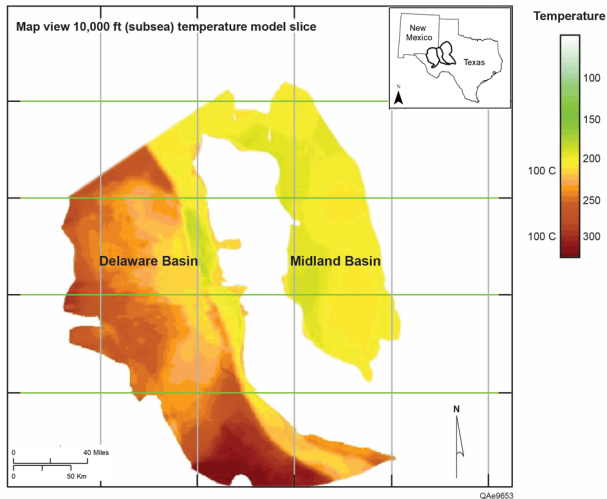


Figure 4.35. Map view of the Permian Basin temperature model at a depth of 10,000 feet (3,048 meters) subsea. Warm colors indicate high temperatures. An approximate scale bar along with an inset map of the Permian Basin in West Texas and New Mexico is shown. Source: Adapted after Keay, et al., 2021

Deep formations in the Permian Basin are overpressured (Wallace, et al., 1978; Rittenhouse, et al., 2016; Lou, et al., 1994). Overpressure may be one of the critical success factors for producing hot brine from the subsurface for geothermal energy production. In the Delaware Basin, especially in the eastern margin of the basin, the third Bone Spring, Wolfcamp, Barnett, and Woodford shale formations are overpressured, with pore pressure often exceeding 0.7 pounds per square inch per feet, which is generally considered as the start of “hard overpressure.” This overpressure might have been generated due to a combination of multiple factors in this basin, including disequilibrium compaction, clay diagenesis, hydrocarbon generation, and tectonism. The temperature gradient across the overpressure zone in the eastern Delaware Basin is 25.1 °C per kilometer, compared to the basin’s average geothermal gradient of 21 °C per kilometer (Wallace, et al., 1978). Temperatures at the top and bottom of the overpressure system are about 80 °C and 115 °C, respectively (Figure 4.36). Below the Woodford, formations have mostly normal pore pressure gradients, however, local variations can exist. Wallace, et al. (1978) stated that the Permian, Mississippian, Devonian, and Ordovician sequences are overpressured in the Delaware Basin.

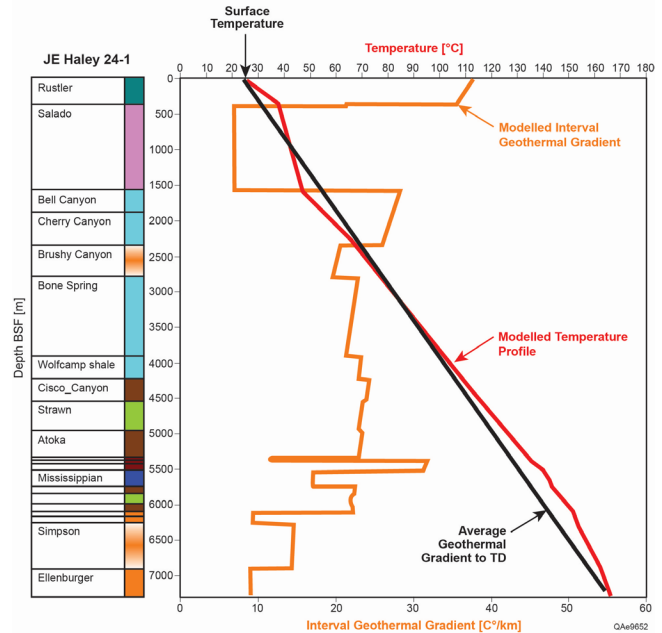


Figure 4.36. Geothermal gradient and temperature profile as a function of depth from a well covering the entire sedimentary strata in the Delaware Basin. Source: Adapted from Deighton, 2015.

A. Potential Geothermal Reservoirs and Reservoir Properties

Based on the available data, the Cambrian-Carboniferous strata in the Permian Basin is considered feasible for deep geothermal resource development. We remove the potential of tight mudrocks, such as Wolfcamp and Bone Spring, from current conventional geothermal consideration since they have very low porosity of about four to eight percent, ultra-low permeability, and other operational constraints, which will be discussed later. Nonetheless these might be attractive targets for Advanced Geothermal Systems, like Closed Loop Systems. The Wolfcamp Formation has high temperature as well as high overpressure in some places, which could be utilized for unconventional geothermal concepts like Engineered and Advanced Geothermal Systems. In addition, the Wolfcamp shale produces voluminous water. These waters could be injected into the deeper reservoirs with favorable reservoir quality, from which hot water could be flowed back to produce geothermal energy. This will be explored later in this Chapter.



1. Ellenburger

The Ordovician-aged Ellenburger is the deepest and laterally most extensive carbonate formation with proven reservoir quality in the Permian Basin. The temperature in the Ellenburger can vary from 99 to 170 °C (210 to 337 °F) (Wallace, et al., 1978; Erdlac, 2006; Kosters, et al., 1990). A significant drop in sea level at the end of Ellenburger deposition resulted in subaerial exposure and widespread karstification and reservoir development (Kerans, 1990). The pore network of the Ellenburger is affected due to dolomitization, karsting, and tectonic fracturing. The upper and lower sections of the Ellenburger have high reservoir quality due to fracture density, breccia, and vugs, compared to the middle section, which is cemented (Sanchez, et al., 2019). In Ellenburger carbonates, matrix porosity is less than 5 percent, consisting of common matrix pore types such as interparticle, moldic, inter-crystalline, or micropores. In general, porosity in the Ellenburger ranges between 2 percent and 20 percent and permeability between 0.1 and 100 millidarcy (Loucks & Kerans, 2019). Although matrix porosity may be low, fractures increase permeability significantly, up to 2,250 millidarcy or more.

2. Simpson Group

Overlying the Ellenburger, the Simpson Group clastic reservoirs are composed of highly mature quartz sandstones having primary interparticle porosity (Schutter, et al., 1992). The Simpson Group is thick in the Delaware Basin, and it is locally porous and permeable. The presence of carbonate cement is one of the factors occluding pores and reducing permeability. Average porosity in the Simpson Group varies from 7 percent to 16 percent in different fields (Tyler, 1991), and permeability ranges between 45 and 164 millidarcy (Galloway, et al., 1983; Wojcik, 1990).

3. Fusselman Formation

The Ordovician-Silurian-aged Fusselman Formation consists of shallow water carbonate platform deposits. It has undergone a variable degree of diagenesis due to episodic sea-level fall. Karst features are also found in this formation. Some of the major Fusselman reservoirs are typically fault-bounded on the Central Basin Platform, and adjacent to part of the Midland Basin (Ruppel, 2019). In general, porosity in this formation varies from 3

percent to 12 percent, whereas permeability is generally between 0.001 and 10 millidarcy (Ruppel, et al., 2019; Kosters, et al., 1990). Apart from the karst, vugs, and fractures, permeability is very low in these reservoirs. The temperature across this formation is generally above 93 °C (200 °F) (Kosters, et al., 1990).

4. Thirtyone Formation

The Devonian-aged Thirtyone Formation is another potential geothermal reservoir in the Permian Basin. These rocks include deepwater cherts, shallow water carbonates, and siliceous ramp limestones (Ruppel, et al., 2019). Each of these facies has significantly different reservoir characteristics that need to be considered while developing geothermal resources. Both carbonates and chert deposits of the Thirtyone Formation have undergone significant alteration since deposition. Chert facies have undergone both early and late episodes of diagenesis that have played important roles in reservoir development. Complete alteration to chert and quartz is likely to result in porosity loss, whereas slower rates favored retention of matrix microporosity. Carbonate dissolution is apparent near the top of the Thirtyone section and along major fault zones. Porosity in the Thirtyone Formation varies from less than 2 percent to 25 percent, with permeability ranging between 10 and 20 millidarcy (Ruppel, et al., 2019). It is highly heterogeneous due to a varying degree of diagenesis and fracturing. Several faults and fault splays intersect these reservoirs, some of which might also act as flow barriers.

Apart from the above deep formations, the Atoka, Strawn, and Cisco formations are potential geothermal targets. These formations are overpressured, especially in the eastern portion of the Delaware Basin. Similar to other carbonate formations, these rocks have undergone diagenesis, which has enhanced their reservoir quality in places.

A recent high level well screening by TGS, a global geophysical services company, showed that there are a few 100 wells and nearby areas that are ripe for repurposing for geothermal development in the Permian Basin (Keay, et al, 2021). They mainly used two criteria for screening: depth about 10,000 feet subsea (about 3,048 meters), implying higher temperature and flow rate (greater than 2,000 barrels per day). These wells contain injectors, shut-ins, and wells near the end of hydrocarbon



production life (based on decline curve analysis). Many of these wells are towards the eastern margin of the Delaware Basin and western margin of the Midland Basin. However, further analysis is needed, as some of the stratigraphic horizons, for example, the Wolfcamp, analyzed by Keay, et al. (2021), are not suitable for conventional geothermal development due to its ultra-low permeability.

The potential for induced seismicity is another major factor, especially in the southwest of the Delaware Basin and towards the western margin of the Midland Basin, for example, Martin County. This area has experienced several instances of elevated seismicity. The injection of voluminous amounts of water for geothermal development can increase the pore pressure and reduce effective stress, and thereby cause existing critically-stressed faults to slip.

Formation water salinity is another uncertainty in these tight formations. Formation water salinity varies significantly in many deep formations in the Permian Basin, including Bone Spring and Wolfcamp formations. Their salinity varies from about 15,000 to 175,000 parts per million due to water mixing from different sources, including connate water, smectite-to-illite transition, and fluid migration from evaporitic sequences along faults and fractures (Nicot, et al., 2020). Salinity close to 15,000 parts per million is an indication of brackish water. This salinity may become an environmental concern, but is also a chemical engineering factor in developing a geothermal plant. Another potential issue in developing geothermal in the shale formations may be the lack of interest among operators to change focus and convert some of their main revenue producing reservoirs and wells to geothermal. Most of the revenue for shale operators in the Permian Basin comes from the Bone Spring, Wolfcamp, and Spraberry plays.

Many recent wells in the Permian Basin target tight formations, including Spraberry, Bone Spring, and Wolfcamp, and some shallower formations, with minimal targeting of deep formations. However, existing deep wells that are either shut-in or near the end of hydrocarbon production life can be converted to geothermal energy production. Water produced from the hydrocarbon producing Bone Spring, Spraberry, and Wolfcamp can be injected back into the deep reservoir for heat production. This reuse would increase the asset life and provide a transparent and predictable

glide path to the energy transition. However, a thorough analysis is needed to determine whether this is possible economically and at scale, and what other resources can be combined for geothermal resources in the oilfield to work economically. A few oil and gas wells here and there in the basin converted to low temperature geothermal wells will neither help reduce carbon emissions, nor provide required electricity to the power grid cheaply. Co-production options (discussed elsewhere in this Report) might provide a multi-revenue stream option that is more economically viable and scalable.

B. Stress Direction and Seismicity in the Permian Basin

Several recent studies have found a strong correlation between saltwater disposal, hydraulic fracturing, and increased seismicity in the Permian Basin (Frohlich, 2012; Lomax & Savvaidis, 2019; Skoumal & Trugman, 2021; Savvaidis, et al., 2019). Some of these earthquakes have a magnitude over 3.0 (Figure 4.37). Due to decades of fluid injection and withdrawal, the state of stress in the basin has evolved. Snee and Zoback (2018) studied the state of stress in the Permian Basin. In the Midland Basin and Central Basin Platform, the direction of the SHmax is approximately east to west, whereas, in the Delaware Basin, SHmax orientation changes progressively from being nearly north to south in the north, to east southeast to west northwest in the south, including the western Val Verde Basin (Snee & Zoback, 2018). Critically stressed faults that are parallel to the SHmax may be prone to slip due to fluid injection.

The current faulting regime in the Midland Basin varies from normal to strike-slip, whereas in the Delaware Basin, it is primarily normal faults. This trend has implications on potential geothermal resource development strategies in the basin depending on the engineering approach. Because water injection will increase the vertical stress in this area, which is already in the normal fault regime, the concern is that the injection may enhance the chance of fault slip. Based on recent studies, some earthquakes in the Permian Basin occur at a greater depth close to the Ellenburger, rather than the shallow Delaware Mountain Group, which is the primary salt water injection zone. Water injection into deep reservoirs such as Ellenburger, which contains high fracture density and vugs, may transmit fluid down to the basement and facilitate pressure build up and fault slip, resulting in induced seismicity.



Therefore, future geothermal sites in the Permian Basin will need to be appropriately planned, instrumented and monitored, and Next Generation concepts like Closed Loop Systems should be considered.

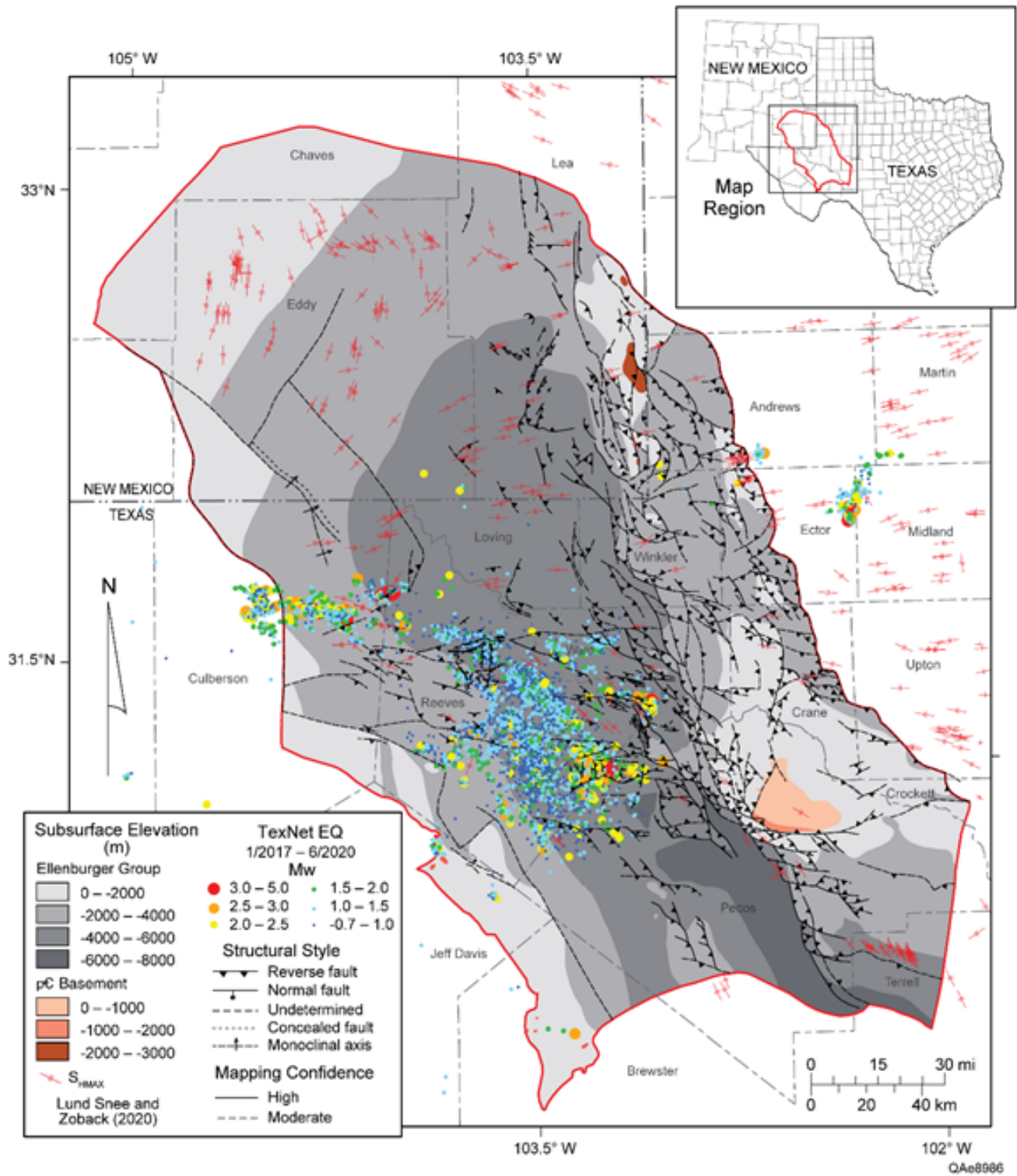


Figure 4.37. The location of interpreted faults and earthquake locations and magnitude in the Permian Basin, focusing on the Delaware Basin. The earthquake locations are analyzed by TexNet, UT Austin.

Sources: Adapted after Horne, et al., 2021.



1. Detailed Review of Crockett County

Crockett County has many oil and gas wells, with the county's southern portion containing more well sites with temperature data available within the NGDS than in the north. It was studied in 2020 as part of the Texas Geothermal Entrepreneurship Organization Project to review a county that included the University of Texas Lands property as a prospect for geothermal development. Crockett County also was chosen for a detailed review because of its location within the Permian Basin, providing a large number of new well BHT data in the last 20 years (Batir & Richards, 2020; 2021).

The updates for Crockett County from the 2011 maps (Blackwell, et al., 2011b) to the 2020 maps (Batir & Richards, 2020; 2021) included an increase of locations from 65 in 2011 to 3,487 sites in 2020. As some of the well sites included more than one temperature-at-depth, there were a total of 3,503 temperatures used (Batir & Richards, 2020; 2021). Most of the new data are from the BEG - NGDS Borehole Observation file. The rest of the data are from the 2014 SMU BHT Heat Flow data file (Figure 4.38). The wells are drilled primarily between 6,560 feet and 9,840 feet (two and three kilometers), yet the deepest wells are at approximately 15,740 feet (4.8 kilometers), and they approximately average 170 °C (338 °F).

Within the BEG Borehole Observation file is a category of SMU Regional Heat Flow data. The data are not included in the SMU 2014 NGDS dataset, and Bureau does not have records as to their origination. One possible source is the work of Erdlac (2006) on the Permian Basin, since this dataset is primarily from wells in the early 2000s, and his report shows plots with large numbers of wells for Crockett County. There is a trend of high gradients with temperatures at 1.9 miles (3 kilometers) greater than 284 °F (140 °C), that were reviewed through the Texas Railroad Commission online data portal. Not all sites included a well log. Those that did were the same or very similar to the dataset temperature at depth. Only a few were not accurate. The increase in BHT values for the newest well logs brings up the potential that those wells drilled most recently are drilled more quickly and, therefore, will have different drilling impacts on the recorded temperature than those from the last century. For this work, a consistent SMU-Harrison Correction (Blackwell, et al., 1990; Richards & Blackwell, 2021) was applied to all well sites, but further research on drilling

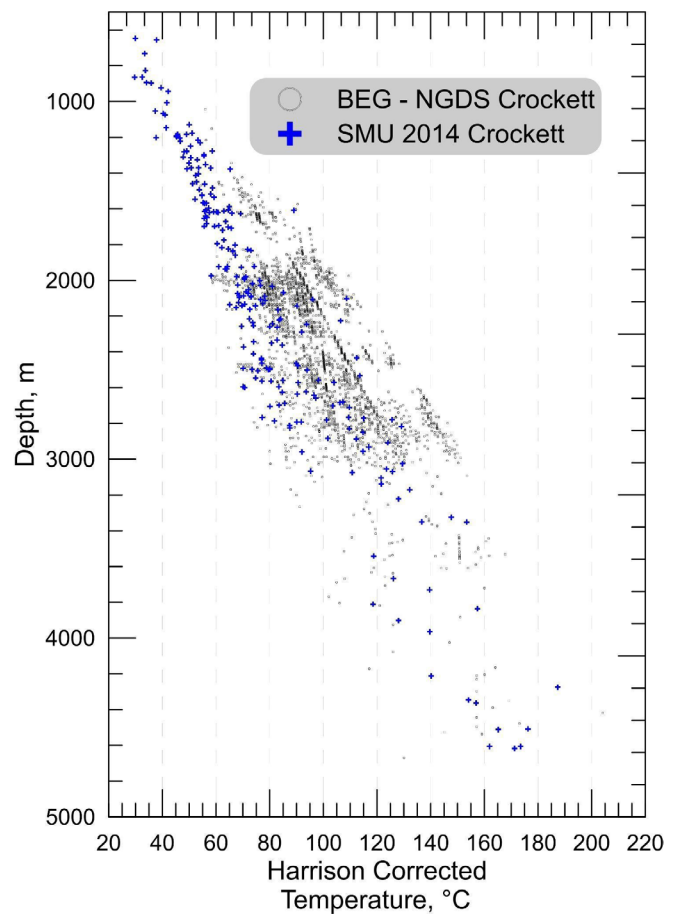


Figure 4.38. Temperature-depth data for Crockett County highlights the immense amount of new data in the NGDS uploaded from the Bureau. The Bureau data (gray circle) also trend warmer than the older SMU BHT data (blue plus). Source: *Future of Geothermal Energy in Texas, 2023*.

impacts of modern wellbores and surrounding formations will most likely change how raw BHT values are corrected for an in-situ setting.

Using the Crockett County BHT data, thermal conductivity values related to those used in the 2011 Blackwell, et al. maps, and two new detailed stratigraphic columns completed as part of the 2020 Batir and Richards study (Batir & Richards, 2020; 2021), an updated heat flow map was produced (Figure 4.39). Comparing the 2020 Batir and Richards map with the 2011 Blackwell, et al. map shows the increased detail possible with additional data. As mentioned above, there is a group of data that are higher gradients than previously known. These data result in the mapped heat flow increasing from a high of 65 to 70 milliwatts per meter squared in 2011 to 80 to 90 milliwatts per meter squared in 2020. The location of University Lands, which are State lands that generate



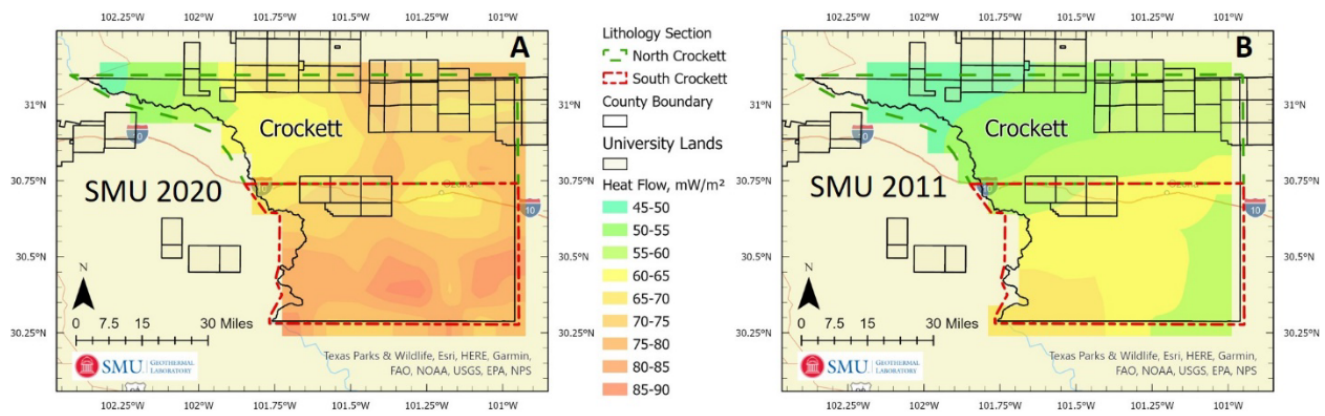


Figure 4.39. The comparison of SMU heat flow maps for Crockett County. (A) the results of detailed geology mapping using 3487 sites by Batir and Richards (2020), and (B) the SMU 2011 subset of U.S. heat flow map by Blackwell, et al. (2011a) with only 65 sites. Sources: Batir and Richards, 2020 and Blackwell, et al., 2011a.

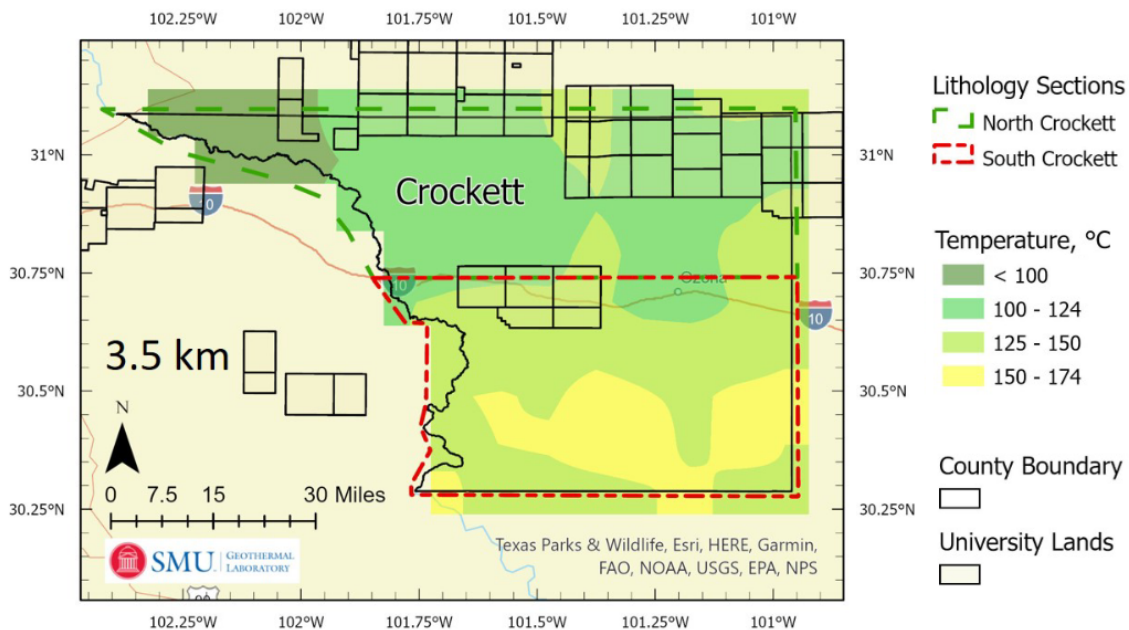


Figure 4.40. The SMU 2020 Crockett County Temperatures-at-Depth Map for 3.5 kilometers. The temperatures range from a low of less than 100 °C (212 °F) in the far northwest corner to over 150 °C (302 °F) in the southeast corner. Source: Batir and Richards, 2020.

revenue for the Permanent University Fund in Texas, are depicted as boxes in the eastern and central portion of the county, which includes higher heat flow values that may lead to developable geothermal resources. Geothermal development potential on University Lands is considered in further depth in [Chapter 13, State Stakeholders Implications and Opportunities](#) of this Report. Figures 4.40, 4.41, and 4.42 are the temperatures-at-depth maps for Crockett County at depths of 11,480 feet, 16,400 feet, and 32,800 feet (3.5 kilometers, 5.0 kilometers, and 10 kilometers) that use the latest heat flow values

as the foundation for the deeper depth temperatures. The highest temperatures at the respective depths are in the southern and eastern portions of the county. Temperatures do not reach 150 °C (302 °F) on University Lands until 3.4 miles (5.5 kilometers) depth, although there are areas at 125 to 150 °C (257 to 302 °F) at 11,480 feet (3.5 kilometers) depth.



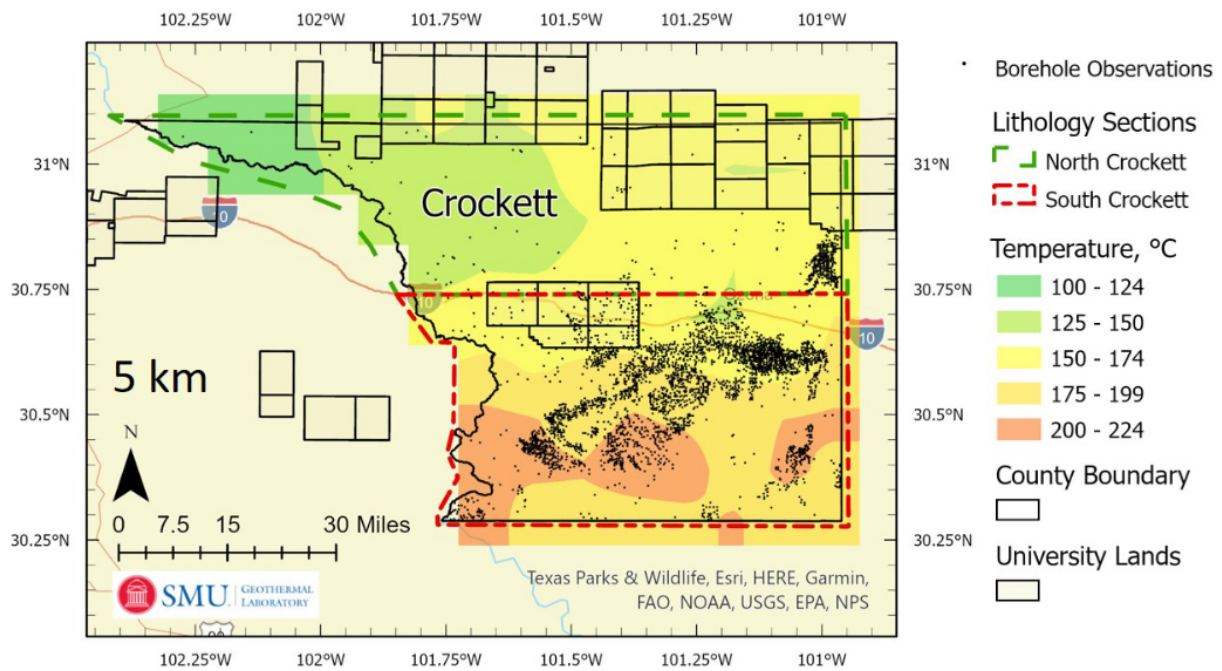


Figure 4.41. The SMU 2020 Crockett County Temperatures-at-Depth Map for five kilometers depth. This map includes the data sites used in the mapping of the temperatures. At this depth, the temperatures range from less than 125 °C (257 °F) in the northwest quadrant to over 200 °C (392 °F) in the southern portion of the map. The University Lands resource temperatures at this depth are approximately 150 °C (302 °F). Source: Batir and Richards, 2020.

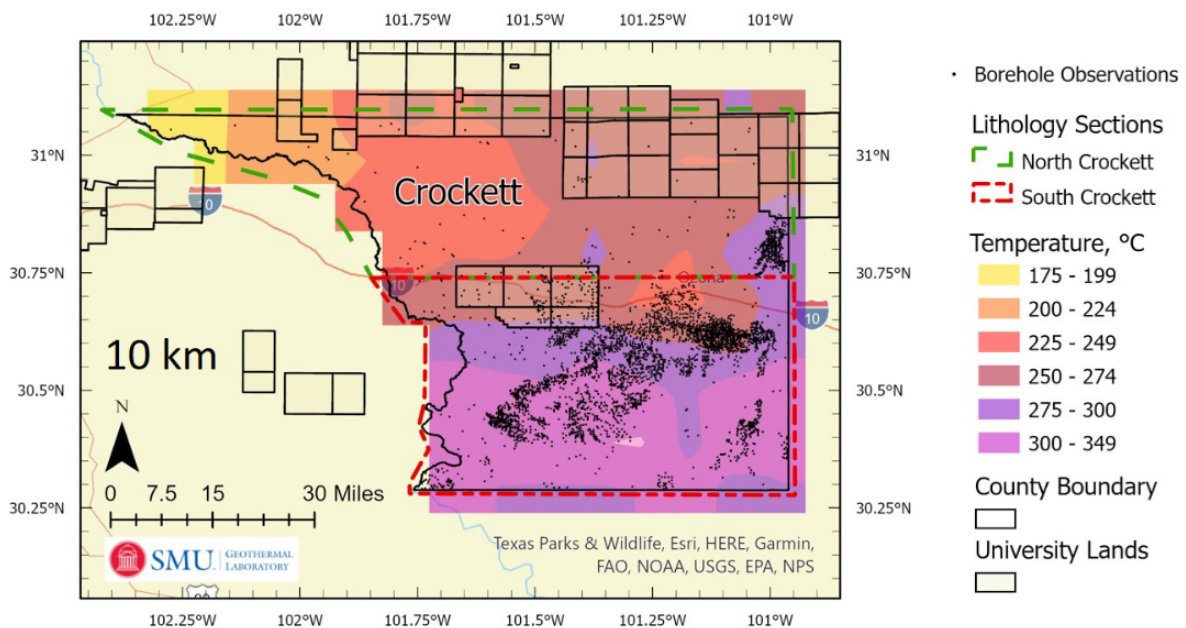


Figure 4.42. The SMU 2020 Crockett County Temperatures-at-Depth Map for ten kilometer depth. This map includes the data sites used in the mapping of the temperatures. At this depth, the temperatures range from less than 200 °C (392 °F) in the northwest quadrant to over 300 °C (572 °F) in the southern portion of the map. The University Lands resource temperatures at this depth are approximately 250 °C (482 °F). Source: Batir and Richards, 2020.



Crockett County is considered part of the Permian Basin and “cold” in terms of geothermal resources. The Heat Flow Map of Texas (Figure 4.4) at the beginning of this Chapter shows this area as blues and greens. The geothermal resources in Crockett County have not changed since the 1990 Geothermal Map of North America (Blackwell, et al., 1990) was produced; instead, our data and knowledge of the geology has grown, allowing for more detailed and accurate mapping of the geothermal resources below Texas.

1. Detailed Review of Webb County

Webb County is dense with oil and gas wells, and much of the related data are in the NGDS. It was studied in 2020 as part of the Texas Geothermal Entrepreneurship Organization Project to improve one county in three regions as an example of changes where many additional BHT sites are newly available (Batir & Richards, 2020; 2021). Webb County is part of the heat flow transition zone from the lower heat flow in Permian Basin to the north, and the higher heat flow in South Texas and the Gulf Coast regions to the south and east. From the previous mapping by Blackwell, et al. (2011a,b), the southern portion of this county, along with Zapata and Starr Counties to the south, had higher temperatures at depth than the surrounding area. These counties are also along the U.S. and Mexico border, therefore, geothermal resources are interesting because developers may qualify for unique funding opportunities.

The updates for Webb County from the 2011 maps to the 2020 maps included an increase for well sites from 387 in 2011 to 1,708 sites in 2020. As some of the well sites included more than one temperature-at-depth, there were a total of 2,087 temperatures used (Batir & Richards, 2020; 2021). The results of the update showed a consistent pattern with the previous mapping efforts that included the addition of more refined sub-county details and an increase overall in temperatures deeper than 2.2 miles (3.5 kilometers).

Besides the additional temperature data, the 2020 studies (Batir & Richards, 2020; 2021) increased the detail for the geology via stratigraphic columns by dividing the county into four different lithology sections that roughly follow the Cretaceous continental shelf edge and the

related sediment influx that defined local depositional environments. The rocks in Webb county are older to the north, with younger sediments to the southeast. Complicating the geology are the growth faults in the deeper structures of the southern portion of the county that thrust the sedimentary formations higher in succession across the county. This change in stratigraphy was also enhanced by a change in thermal conductivity, from a simple model used in 2011 (Blackwell, et al., 1990; Blackwell & Richards, 2004) to assign thermal conductivity values based on related geology from McKenna and Sharp (1998), and a study of the same formations, though the location of this study was Louisiana (Pitman & Rowan, 2012).

The increased volume of temperature data and improved thermal conductivity values make a noticeable change in the resulting heat flow map when compared between the 2020 and 2011 maps (Figure 4.43). The previous heat flow averaged between 60 and 70 milliwatts per meter squared, and the 2020 calculated heat increases to a low of 70 milliwatts per meter squared and a high of 100 milliwatts per meter squared. These changes also impact the temperatures-at-depth, with more data measured at 2.2 miles (3.5 kilometers) and the improved geological relevancy of the deeper calculated temperatures at 4 miles to 6.2 miles (6.5 kilometers and 10 kilometers) (Figures 4.44 through 4.46) (Batir & Richards, 2020; 2021).

The new temperatures-at-depth are generally coldest to the northwest and hottest in the southeastern portion of the county. The 6.2 miles (10 kilometers) map shown in Figure 4.46 includes the well site locations for all the maps, highlighting the data density in the oil and gas fields with few-to-no points in the northwest portion of the county. Although the temperatures are also coldest in this few-to-no data area, geology trends do not indicate a reason for higher temperatures if more well-site data were available. At 2.2 miles (3.5 kilometers) depth, the temperatures are between 125 °C and 175 °C (257 °F and 347 °F). At 4 miles (6.5 kilometers) is where the source of the values change from measured BHT values to calculated between 200 °C and 300 °C (392 °F and 572 °F). By 6.2 miles (ten kilometers), the calculated temperatures are expected to be at least 300 °C to over 375 °C (572 °F to over 707 °F).



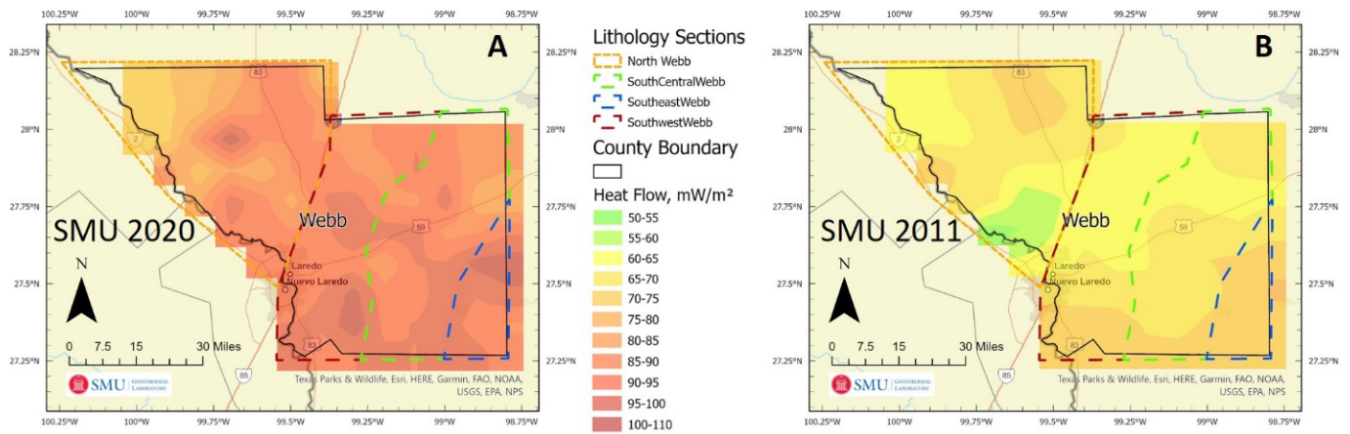


Figure 4.43. Webb County heat flow comparison between the Batir and Richards (2020) detailed study and the Blackwell, et al. (2011) generalized mapping as part of a national map. (A) SMU 2020 assessment. (B) SMU 2011 subset of U.S. heat flow map. The dashed lines divide the county into four sub-county stratigraphic columns used for the 2020 thermal conductivity determinations. *Source: Adapted from Batir and Richards, 2020.*

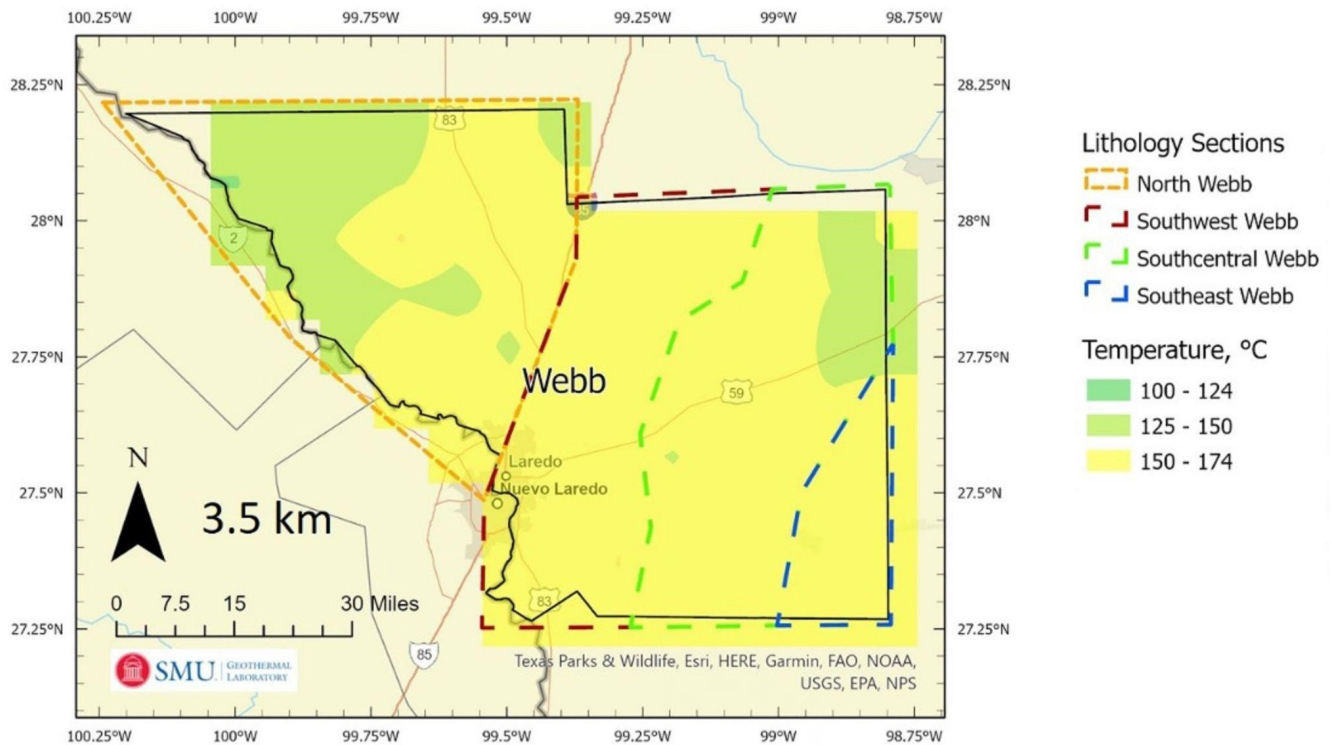


Figure 4.44. Webb County temperatures at 3.5 kilometers depth based on oil and gas well data and the lithology sections used for detailed thermal conductivity values. *Source: Adapted from Batir and Richards, 2020.*

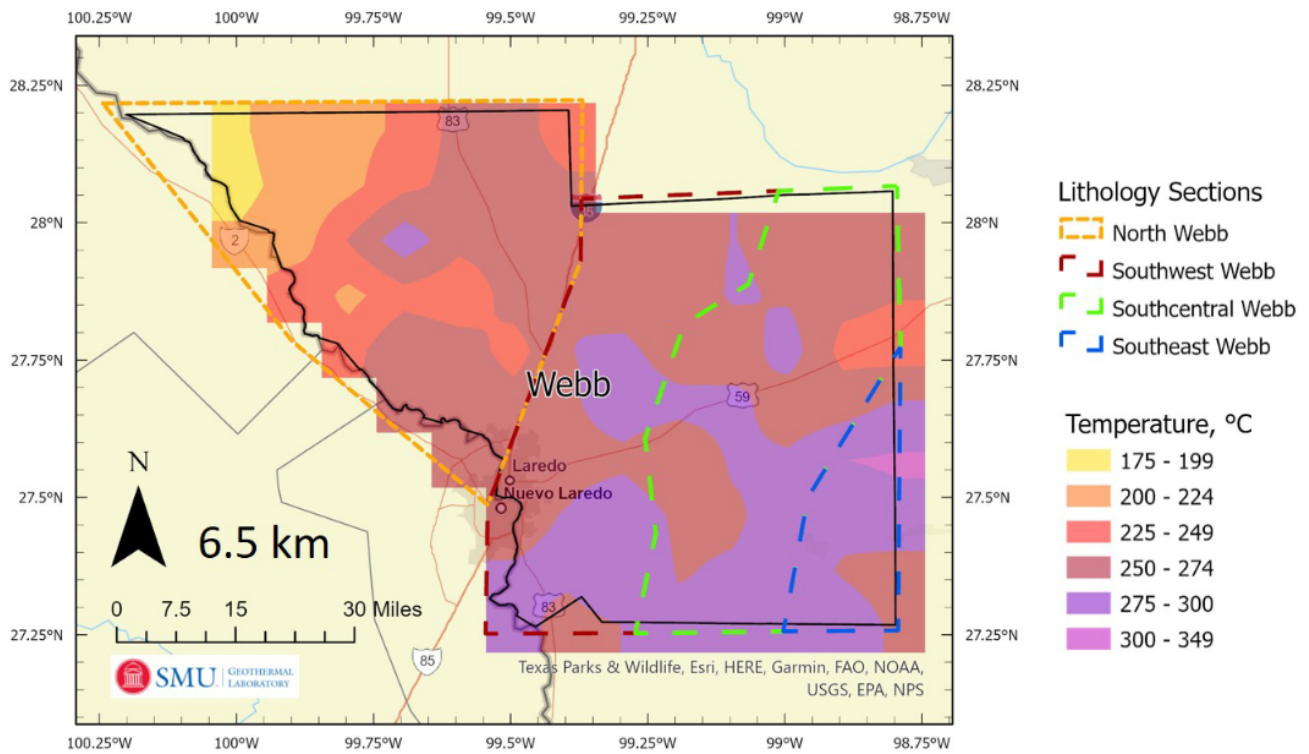


Figure 4.45. Webb County temperatures at 6.5 kilometers depth based on oil and gas well data and the lithology sections used for detailed thermal conductivity values. Source: Adapted from Batir and Richards, 2020.

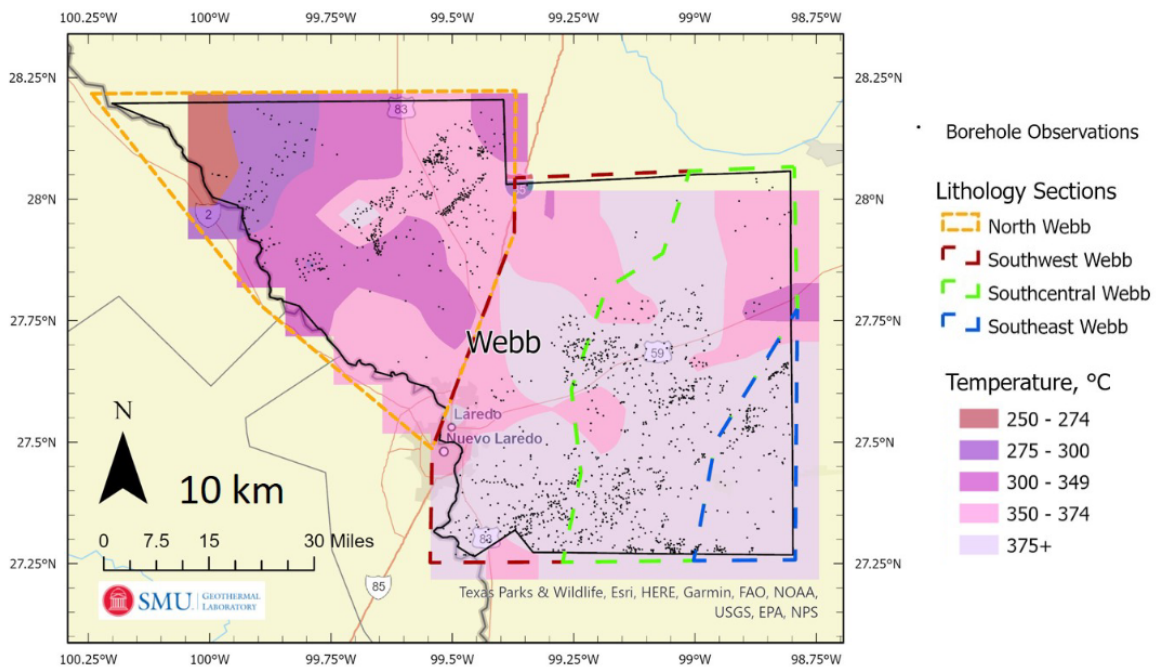


Figure 4.46. Webb County temperatures at ten kilometers depth based on oil and gas well sites that are typically less than 4.0 kilometers in depth (shown here as Borehole Observations) and the lithology sections used for detailed thermal conductivity values. Source: Adapted from Batir and Richards, 2020.



Webb County, and its related region of South Texas, have some of the highest potentials for geothermal resources based on the current oil and gas data. The deep sedimentary formations allow for an average of 7.4 kilometers of sediments in this region, with the deepest sediments to the southeastern portion of the county. As shown by the increase in data volume between the 2011 and 2020 maps, with each assessment and improved data resolution, the geothermal resources are better defined with more variability and reliability, yet with trends expected to be similar to those of the oil and gas fields.

XI. Anadarko Basin (North Texas)

The Anadarko Basin is primarily located in Oklahoma and extends to the northern Texas Panhandle (Figure 4.47). The Anadarko Basin is considered one of the deepest foreland Paleozoic basins in the North American craton. The basin is bound by different structural highs, including the Amarillo-Wichita uplift (south), Nemaha uplift (east), and Cimarron Arch (west) (Johnson, 1989). Most of the published studies cover the Oklahoma portion of the basin. There are very few studies in Anadarko of North Texas (Kosters, et al., 1990). The present day Anadarko Basin started from its predecessor, the Oklahoma Basin. The Oklahoma Basin started as a broad embayment, which received a thick sequence of carbonates interbedded with shale and sandstone (Johnson, et al., 1988). The Oklahoma Basin underwent an orogenic episode during the Pennsylvanian period. The Oklahoma Basin was fragmented into multiple uplifts and major basins during this time, including the Anadarko Basin. The basin subsided throughout the Pennsylvanian-Permian period and continued to receive voluminous sediment. The late epeirogenic history of the basin is characterized by the Permian carbonates, red beds, and evaporites.

Based on the limited data, the heat flow decreases to the southeast of the basin in Oklahoma (Carter, et al., 1998; Gallardo & Blackwell, 1999; Frone, 2014). The western and northern portions of the basin have higher heat flow (between 54 and 62 milliwatts per meter squared) than the southern portion of the basin (between 39 and 47 milliwatts per meter squared) in Oklahoma. Figure 4.48 shows a temperature profile along with the depth in a deep well. Similar to the other basins in Texas, some areas in the Anadarko Basin are overpressured, especially southwest Oklahoma (Lee & Deming, 2002) and some

areas are underpressured. The pressure variation in the basin is related to two distinct geologic events, rapid burial and uplift/erosion. Based on the U.S. Geological Survey report (Nelson & Gianoutsos, 2011), a portion of North Texas Anadarko Basin (away from the Oklahoma border) is underpressured, however, a few places, such as Collingsworth and Wheeler Counties close to the Oklahoma border, might be overpressured. This border region is where the Anadarko Basin is deepest. There is not enough published pressure data in this specific area to draw meaningful conclusions for the North Texas Anadarko Basin. More formation-by-formation study is needed in the Anadarko Basin in north Texas.

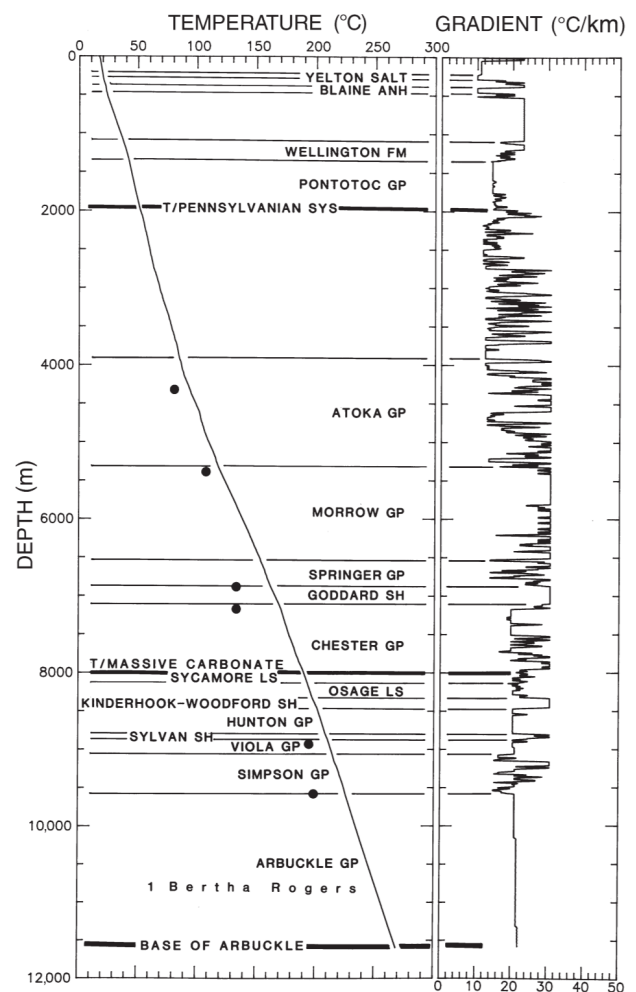


Figure 4.47. The location of the Anadarko Basin, along with prominent structural features. Source: Johnson et al., 1989; Gallardo and Blackwell, 1999. Used with permission of Geological Society of America from *Sedimentary cover, North American Craton, U.S.*, Sloss, L., D-2, 1988; permission conveyed through Copyright Clearance Center, Inc.



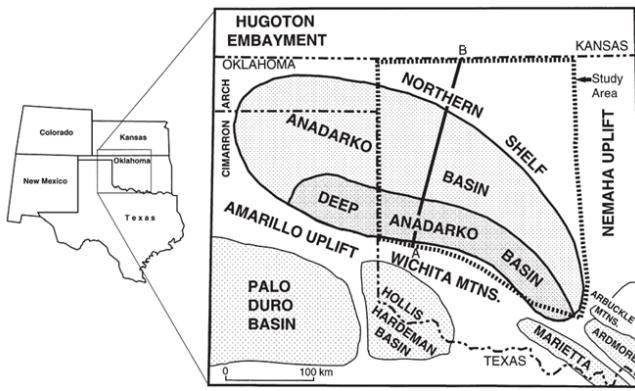


Figure 4.48: Calculated temperature-depth and gradient-depth model for a representative deep-basin well, along with the formations (Lone Star 1 Bertha Rogers well, Washita County, Oklahoma). Large dots are bottom-hole temperatures at well total depth. Source: Gallardo and Blackwell, 1999.

The Cambro-Ordovician Arbuckle Group is the deepest reservoir in the basin. The Arbuckle and its equivalents are all composed of very thick carbonate successions that are often dolomitized. The Arbuckle Group is fractured and contains vugs, similar to Ellenburger in the Permian Basin. Based on a study by NRG Associates (1986), porosity in the Arbuckle varies with depth, for example, 12.5 percent, 7 percent, and 6.2 percent at depths of 6,000 feet (1,829 meters), 7,664 feet (2,336 meters), and 18,240 feet (5,560 meters), respectively, which is indicative of an increasing degree of cementation. Based on the published data, horizontal matrix permeability varies from less than 0.16 millidarcy to 309 millidarcy, whereas vertical matrix permeability varies from less than 0.16 millidarcy to 197 millidarcy (Morgan & Murray, 2015). The presence of fractures enhances permeability greatly. Figure 4.49 shows the geothermal gradient in the Arbuckle is about 22 °C per kilometer, and extrapolated temperature is about 250 °C (482 °F) at about 11,000 feet (3,353 meters) in one borehole location.

Overlying the Arbuckle Group, the Mid-Ordovician Simpson Group is also a potential geothermal reservoir composed of limestones, sandstones, and shales. The porosity of this group ranges between 10 to 18 percent over a depth of 3,500 feet (1,067 meters) to 11,000 feet (3,353 meters) (Ball, et al., 1991). Permeabilities vary between 15 and 300 millidarcy with an average of 120 millidarcy over the same depth range (Harrison & Routh, 1981). The Simpson Group has a temperature of about 200 °C (392 °F) at about 9,600 ft (2,926 meters) (Figure 4.49). The overlying Viola Group

is generally a tight carbonate section, however, locally dolomitized sections have good reservoir quality (Adler, et al., 1971). Other potential reservoirs include the Hunton, Meramec, and Morrow Groups, where temperatures are high enough to produce productively hot brine.

The Granite Wash is another potential geothermal reservoir straddling the Oklahoma and Texas border on the northern flank of the Amarillo-Wichita uplift, and occurs beneath Hemphill, Roberts, and Wheeler Counties in Texas. The Granite Wash is primarily composed of arkosic sandstones and conglomerates with low porosity (1 to 16 percent, average 8 percent) and permeability generally less than 0.1 millidarcy (Mitchell, 2014; Wei & Xu, 2016). However, there are prospective sections consisting of chert (Morrowan Granite Wash) and carbonate (Atokan Granite Wash). This reservoir is both structurally and stratigraphically complex due to its position near the Amarillo-Wichita uplift area. Since 2008, several horizontal oil and gas wells have been drilled in the deep Granite Wash play (9,000 to 15,000 feet or 2,743 to 4,572 meters), which has enabled a better understanding of the Granite Wash. The Stiles Ranch field in Wheeler County of North Texas is an example). The deep wells offer an opportunity to attain high temperatures and are also targets for repurposing depleted wells into geothermal wells. However, because of the lack of published studies, there is a need for detailed research on the subsurface in North Texas focused on geothermal energy potential.

Induced seismicity is a concern in the Anadarko Basin. There are some major faults along northwest to southeast in north Texas. The present day principal maximum horizontal stress direction is also along northwest to southeast (Lund Snee & Zoback, 2020). Therefore, water injection into deep reservoirs close to faults may result in fault slip and earthquakes. However, this should not be a significant concern for Advanced Geothermal Systems, like Closed Loop Geothermal Systems.

XII. Other Settings

A. The Llano Uplift

The Llano Uplift is a unique geologic province in Texas, depicted in the Central Texas Uplift in Figure 4.1. It is an area of approximately 62 by 37 miles (100 by 60 kilometers) of igneous and metamorphic rocks at the surface. The only other region like it is in far West Texas.



The uplift is a window into a rather complex mixture of ancient rocks that were part of the core of a mountain chain of Precambrian age, which is greater than one billion years old (Mosher, et al., 2008). It consists primarily of igneous and metamorphic basement rocks that have been uplifted relative to their surroundings due to several periods of tectonic activity starting in the Precambrian (Ewing, 2016). For the purposes here, the main point of the geology is that it consists of “hard” rocks instead of the general “soft” rock (sedimentary) geology of most of the rest of Texas. The “hard” rocks make deep drilling slower, more difficult, and therefore more expensive in this setting. The nature of these rocks and their history also means there is no petroleum in the uplift region. In turn, this results in a complete lack of wells in the region, other than shallow water wells. The well data map of Texas (Figure 4.3) is the empty region west of Austin and the Hill Country.

The lack of data does not prevent building a reasonable picture of the thermal state of the crust. The regions around the uplift, characterized by much better temperature data, are relatively stable and have constant crustal heat flow in the 35 to 45 milliwatts per square meter range. Given the lack of geologically recent activity in the Llano uplift, it is reasonable to expect to find a similar 35 to 45 milliwatts per square meter heat flow throughout the uplift. The uplift rocks are very low permeability, thus, there is no thermal disturbance due to fluid movement in the crust. Finally, reasonable thermal conductivity measurements are available for the rock types in the region. Combining the data allows for a reasonable determination of the temperature at depth model, as shown in Figures 4.5 through 4.7 at the beginning of this Chapter.

From the heat flow and temperature at depth maps, it is evident that the uplift is one of the cooler regions of Texas, as shown in Figures 4.4 through 4.7. Even at 6.2 miles (10 kilometers) depth, the temperatures are between the 150 and 175 °C (302 and 347 °F) range. While these temperatures might be a reasonable target for certain geothermal technologies, they are less attractive compared to other areas of Texas. The depths and hard rock in the Llano Uplift will result in more expensive drilling, and the region will benefit from the development of cheaper methods to drill hard rock.

B. El Paso – The Edge of the Basin & Range

The far west of Texas, around El Paso, is on the edge of the Basin and Range province. This is a region of ongoing crustal extension. This crustal extension results in a thinner crust. Since the temperature boundary conditions on the top and bottom of the crust are unchanged, the thermal gradient must increase. The temperature maps for Texas (Figures 4.5 through 4.7) show that the highest temperatures in Texas underlie this region and may exceed 350 °C (662 °F) at 6.2 miles (ten kilometers) depth.

Besides the high background temperatures due to thin crust, the Basin and Range province is characterized by deep extensional faulting. This faulting, in many parts of the Basin and Range, creates permeable pathways. Water heated by deep circulation into the crust along those pathways can rapidly flow to the surface, creating exploitable Conventional Hydrothermal Systems. While there are no producing geothermal systems in this region, there have been exploration projects on Fort Bliss, a large military base that stretches from Texas into New Mexico, with the latest announced in 2020 (Richter, 2020).

Historically, the region has not been of interest to the oil industry, and is thus sparsely drilled (Figure 4.3), but there have been some geothermal exploration programs because of the known high heat flow in the area. Most of the drilling and data is relatively shallow and is indicative mainly of shallow fluid flow; there have been deep wells of around 3,280 feet (one kilometer) that reached temperatures of 93 °C (200 °F) (Lear, et al., 2016). Taking an average surface temperature of 18 °C (64 °F) results in a gradient of 75 °C per kilometer (4.1 °F per 100 feet). While this measurement is possibly elevated due to fluid convection, it still indicates significant temperatures in the shallow to intermediate subsurface.

As high as any in Texas, these temperatures clearly make this region a high priority for further geothermal exploration and development. However, the current data is relatively sparse. Texas’ other “hot” regions, the Gulf Coast and East Texas, have rich data sets that quantitatively delineate the resource at the region to county scale. The relative lack of data in Texas’ Basin and Range region means that the apparent high temperatures are not well constrained. In other western states, the Basin and Range is the site of most U.S. hydrothermal geothermal systems (by number, not generation capacity),



but there are no known hydrothermal systems in the Texas zone. It is estimated that there are three to five times as many undiscovered Blind Hydrothermal Systems (“BHS”) in the western United States (BHS are Conventional Hydrothermal Systems with no surface manifestations). By extension, there may be multiple BHS to be discovered in the Texas Basin and Range region.

Thus, the Basin and Range region of Texas appears to have significant geothermal potential both for the development of Conventional and Next Generation Geothermal Systems. A more precise and certain thermal picture of the area is needed. A program of intermediate-depth drilling across the region is called for to define the thermal picture of the region. Confidence in the regional temperature landscape would, in turn, spur site-specific exploration and investment in geothermal projects.

C. Central Texas/Edwards Plateau

The Central Texas Hill Country was a region of Cretaceous age limestones when much of Texas was covered by shallow seas. The region is bounded on the south and east by the Balcones Fault Zone, which forms the boundary with the coastal plains, and extends west to the Llano Uplift, surrounding it. West of the Llano Uplift, the limestones continue as the Edwards Plateau. These areas have experienced limited petroleum exploration except in the far west of the region, where it grades into the Permian Basin. Like the Llano Uplift, a reasonable picture of the thermal condition of the subsurface of Central Texas and the Edwards Plateau is possible but is not well constrained.

As shown in Figures 4.5 through 4.7, this region is relatively cool. Unlike the Llano Uplift, however, the rocks, limestones, are considered “soft” rocks. Thus, while the temperatures are not any hotter than in the adjacent Llano area, the cost of reaching the same depths is much less. This makes the region an easier geothermal exploration target than the Llano Uplift. Also, like the basin and Range, data is relatively sparse and would benefit from a systematic data collection program.

XIII. Conclusion

Texas has an immense resource at hand in the form of accessible heat for geothermal energy production – thousands of times our current energy usage in Texas. Texas also has a wide variety of geologic/geophysical settings, thus there is no “one size fits all” approach to understanding and assessing the geothermal potential of Texas. This variation and complexity in the geologic and geophysical setting will require thoughtful research and planning as entities seek to develop geothermal resources in the State.

This Chapter provides a solid starting point for project planning and understanding the general conditions in an area or region. Site specific analysis is still needed to reduce risk and better understand this natural and reoccurring exploitable resource in Texas. The Lone Star State is unique to possess substantial information about the subsurface, although more of this data needs to be analyzed with a view toward geothermal development. Where there has not been oil and gas development (see Figure 4.3), our knowledge of the subsurface is weak. These sparsely drilled areas include most of the population centers outside of the Gulf Coast. **Of significant note, where we have taken deeper dives at the county scale in this Report, we find that the subsurface heat resource is better than previously estimated in the most recent mapping of the Texas heat resource, last conducted in 2011.** This is due to more refined approaches, a large increase in well drilling and available data since 2011, and a comprehensive update of county level mapping in Texas.

Going forward, government, industry, and academic cooperation and coordination is needed to fill in the gaps in our knowledge of the Texan subsurface, and provide a foundation for accelerating geothermal development. Texas has everything needed to help launch the future of geothermal, including the resource, and can lead the world in the Geothermal Anywhere movement.



Conflict of Interest Disclosure

Ken Wisian serves as an Associate Director of The Bureau of Economic Geology, Jackson School of Geoscience at the University of Texas at Austin, and is compensated for this work. His main area of research for 30 plus years in geothermal systems. Outside of this role, Ken Wisian certifies that he has no affiliations, including board memberships, stock ownership and/or equity interest, in any organization or entity with a financial interest in the contents of this manuscript, and has no personal or familial relationship with anyone having such an affiliation or financial interest.

Shuvajit Bhattacharya serves as a Research Associate at Bureau of Economic Geology, The University of Texas at Austin, and is compensated for this work. His main research expertise are in petrophysics, seismic interpretation, and integrated subsurface characterization. He has contributed to the regional geology and formation characteristics of the Gulf Coast, Permian Basin (West Texas), and Anadarko Basin (North Texas) portion of this chapter. Outside of this role, Shuvajit Bhattacharya certifies that he has no affiliation, including board memberships, stock ownership and/or equity interest, in any organization or entity with a financial interest in the contents of this manuscript, and has no personal or familial relationship with anyone having such an affiliation or financial interest.

Maria Richards serves as the Coordinator of the SMU Geothermal Laboratory in the Roy M. Huffington Department of Earth Sciences, and is compensated for this work. Her main area of research for 26 years is in geothermal resource exploration. Outside of this role, Maria Richards certifies that she has no affiliation, including board memberships, stock ownership and/or equity interest, in any organization or entity with a financial interest in the contents of this manuscript, and has no personal or familial relationship with anyone having such an affiliation or financial interest.



Chapter 4 References

- Adams, R. L. (2009). Basement tectonics and origin of the Sabine uplift. *Gulf Coast Association of Geological Societies Transactions*, 59, 3-19.
- Adler, F. J., Caplan, W. M., Carlson, M. P., Goebel, E. D., Henslee, H. T., ... & Wells, J. S. (1971). Future Petroleum Provinces of the Mid-Continent, Region 7, in AAPG Special Volume M15 Future Petroleum Provinces of the United States—Their Geology and Potential, 2985-1042.
- Ball, M. M., Henry, M. E., & Frezon, S. E. (1991). Petroleum geology of the Anadarko Basin region, province (115), Kansas, Oklahoma, and Texas (pp. 1-36). Denver, Colorado: US Geological Survey.
- Batir, J.F., & Richards, M. C., (2021). Updated Heat Flow and Temperature-at-Depth Maps of Three Texas Counties, Geothermal Resources Council Transactions, 45, 20. 1952-1970.
- Batir, J. F. and Richards, M. C. (2020a). Upshur County Geothermal Assessment, Unpublished Report for Clearwater Reserves, LLC by SMU Geothermal Laboratory, Dallas, TX.
- Batir, J. F. & Richards, M. C. (2020b). Analysis of Geothermal Resources in Three Texas Counties (No. 1291). USDOE Geothermal Data Repository (United States); Southern Methodist University Huffington Department of Earth Sciences.
- Batir, J. F., Richards, M. C., & Schumann, H. (2018). Reservoir Analysis for Deep Direct-Use Feasibility Study in East Texas. *GRC Transactions*, 42, 20.
- Bebout, D. G., Weise, B. R., Gregory, A. R., & Edwards, M. B. (1982). Wilcox sandstone reservoirs in the deep subsurface along the Texas Gulf Coast: their potential for production of geopressured geothermal energy. Report of Investigations No. 117 (No. DOE/ET/28461-T2). Texas Univ., Austin (USA). Bureau of Economic Geology.
- Bebout, D. G., Gutierrez, D. R., & Bachman, A. L. (1981). Geopressured geothermal resource in Texas and Louisiana: geological constraints (No. CONF-811026-3). Louisiana Geological Survey, Baton Rouge.
- Longman, M. W., & Mench, P. A. (1978). Diagenesis of Cretaceous limestones in the Edwards aquifer system of south-central Texas: a scanning electron microscope study. *Sedimentary Geology*, 21(4), 241-276.
- Blackwell, D. D., Richards, M. C., Frone, Z. S., Batir, J. F., Williams, M. A., Ruzo, A. A., & Dingwall, R. K. (2011a). SMU geothermal laboratory heat flow map of the conterminous United States, 2011. Southern Methodist University Huffington Department of Earth Sciences.
- Blackwell, D., Richards, M., Frone, Z., Batir, J., Ruzo, A., Dingwall, R., & Williams, M. (2011b). Temperature-at-depth maps for the conterminous US and geothermal resource estimates (No. GRC1029452). Southern Methodist University Geothermal Laboratory, Dallas, TX (United States).
- Blackwell, D., Richards, M., & Stepp, P. (2010). Final report, Texas geothermal assessment for the 135 corridor east, for Texas state energy conservation office, contract CM709. SMU geothermal laboratory, Dallas, Texas, USA, 80.
- Blackwell, D. D., & Richards, M. (2004a). Geothermal Map of North America: American Association of Petroleum Geologists. Tulsa, Oklahoma, scale (1: 6,500,000).
- Blackwell, D., & Richards, M. C. (2004b). The 2004 geothermal map of North America, explanation of resources and applications. *Geothermal Resource Council Transactions*, 28, 317-320.
- Blackwell, D. D., Steele, J. L., & Carter, L. C. (1990). Heat flow patterns of the North American continent: A discussion of the DNAG geothermal map of North America. DOE EEGTP (USDOE Office of Energy Efficiency and Renewable Energy Geothermal Tech Pgm).
- Bruner, K. R., & Smosna, R. A. (2011). A comparative study of the Mississippian Barnett shale, Fort Worth basin, and Devonian Marcellus shale, Appalachian basin (NETL-2011/1478, 2011). US Department of Energy.
- Budd, D. A. (1981). Smackover and lower Buckner formations, south Texas: depositional systems on a Jurassic carbonate ramp. Report of Investigations 112, Texas Univ., Austin (USA). Bureau of Economic Geology.
- Burke, L. A., Kinney, S. A., Dubiel, R. F., & Pitman, J. K. (2013). Regional maps of subsurface geopressure gradients of the onshore and offshore Gulf of Mexico Basin. US Department of the Interior, US Geological Survey.
- Carter, L. S., Kelley, S. A., Blackwell, D. D., & Naeser, N. D. (1998). Heat flow and thermal history of the Anadarko Basin, Oklahoma. *AAPG bulletin*, 82(2), 291-316.



- Christie, C.H. (2014). Possible Causes for the Variation of Geothermal Gradients Across the Northern Continental Shelf of the Gulf of Mexico, MS Thesis, Texas Tech University.
- Claypool, G. E., & Mancini, E. A. (1989). Geochemical relationships of petroleum in Mesozoic reservoirs to carbonate source rocks of Jurassic Smackover Formation, southwestern Alabama. *AAPG bulletin*, 73(7), 904-924.
- Cornelius, S., & Emmet, P. A. (2020). Relationship between Geothermal and Geopressure Gradients in the Western Gulf of Mexico. *GeoGulf, Gulf Coast Association of Geological Societies Transactions* (70:1), 85-94.
- Davies, J. H., & Davies, D. R. (2010). Earth's surface heat flux. *Solid Earth*, 1(1), 5-24.
- Davis, R. J., Conover, M. F., Keeney, R. C., Personett, M. L., & Richmann, D. L. (1981). Texas geothermal RD&D program planning: Texas Energy Development Fund. DHCSRAC/EDF-045, DE83900796.
- Deighton, I. (2015). Basin Temperature Modeling Using Large Bottom Hole Temperature Datasets. In Oral presentation given at the SMU Power Plays Geothermal Conference, Dallas (Vol. 20).
- Dixon, S. A., Summers, D. M., & Surdam, R. C. (1989). Diagenesis and preservation of porosity in Norphlet Formation (Upper Jurassic), southern Alabama. *AAPG bulletin*, 73(6), 707-728.
- Dutton, S. P., & Loucks, R. G. (2010). Diagenetic controls on evolution of porosity and permeability in lower Tertiary Wilcox sandstones from shallow to ultradeep (200-6700 m) burial, Gulf of Mexico Basin, USA. *Marine and Petroleum Geology*, 27(1), 69-81.
- Dutton, S. P., Kim, E. M., Broadhead, R. F., Breton, C. L., Raatz, W. D., Ruppel, S. C., & Kerans, C. (2004). Play analysis and digital portfolio of major oil reservoirs in the Permian Basin: application and transfer of advanced geological and engineering technologies for incremental production opportunities, Final Report.
- Edwards, M. B. (1981). Upper Wilcox Rosita delta system of south Texas: Growth-faulted shelf-edge deltas. *AAPG Bulletin*, 65(1), 54-73.
- Endicott, J.R., (1995). Case history—three McMullen County fields (Texas). *Oil and Gas Journal*, 54, 228-230.
- Erdlac Jr, R. J. (2006). A resource assessment of geothermal energy resources for converting deep gas wells in carbonate strata into geothermal extraction wells: a Permian Basin evaluation (No. DOE/GO/85023). The University of Texas of the Permian Basin Center for Energy & Economic Diversification, Odessa, Texas.
- Esposito, A., & Augustine, C. (2012). Recoverable Resource Estimate of Identified Onshore Geopressured Geothermal Energy in Texas and Louisiana. US Department of Energy, Office of Energy Efficiency and Renewable Energy, National Renewable Energy Laboratory.
- Ewing, T. E. (2016). Texas through time: Lone Star geology, landscapes and resources. Texas Univ., Austin (USA). Bureau of Economic Geology.
- Ewing, T. E., Budnik, R. T., Ames, J. T., Ridner, D. M., & Dillon, R. L. (1990). Tectonic map of Texas. Texas Univ., Austin (USA). Bureau of Economic Geology.
- Ewing, T.E., & Salvador, A. (Ed.). (1991). Structural Framework. *The Geology of North America: The Gulf of Mexico Basin* (Vol. 10, 31-52). Boulder, Colorado: Geological Society of America.
- Fasola, S. L., Brudzinski, M. R., Skoumal, R. J., Langenkamp, T., Currie, B. S., & Smart, K. J. (2019). Hydraulic fracture injection strategy influences the probability of earthquakes in the Eagle Ford shale play of South Texas. *Geophysical Research Letters*, 46(22), 12958-12967.
- Fisher, W. L., Brown Jr, L. F., Scott, A. J., & McGowen, J. H. (1969). Delta systems in the exploration for oil and gas. University of Texas at Austin, Bureau of Economic Geology.
- Frohlich, C. (2012). Two-year survey comparing earthquake activity and injection-well locations in the Barnett Shale, Texas. *Proceedings of the National Academy of Sciences*, 109(35), 13934-13938.
- Frone, Z. (2014). Heat flow and thermal history of the Anadarko Basin, Oklahoma. *AAPG Search and discovery Article*, 10657, 28. Retrieved December 20, 2022 from https://www.searchanddiscovery.com/documents/2014/10657frone/ndx_frone.pdf.
- Gallardo, J., & Blackwell, D. D. (1999). Thermal structure of the Anadarko Basin. *AAPG bulletin*, 83(2), 333-361.
- Galloway, W. E., Ewing, T. E., Garrett, C. M., Tyler, N., & Bebout, D. G. (1983). Atlas of major Texas oil reservoirs. Texas Univ., Austin (USA). Bureau of Economic Geology.
- Galloway, W. E., Hobday, D. K., & Magara, K. (1982). Frio Formation of the Texas Gulf Coast Basin: depositional systems, structural framework, and hydrocarbon, origin, migration, distribution, and exploration potential. Report of investigations No. 122 (No. NP-3901764). Texas Univ., Austin (USA). Bureau of Economic Geology.



- Godo, T. (2019). The Smackover–Norphlet petroleum system, deepwater Gulf of Mexico: oil fields, oil shows, and dry holes. *Gulf Coast Association of Geological Societies Journal*, 8, 104-152.
- Granata Jr, W. H. (1960). Cretaceous stratigraphy and structural development of the Sabine uplift area, Texas and Louisiana. Ph.D. Thesis, University of Wyoming.
- Hamlin, H. S., & Tyler, N. (1988). Consolidation of Geologic Studies of Geopressed Geothermal Resources in Texas. Annual Report under US Department of Energy and The University of Texas at Austin Cooperative Agreement No. DE-FC07-85-NV, 1041.
- Harrison, W. E., & Routh, D. L. (1981). Reservoir and fluid characteristics of selected oil fields in Oklahoma. *Oklahoma Geological Survey Spec. Publication;(United States)*, 81.
- Hartman, B. M., & Scranton, D. F. (1992). Geologic map of Texas: Bureau of Economic Geology. The University of Texas at Austin, scale, 1(500,000).
- Hornbach, M. J., DeShon, H. R., Ellsworth, W. L., Stump, B. W., Hayward, C., Frohlich, C., ... & Luetgert, J. H. (2015). Causal factors for seismicity near Azle, Texas. *Nature communications*, 6(1), 1-11.
- Horne, E. A., Hennings, P. H., Zahm, C. K., Callahan, O. A., & Eichhubl, P. (2021). The geologic basement of Texas: A volume in honor of Peter T. Flawn. Bureau of Economic Geology Report of Investigations, No. 286.
- Hovorka, S. D., Doughty, C. A., Knox, P. R., Green, C. T., Pruess, K., & Benson, S. M. (2001). Evaluation of brine-bearing sands of the Frio Formation, Upper Texas Gulf Coast for geologic sequestration of CO₂. GCCC Texts and Reports, Texas Univ., Austin (USA). Bureau of Economic Geology.
- Hurd, G. S., Kerans, C., Fullmer, S., & Janson, X. (2016). Large-scale inflections in slope angle below the shelf break: A first order control on the stratigraphic architecture of carbonate slopes: Cutoff Formation, Guadalupe Mountains National Park, West Texas, USA. *Journal of Sedimentary Research*, 86(4), 336-362.
- Jennings, S., Hasterok, D., & Payne, J. (2019). A new compositionally based thermal conductivity model for plutonic rocks. *Geophysical Journal International*, 219(2), 1377-1394.
- John, C. J., Maciasz, G., & Harder, B. J. (1998). Gulf Coast geopressed-geothermal program summary report compilation. Volume 2-B: Resource description, program history, wells tested, university and company based research, site restoration (No. DOE/ID/13366-T1-Vol. 2B). Louisiana State Univ., Basin Research Inst., Baton Rouge, LA (United States).
- Johnson, K. S. (1989). Geologic evolution of the Anadarko basin. *Oklahoma geological survey circular*, 90(10)
- Johnson, K. S., Amsden, T. W., Denison, R. E., Dutton, S. P., Goldstein, A. G., Rascoe, B., ... & Thompson, D. M. (1988). Southern midcontinent region. *Sedimentary Cover–North American Craton: United States*. The Geological Society of America.
- Jordan, T. E., Richards, M. C., Horowitz, F. G., Camp, E., Smith, J. D., Whealton, C. A., ... & Bolat, R. (2016). Low Temperature geothermal play fairway analysis for the Appalachian basin: phase 1 revised report November 18, 2016 (No. DE-EE0006726). Cornell Univ., Ithaca, NY (United States).
- Keay, J., O'Reilly, C., Mayer, M., Valenciano, A., & Richards, M. (2021). New life for old wells—Repurposing oil and gas well data for geothermal prospecting. In *First International Meeting for Applied Geoscience & Energy* (pp. 3345-3348). Society of Exploration Geophysicists.
- Kerans, C. (1990). Karst-Controlled Reservoir Heterogeneity in Ellenburger Group Carbonates of West Texas: Reply (1). *AAPG Bulletin*, 74(7), 1124-1125.
- Kerans, C., Playton, T., Phelps, R., & Scott, S. Z. (2014). Ramp to rimmed shelf transition in the Guadalupian (Permian) of the Guadalupe Mountains, West Texas and New Mexico. in *Deposits, Architecture, and Controls of Carbonate Margin, Slope and Basinal Settings*. SEPM Society for Sedimentary Geology, vol. 105.
- Kosters, E. C., Bebout, D. G., Seni, S. J., Garret, C. M., Brown, L. F., Hamlin, H. S., ... & Tyler, N. (1990). Atlas of major Texas gas reservoirs. p. 161.
- Kreitler, C. W., Akhter, M. S., & Donnelly, A. C. (1990). Hydrologic hydrochemical characterization of Texas frio formation used for deep-well injection of chemical wastes. *Environmental Geology and Water Sciences*, 16(2), 107-120.
- Kweik, R. S. (2014). Thermal and mass history of Fairway Field in east Texas: Implication for geothermal energy development in an oil and gas setting. Diss. Southern Methodist University.
- Kweik, R. S., Blackwell, M., Hornbach, M. & Richards, M. (2014). Thermal and Mass History of Fairway Field in East Texas. *GRC Transactions*, 38, 349-654.



- Land, L. S. (1984). Frio Sandstone Diagenesis, Texas Gulf Coast: A Regional Isotopic Study. Part 1. Concepts and Principles. in *Clastic Diagenesis*, American Association of Petroleum Geophysicists, Special Volume, M37, 47-52.
- Land, L. S., & Fisher, R. S. (1987). Wilcox sandstone diagenesis, Texas Gulf Coast: a regional isotopic comparison with the Frio Formation. *Geological Society, London, Special Publications*, 36(1), 219-235.
- Bruce, C. H. (1973). Pressured shale and related sediment deformation: mechanism for development of regional contemporaneous faults. *AAPG Bulletin*, 57(5), 878-886.
- Lear, J., Bennett, C., Lear, D., Jones, P. L., Burdige, M., Barker, B., ... & Taylor, N. (2016). El Paso County Geothermal Project at Fort Bliss. Final Project Report (No. DE-EE0002827-FINAL). El Paso County, TX (United States).
- Lee, Y., & Deming, D. (2002). Overpressures in the Anadarko basin, southwestern Oklahoma: Static or dynamic?. *AAPG bulletin*, 86(1), 145-160.
- Li, P., Huang, G. C. D., Savvaidis, A., Kavoura, F., & Porritt, R. W. (2021). Characteristics of seismicity in the Eagle Ford shale play, southern Texas, constrained by earthquake relocation and centroid moment tensor inversion. *Seismological Research Letters*, 92(6), 3504-3515.
- Lindquist, S. J. (1977). Secondary porosity development and subsequent reduction, overpressured Frio Formation sandstone (Oligocene), south Texas. *Gulf Coast Association of Geological Societies Transactions* (27), 99-107.
- Lindquist, S. (1976). Leached Porosity in Overpressured Sandstone—Frio Formation (Oligocene), South Texas. *Gulf Coast Association of Geological Societies Transactions* (26), 332.
- Lofton, C. L., & Adams, W. M. (1971). Possible Future Petroleum Provinces of Eocene and Paleocene, Western Gulf Basin, in Cram, I. H., ed. *Future Petroleum Provinces of the United States—Their Geology and Potential*, Volumes 1 & 2. AAPG Memoir 15, 855-886
- Lomax, A., & Savvaidis, A. (2019). Improving absolute earthquake location in west Texas using probabilistic, proxy ground-truth station corrections. *Journal of Geophysical Research: Solid Earth*, 124(11), 11447-11465.
- Loucks, R. G. (1978). Sandstone Distribution and Potential for Geopressured Geothermal Energy Production in the Vicksburg Formation Along the Texas Gulf Coast (1). *Gulf Coast Association of Geological Societies Transactions* (28), 239-271.
- Loucks, R. G., Dodge, M. M., & Galloway, W. E. (1984). Regional controls on diagenesis and reservoir quality in lower Tertiary sandstones along the Texas Gulf Coast: Part 1. Concepts and principles. In *Clastic Diagenesis*, AAPG, Special Volume, M37, 15-45.
- Loucks, R. G., Dodge, M. M., & Galloway, W. E. (1979). Importance of Secondary Leached Porosity in Lower Tertiary Sandstone Reservoirs Along the Texas Gulf Coast (1). *Gulf Coast Association of Geological Societies Transactions* (29), 164-171.
- Loucks, R. G., & Kerans, C. (2019). Geologic Review of the Lower Ordovician Ellenburger Group of the Permian Basin, West Texas and Southeast New Mexico. in Ruppel, S, ed. *Anatomy of a Paleozoic basin: the Permian Basin, USA*, Volumes 1 and 2, The University of Texas Bureau of Economic Geology (Report of Investigations 285) and The American Association of Petroleum Geologists (Memoir 118), 399 pp., doi: doi.org/10.23867/RI0285-1., 295-330.
- Lund Snee, J. E., & Zoback, M. D. (2020). Multiscale variations of the crustal stress field throughout North America. *Nature communications*, 11(1), 1-9.
- Luo, M., Baker, M. R., & LeMone, D. V. (1994). Distribution and generation of the overpressure system, eastern Delaware basin, western Texas and southern New Mexico. *AAPG bulletin*, 78(9), 1386-1405.
- Macpherson, G. L. (1992). Regional variations in formation water chemistry: major and minor elements, Frio formation fluids, Texas. *AAPG bulletin*, 76(5), 740-757.
- McBride, E. F., Land, L. S., & Mack, L. E. (1987). Diagenesis of eolian and fluvial feldspathic sandstones, Norphlet Formation (Upper Jurassic), Rankin County, Mississippi, and Mobile County, Alabama. *AAPG Bulletin*, 71(9), 1019-1034.
- McKenna, T. E. (1997). Fluid flow and heat transfer in overpressured sediments of the Rio Grande embayment, Gulf of Mexico basin. *Gulf Coast Association of Geological Societies Transactions*, (47), 351-366.
- McKenna, T. E., Sharp Jr, J. M., & Lynch, F. L. (1996). Thermal conductivity of Wilcox and Frio sandstones in south Texas (Gulf of Mexico Basin). *AAPG bulletin*, 80(8), 1203-1215.
- Mitchell, J. R. (2014). Stratigraphy and Hydrocarbon Production from Pennsylvanian Age Granite Wash Reservoirs in the Western Anadarko Basin, Oklahoma and Texas, Fall River Exploration LLC, Tulsa, Oklahoma, November 13, 2014. Retrieved November 30, 2022, from <http://www.ogs.ou.edu/MEETINGS/Presentations/GraniteWashNov2014/MitchellGWN014.pdf>.
- Morgan, B. C., & Murray, K. E. (2015). Characterizing small-scale permeability of the Arbuckle Group, Oklahoma. *Okla. Geol. Surv. Open-File Rept. OF2-2015*, 1-12.



- Mosher, S., Levine, J. S. F., & Carlson, W. D. (2008). Mesoproterozoic plate tectonics: A collisional model for the Grenville-aged orogenic belt in the Llano uplift, central Texas. *Geology*, 36(1), 55-58.
- Nagihara, S., Sclater, J. G., Phillips, J. D., Behrens, E. W., Lewis, T., Lawver, L. A., ... & Maxwell, A. E. (1996). Heat flow in the western abyssal plain of the Gulf of Mexico: Implications for thermal evolution of the old oceanic lithosphere. *Journal of Geophysical Research: Solid Earth*, 101(B2), 2895-2913.
- Nagihara, S., & Smith, M. A. (2008). Regional overview of deep sedimentary thermal gradients of the geopressed zone of the Texas-Louisiana continental shelf. *AAPG bulletin*, 92(1), 1-14.
- Negraru, P. T., Blackwell, D. D., & Erkan, K. (2008). Heat flow and geothermal potential in the South-Central United States. *Natural Resources Research*, 17(4), 227-243.
- Nehring, R. G. (1992). *The Significant Oil and Gas Fields of the United States Database*. NRG Assocs.
- Nelson, P. H., & Gianoutsos, N. J. (2011). Evolution of overpressured and underpressured oil and gas reservoirs, Anadarko Basin of Oklahoma, Texas, and Kansas (No. 2011-1245). US Geological Survey.
- Nestell, M. K., Nestell, G. P., Wardlaw, B. R., & Ruppel, S. C. (2019). Integrated fusulinid, conodont, and radiolarian biostratigraphy of the Guadalupian (Middle Permian) in the Permian Basin region, USA. in Ruppel, S, ed. *Anatomy of a Paleozoic basin: the Permian Basin, USA, Volumes 1 and 2, The University of Texas Bureau of Economic Geology (Report of Investigations 285) and The American Association of Petroleum Geologists (Memoir 118)*, 399 pp., 251-291.
- Nicot, J. P., Darvari, R., Eichhubl, P., Scanlon, B. R., Elliott, B. A., Bryndzia, L. T., ... & Fall, A. (2020). Origin of low salinity, high volume produced waters in the Wolfcamp Shale (Permian), Delaware Basin, USA. *Applied Geochemistry*, 122, 104771.
- NRG Associates. (1986). *The significant oil and gas fields of the United States database: Colorado Springs, Colorado*. (proprietary database)
- Ogg, J. G., Ogg, G., & Gradstein, F. M. (2016). *A concise geologic time scale: 2016*. Elsevier.
- Pitman, J. K., & Rowan, E. L. (2012). Temperature and petroleum generation history of the Wilcox Formation, Louisiana (No. 2012-1046, pp. i-51). US Geological Survey.
- Pribnow, D. F., & Sass, J. H. (1995). Determination of thermal conductivity for deep boreholes. *Journal of Geophysical Research: Solid Earth*, 100(B6), 9981-9994.
- Richards, M. C., & Blackwell, D. D. (2012). Developing geothermal energy in Texas: mapping the temperatures and resources. *Transactions, Gulf Coast Association of Geological Societies*, 62.
- Richards, M., Blackwell, D. D., Williams, M., Frone, Z., Dingwall, R., Batir, J., & Chickering, C. (2012). Proposed reliability code for heat flow sites. *Geothermal Resources Council Transactions*, 36, 211-217.
- Richter, A. (2020) U.S. Army receives funding to explore geothermal district heating option, Think Geoenergy, 19 January 2020, retrieved December 20, 2022 from <https://www.thinkgeoenergy.com/u-s-army-receives-funding-to-explore-geothermal-district-heating-option>.
- Riney, T. D. (1991). Pleasant Bayou Geopressed-Geothermal Reservoir Analysis-January 1991 (No. SSS-TR-91-12162 Draft). DOE EEGTP (USDOE Office of Energy Efficiency and Renewable Energy Geothermal Tech Pgm).
- Ritch, H. J., & Kozik, H. G. (1971, May). Petrophysical Study Of Overpressured Sandstone Reservoirs, Vicksburg Formation Mc Allen Ranch Field Hidalgo County, Texas. In SPWLA 12th Annual Logging Symposium. OnePetro.
- Rittenhouse, S., Currie, J., & Blumstein, R. (2016). Using mud weights, DST, and DFIT data to generate a regional pore pressure model for the Delaware basin, New Mexico and Texas. In SPE/AAPG/SEG Unconventional Resources Technology Conference. OnePetro.
- Ruppel, S., Nance, S., Hamlin, S., Harrington, R., Loucks, R., Kerans, C., ... & Wright, W. *Anatomy of a Paleozoic Super Basin—The Permian Basin, USA: Geology, Depositional History, Basin Evolution, and Reservoir Development*. In 2019 AAPG Annual Convention and Exhibition.
- Sanchez, T., Loughry, D., & Coringrato, V. (2019, October). Evaluating the Ellenburger Reservoir for Salt Water Disposal in the Midland Basin: An Assessment of Porosity Distribution Beyond the Scale of Karsts. In Unconventional Resources Technology Conference, Denver, Colorado, 22-24 July 2019 (pp. 4436-4452). Unconventional Resources Technology Conference (URTeC); Society of Exploration Geophysicists.
- Savvaiddis, A., Young, B., Huang, G. C. D., & Lomax, A. (2019). TexNet: A statewide seismological network in Texas. *Seismological Research Letters*, 90(4), 1702-1715.



- Scanlon, B. R., Reedy, R. C., Male, F., & Walsh, M. (2017). Water issues related to transitioning from conventional to unconventional oil production in the Permian Basin. *Environmental science & technology*, 51(18), 10903-10912.
- Schumacher, S., & Moeck, I. (2020). A new method for correcting temperature log profiles in low-enthalpy plays. *Geothermal Energy*, 8(1), 1-23.
- Schutter, S. R., Webby, B. D., & Laurie, J. R. (1992). Ordovician hydrocarbon distribution in North America and its relationship to eustatic cycles. *Global perspectives on Ordovician geology*, 432.
- Shew, R. D. (1992). Origin and Variability of H₂S Concentrations in Siliciclastic and Carbonate Reservoirs—Smackover and Norphlet Formations of Central and Eastern Mississippi, Search and Discovery Article. AAPG. Retrieved December 20, 2022 from <https://www.searchanddiscovery.com/abstracts/html/1992/annual/abstracts/0118b.htm>.
- Skoumal, R. J., & Trugman, D. T. (2021). The proliferation of induced seismicity in the Permian Basin, Texas. *Journal of Geophysical Research: Solid Earth*, 126(6), e2021JB021921.
- SMU Node of National Geothermal Data System, Texas. (2022). Retrieved December 12, 2022 from <http://geothermal.smu.edu/static/DownloadFilesButtonPage.htm>.
- Snee, J. E. L., & Zoback, M. D. (2018). State of stress in the Permian Basin, Texas and New Mexico: Implications for induced seismicity. *The Leading Edge*, 37(2), 127-134.
- Swanson, S. M., Karlsen, A. W., & Valentine, B. J. (2013). Geologic Assessment of Undiscovered Oil and Gas Resources: Oligocene Frio and Anahuac Formations, United States Gulf of Mexico Coastal Plain and State Waters, Open-File Report 2013-1257. USGS.
- Swanson, R. K., Oetking, P., Osoba, J. S., & Hagens, R. C. (1976). Development of an assessment methodology for geopressured zones of the upper Gulf Coast based on a study of abnormally pressured gas fields in south Texas (No. C00-2687-5). Energy Research and Development Administration, Washington, DC (USA). Div. of Geothermal Energy.
- Tester, J. W., Anderson, B. J., Batchelor, A. S., Blackwell, D. D., DiPippo, R., Drake, E. M., ... & Veatch, R. J. (2006). The Future of Geothermal Energy: Impact of Enhanced Geothermal Systems (EGS) on the United States in the 21st Century. (2006). Massachusetts Institute of Technology. Chapter 2, Appendix A, p. 93.
- Tester, J. W., Anderson, B. J., Batchelor, A. S., Blackwell, D. D., DiPippo, R., Drake, E. M., ... & Veatch Jr, R. W. (2006). The future of geothermal energy in the 21 century impact of enhanced geothermal systems (EGS) on the United States. MIT.
- Texas Seismological Network Earthquake Catalog - TexNet. (2022.) University of Texas, Austin. Retrieved December 20, 2022, from <https://www.beg.utexas.edu/texnet-cisr/texnet/earthquake-catalog>.
- Turchi, C. S., McTigue, J. D. P., Akar, S., Beckers, K. J., Richards, M., Chickering, C., ... & Slivensky, D. (2020). Geothermal Deep Direct Use for Turbine Inlet Cooling in East Texas (No. NREL/TP-5500-74990). National Renewable Energy Lab.(NREL), Golden, CO (United States).
- Tyler, N. (1991). Integrated characterization of Permian basin reservoirs, University Lands, west Texas: targeting the remaining resource for advanced oil recovery (Vol. 203). Texas Univ., Austin (USA). Bureau of Economic Geology.
- U.S. Department of Energy - DOE. (2022). WINDExchange: U.S. Installed and Potential Wind Power Capacity and Generation, Retrieved December 2, 2022, from <https://windexchange.energy.gov/maps-data/321>.
- U.S. Energy Information Administration - EIA. (2022a). How much electricity does an American home use? (faq) Retrieved November 14, 2022, from <https://www.eia.gov/tools/faqs/faq.php?id=97>.
- U.S. Energy Information Administration - EIA. (2022b), Texas Electricity Profile 2021, Retrieved December 12, 2022 from <https://www.eia.gov/electricity/state/texas/>.
- Vacquier, V., Mathieu, Y., Legendre, E., & Blondin, E. (1988). Experiment on estimating thermal conductivity of sedimentary rocks from oil well logging. *AAPG Bulletin*, 72(6), 758-764.
- Vasseur, G., Brigaud, F., & Demongodin, L. (1995). Thermal conductivity estimation in sedimentary basins. *Tectonophysics*, 244(1-3), 167-174.
- Waite, L. E. (2009). Edwards (Stuart City) shelf margin of south Texas: new data, New Concepts. Tulsa Geological Society, Tulsa, Oklahoma, USA., in AAPG Search and Discovery archive, Retrieved December 22, 2022 from <https://www.searchanddiscovery.com/documents/2009/10177waite/images/waite>.
- Wallace Jr, R. H., Kraemer, T. F., Taylor, R. E., & Wesselman, J. B. (1978). Assessment of Geopressured-Geothermal Resources. *Geological Survey Circular*, 790, 132-155.



- Webster, R. E., Luttner, D., & Liu, L. (2008). Fairway James Lime Field, East Texas: Still Developing After 48 Years. In American Association of Petroleum Geologists Search and Discovery Article# 110061. Retrieved December 20, 2022 from https://www.searchanddiscovery.com/pdfz/documents/2008/08092webster/ndx_webster.pdf.html.
- Wei, Y., & Xu, J. (2016). Granite Wash Tight Gas Reservoir, in Ma, YZ & Holditch, S. eds. Unconventional oil and gas resources handbook: Evaluation and Development. Gulf Professional Publishing, 449-473.
- Weijermars, R., Burnett, D., Claridge, D., Noynaert, S., Pate, M., Westphal, D., ... & Zuo, L. (2018). Redeveloping depleted hydrocarbon wells in an enhanced geothermal system (EGS) for a university campus: Progress report of a real-asset-based feasibility study. *Energy strategy reviews*, 21, 191-203.
- Wermund, E. G. (1996). Physiographic map of Texas: Bureau of Economic Geology. Bureau of Economic Geology, The University of Texas at Austin, Texas, plate.
- White, D. E., & Williams, D. L. (1975). Assessment of geothermal resources of the United States, 1975 (No. 726-730). US Department of the Interior, Geological Survey.
- Wojcik, R. (1990). Oil and gas fields in West Texas. *West Texas Geological Society Publication*, 5, 71-72
- Womack, R. H. (1971). Geological investigation downdip Wilcox trend of Live Oak, McMullen and Duval Counties, Texas. *South Texas Geological Society Bulletin* 12, 5-23.
- Wood, D. H., & Guevara, E. H. (1981). Regional structural cross sections and general stratigraphy. East Texas Basin: Texas Univ., Austin (USA). Bureau of Economic Geology.
- Woodruff Jr, C. M., Macpherson, G. L., Gever, C., Caran, S. C., & El Shazly, A. G. (1984). Geothermal potential along the Balcones/Ouachita trend, central Texas: ongoing assessment and selected case studies (No. DOE/ID/12057-T6). Texas Univ., Austin (USA). Bureau of Economic Geology.
- Woodruff Jr, C. M., & McBride, M. W. (1979). Regional assessment of geothermal potential along the Balcones and Luling-Mexia-Talco Fault Zones, Central Texas. Final report (No. DOE/ET/28375-1). Texas Univ., Austin (USA). Bureau of Economic Geology.
- Zafar, S. D., & Cutright, B. L. (2014). Texas' geothermal resource base: A raster-integration method for estimating in-place geothermal-energy resources using ArcGIS. *Geothermics*, 50, 148-154.

